STRUCTURE-SOIL INTERACTION IN FRAMED BUILDINGS WITH ORTHOTROPIC WALL INFILLS

A Thesis

by

SAEEDA NAZNEEN

Submitted to the Department of Civil Engineering of Bangladesh University of Engineering & Technology, Dhaka in partial fulfilment of the requirements for the degree

of

MASTER OF SCIENCE IN CIVIL ENGINEERING

August, 1986

STRUCTURE-SOIL INTERACTION IN FRAMED BUILDINGS

WITH ORTHOTROPIC WALL INFILLS

A Thesis

by

SAEEDA NAZNEEN

Approved as to style and content by:

(Dr. M. Azadur Rahman) Supervisor
Professor,
Dept. of Civil Engineering,
BUET, Dhaka.

(Dr. M. Shamim Z. Bosunia) Member
Professor and Head
Dept. of Civil Engineering,
BUET, Dhaka.

A. M. M. Safiullah

(Dr. A.M.M. Safiullah) Member
Professor,
Dept. of Civil Engineering,
BUET, Dhaka.

(Dr. M. Mizanul Huq) Member (External)
Director,
Sthapatya Shilpa
Dhaka.

August, 1986

ACKNOWLEDGEMENT

The author is grateful to her supervisor Professor M. Azadur Rahman for his invaluable advice and guidance throughout the course of this thesis. The author wishes to thank Professor M. Shamim Z. Bosunia, Head, Department of Civil Engineering for his encouragement and co-operation.

The author is indebted to Mr. Mallick Shamim Ahsan for his co-operation and technical advice during the installation of the computer program. Gratitude is also expressed to Computer Centre staff for their co-operation in ensuring a fast turnaround of jobs. The assistance of Mr. M.A. Malek and Mr. Shahiduddin in preparing the thesis is gratefully acknowledged.

SUMMARY

The thesis considers the interaction between structures with orthotropic wall infills and their supporting soil. The finite element method is employed and a general computer program is developed for the non-linear three dimensional structure-soil interaction analysis. The propagation of crack and tensile separations in the soil is taken care of. Novel techniques for the efficient storage of the various matrices and also for solution of simultaneous equations are employed. These resulted in the economy of both computer storage and time and the development of a program viable for computers of even moderate size.

A planned scheme of analyses of various structures with different configurations and having frames with orthotropic wall infills were undertaken. Parameters such as deflections, bending moments, soil stresses, wall stresses and crack propagation were examined in detail. The actual contribution of orthotropic infill walls in increasing the lateral stiffness of framed structures was found to be less than what is apparent from conventional fixed base analyses. However, they were found to reduce significantly the formation and propagation of cracks in the soil. The stresses and the strains in the soil were also studied in order to establish the extent of the soil to be included in the finite element analysis. The rapid reduction of the strains in the soil with depth indicated that this extent need not be very large.

CONTENTS

Chapter 1

GENERAL INTRODUCTION

1.1 INTRODUCTION

The traditional approach of isolation and separate treatment of a structure and its supporting soil has been proved to be irrational and often incorrect. A study of the interaction between the two leads to a more precise understanding of the behaviour of both. Such a study fulfills the need to estimate the form and magnitude of the relative deflections which are used to assess the likelihood of damage. It also reveals the actual distribution of forces and stresses within the structure resulting from the fact that the supports are not unyielding.

To achieve a satisfactory interactive analysis, the soil, the substructure and the superstructure are mathematically modelled. Traditionally, however, extensive simplifying assumptions are made in arriving at these models. This is even so in conventional rigid base analyses. In the design of framed buildings, for instance, the contributions of walls, partitions and floor slabs to the overall stiffness are often not recognized or are recognized only tacitly. The structure is frequently analysed as a bare frame without claddings and infills. In reality, the infills participate in supporting the load and provide a significant amount of stiffness to the structure. For strength calculations these assumptions, being conservative, may be reasonable, but for predicting deformations the simplification is not as easy to justify. Specially, for a realistic analysis of structure-soil interaction, a more explicit recognition of these contributions is required.

Two committees were formed by the Institution of Structural Engineers who published their reports in 1974 (Littlejohn and Macleod) and in 1978 (Thorburn). Both these reports recommended research into analytical methods of solving structure-soil interaction. Although extensive research work followed these reports, many aspects of the problem, including that of infilled frames await due attention.

Brickwork is the traditional material with which infill walls are built in framed buildings. The material is essentially anisotropic and has often been simplified as orthotropic, Rahman and Sawko (1980). The present work considers these orthotropic wall panels as integral infills of the frame. The interaction of the structure and the soil and the contribution of the infill are then studied for various plan configurations and loading conditions. The important aspect of the propagation of cracks in the soil resulting from its inherent tensile weakness has also been duly incorporated in the study. The finite element method, with its versatility and accuracy, has been chosen as the analytical tool. This thesis describes the objectives, the methodology and the findings of this research.

1.2 REVIEW OF METHODS OF INTERACTION ANALYSIS

The interaction of building frames with their supporting soil and the need for inclusion of structural rigidity in calculating settlement of their supports were first appreciated by Meyerhof (1947). A growing interest has since been shown in this field with the necessity of building cheaper and more complex structures on less favourable grounds. The traditional approach treats the problem as a two phase system. Either the soil is analysed, with the structure being represented by an artificial model, or the structure is supported by a fictitious soil.

The relative complexity of the soil behaviour has lead to various simplified soil models. These can be classified as mechanical or mathematical. The most widely used mechanical model is Winkler spring where the soil is replaced by a series of discrete springs. This simple spring concept has been modified further by many authors (Fletcher and Hermann, 1971) to extend its applicability.

Empirical or mathematical models of the soil idealize the soil as an elastic, isotropic, homogeneous and semi-infinite continuum. The mathematical solution of this continuum is based on the classical Boussinesq problem of a point load on the surface of a semi-infinite body. Such models with different modifications were used by Milovic and Tournier (1974) and others. Various simplified continuum representations were also developed to eradicate mathematical difficulties in connection with the inclusion of structural rigidity in the analysis.

Simplified methods of interactive analysis with the soil represented by one of the models described above have been proposed by some investigators. Lee and Harrison (1970) and Seetharamulu and Kumar (1973) analysed framed structures supported on soil.

Chamecki (1956) proposed a method for calculating the settlements of structural supports in which the rigidity of the structure was considered in terms of some load transfer coefficients. Later many authors (Chamecki, 1969; Larnach, 1970; Larnach and Wood, 1972; Komornik and Mazurik, 1974) extended and generalized the above method by using the matrix displacement method to analyse the structure considering the progressive time depended settlements of the soil.

With the development of numerical techniques such as finite element method, a more rigorous treatment of the structure and the soil as an integral system became possible. Cheung and Zienkiewicz (1965) presented a finite element method for the analysis of slabs and tanks resting on an Winkler foundation. Then Cheung and Nag (1968), Smith (1970) and others extended the above method to care for horizontal contact pressure and vertical tension separation of the structure-soil boundary and soil inhomogeneity etc.

Majid and Craig (1972) used an incremental technique to perform an interactive analysis for two dimensional problems with a soil showing non-linear properties.

King and Chandrasekaran (1974) described a method for analysing a multistorey space frame on a raft foundation supported by a non-homogeneous soil represented by three-dimensional finite elements with variable properties. But the method does not treat the structure and soil as an integral unit and the influence of one on the other is considered in several separate analyses.

Cunnell (1974) and Majid and Cunnell (1976) proposed a three-dimensional finite element interaction analysis method in which the non-linear stress-strain property of the soil was followed. The structure, the foundation and the soil were represented by suitable three-dimensional finite elements and analysed as an integral system. But the tension separation in the soil mass as well as in the soil-foundation interface were ignored. Additionally the approach has severe limitations in computational aspects.

Rahman (1978) applied finite element method for three-dimensional non-linear analysis of the superstructure, the foundation and the soil as an integral system. The non-linear properties of the soil were duly incorporated and an incremental analysis technique was followed and an iterative method of analysis was proposed for long term settlements of soils. Tensile separations at the foundation-soil interface and within the soil mass were taken care of. A computer program was developed and two large practical structures and their supporting soil were analysed to investigate into their interactive behaviour.

A detailed investigation has been carried out by Sankaran and Srinivasaraghavan (1981) to study the interaction between a superstructure, its raft foundation and the underlying soil system. The results of the analysis of this three phase system using finite element programme are presented in terms of differential settlement and member forces of the raft. Analysis has also been made of a raft and soil system only ignoring the interaction of the superstructure. Comparison of the results of the two analyses, the effect of superstructure interaction and the optimisation of raft thickness for satisfying the conflicting limiting requirements for differential settlement and member forces have been revealed clearly in this analysis.

Desai et al (1982) presented a finite element procedure for general problem of three-dimensional soil-structure interaction involving non-linearities caused by material behaviour, geometrical changes, and interface behaviour. The formulation is based on the updated Lagrangian or approximate Eulerian approach with appropriate provision for constitutive laws. Consideration is given to the mathematical and experimental aspects related to the important topic of development and adoption of a constitutive law for geologic medium. Development and use of an interface element to describe the three-dimensional interface behaviour is described. The influence of cracking and tensile stress conditions in the soil and interfaces is allowed by using the stress transfer approach. The procedure was verified by comparing predictions with observation of a structure pushed in the soil in a special soil-bin test facility.

Desai and Sargard (1984) developed a stress hybrid finite element procedure for non-linear, elastic and elastic-plastic analysis of soil-structure interaction including simulation of construction sequences. In this method, both displacements and stresses are assumed independently within an element and on its boundaries. As a result, it is possible to choose different and higher order stress distributions if warranted by the physical characteristics of the problem, such as interfaces and excavated surface.

Demeneghi (1981) proposed a procedure of analysing in an integral form the soil-structure interaction for a reticular continuous structure and for a distributed reaction of compressible soil.

From the above study of the available works the effectiveness of the finite element method in performing a three-dimensional non-linear analysis of structure-soil interaction problems is evident. The method is easily programmable and a broad class of structures with various types of elements and loading conditions can be efficiently handled. The method can also easily cater for the varying properties of soil including low tensile strength and low resistance to cracks. Considering these, employment of the method in conducting the present research work is justifiable.

1.3 ANALYSIS OF INFILLED FRAMES

A realistic allowance for the in-plane stiffness of walls and partitions, particularly where these are built as infill panels or as continuous shear walls is desirable when a structure-soil interaction analysis is being conducted. A review of the available works show an inadequate consideration in this regard. However, definite progress has been made for the inclusion of infill panels in framed structures for traditional analyses without regard to structure-soil interaction.

Investigations of infilled frames made in the fifties and the sixties (Wood, 1958; Polyakov, 1960; Holmes, 1961; Stafford Smith, 1966) were concerned with strength and stiffness characteristics of non-integral infilled frames, in which weak bond and friction might develop at the interface between the infills and the frames; no attempt was, however, made to improve the integrity at the interface. Irregularities and unevenness at the interface produce considerable variation in structural strength and stiffness making them unreliable for theoretical predictions and design purposes.

Investigations of integral infilled frames of the seventies (Liauw, 1970, 1973; Mallick and Garg, 1971; Liauw and Lee, 1977; Wood, 1978) provided deeper understanding of their behaviour, and realization of improved structural characteristics. The problems inherent in a non-integral frame can be overcome by the introduction of materials with strong bond (Kadir and Hendry, 1975) or shear connectors (Liauw and Lee, 1977; Liauw and Kwan, 1982) at the frame-infill interface, resulting in a more reliable structure not only for analytical prediction and design purposes, but also for engineering the structure to give a better performance.

Apart from nonintegral and fully-integral infilled frames, other types which have been investigated can be grouped as semi-integral infilled frames, where the panels are partially integrated to the frames, e.g., provision of vertical slits in each panel or provision of vertical gaps on both sides of each panel which is integral with the beam only.

Although the analysis of infilled frame structure has been attempted using the theory of elasticity (Sachanski, 1960; Liauw, 1970) and by finite element analyses (Karamanski, 1967; Mallick and Severn, 1967; Kadir, 1974), the rather uncertain boundary conditions between the infill and the frame suggest that an approximate solution would be appropriate. Various approximations (Wood, 1958; Benjamin and Williams, 1958; Liauw, 1972) have been proposed, the most highly developed being that based on the concept of an equivalent diagonal strut, which was originally proposed by Polyakov (1960) and subsequently developed by other investigators (Holmes, 1961; Stafford Smith, 1962, 1966; Mainstone, 1971). The essential problems in this approach are (1) to determine the contact length between the frame and the brickwork, (2) to find the effective width for the equivalent strut and (3) to establish the mode of failure and strength of the brickwork. The contact length depends on the relative stiffness of the frame and infill, and on the geometry of the panel. Stafford Smith (1966) first developed the analogy of the problem with a beam on an elastic foundation. The relationship between the force acting on the equivalent diagonal and the normal stress at the centre of the panel has been suggested by Kadir (1974) following work by Seddon (1956) on partially loaded concrete wall. Kadir has carried out an elastic analysis to obtain a relationship giving the percentage of the total lateral force applied to the frame-wall system carried by the wall. Kadir also found that the equivalent diagonal strut method could be applied to multi-storey frames with reasonable accuracy.

Infill panels frequently contain door or window opening which will obviously reduce their effectiveness in stiffening the surrounding frame to an extent dependent on their size. Experiments by a number of investigators (Sachanski, 1960; Holmes, 1961; Benjamin and Williams, 1958; Liauw and Lee, 1977) have indicated that centrally located openings may reduce the strength and stiffness of an infilled frame by about 50% and 70% respectively. The results of a number of model-scale tests by Kadir illustrate the effect of various sized centrally placed openings in a square infilled panel. However, because of the variability in the test results and the small number of experiments no definite conclusions could be drawn. For unreinforced openings in the infill panels, it is suggested that where openings cut the diagonal which forms the axis of the effective strut and occupy more than a sixth of the frame opening, the infill panel in question should be ignored. Where the openings are of lesser size or do not cut the diagonal, the infill panels should be rated at half the stiffness of similar full infill panels, although small openings in corners that the interaction analysis shows to be unloaded may be ignored completely. Liauw (1977) has put forward a method for the calculation of the stiffness and strength of infilled frames with openings that uses a strain energy method to establish the area of the equivalent strut. An infill with a centrally placed door opening is replaced by two members, one horizontal and one vertical and connected by a rigid joint. Interactive forces between the surrounding frame and the infill are assumed to be concentrated at two diagonally opposite corners. Stafford Smith (1966) investigated the behaviour of diagonally loaded infilled frames and laterally loaded single and multistorey infilled frames. The members of the frame were of the same section and rigidly connected together, the infills were square and of isotropic material with a plastic type of compressive failure, similar to concrete.

There are many experimental data on the behaviour of brick work (Polyakov, 1960; Sachanski, 1960; Fiorato, 1970;

Mainstone, 1970, 1971), concrete (Benjamin and Williams, 1960; Stafford Smith, 1966; Simms, 1967; Stafford Smith and Carter, 1969; Mainstone, 1971) and Steel (El-Dakhakhni and Daniels, 1973; Nyberg, 1976) infills. Virtually nothing has been done on infill panels of other materials.

The contribution of the panels to the overall stiffness of above ground structure is dependent on their tightness of fit in the frame. In the tests referred to, with rare exceptions, early separations of the unloaded corners of the infill panels from the frames, usually coupled at slightly higher deflections with some internal cracking, led to the infill panels behaving essentially as diagonal struts. For design purposes it therefore seems preferable to regard them so, rather than as true shear panels with nominal shear moduli to compensate for the highly non-uniform and predominantly compressive internal stress patterns.

Many reinforced concrete frames are built with brickwork infill which adds considerably to the strength and rigidity of the structure as a whole. A considerable amount of research work has been carried out on the stiffening effect of infill panels although very little use of this appears to be made in practical design. This is possibly because of uncertainity of the composite action when, as is usual, the brickwork is not completely bonded to the frame and there is the fear that infill panels may be removed at some stage in the life of the building. Moreover infill panels are highly non-homogeneous. Nominally identical infill panels will differ markedly from one another in the precise distribution of this non-homogeneity and may, in consequence, differ considerably in behaviour. Cracking and partial separations between the infill panel and the frame may soon develop as the latter distorts. Ultimate loads of the combined frame-infill system will be reached only after excessive cracking. A typical load-deflection response is not only significantly non-linear, but also time dependent and influenced initially by the construction sequence. An infilled frame may over a relevant range of distortions, be an order of magnitude stiffer than the bare frame. Hence, a realistic treatment of the infill panels must be regarded as essential to a meaningful interaction analysis.

Infill panels of plain concrete are more nearly homogeneous, and the only tests that have permitted a direct comparison with brickwork infill panels (Mainstone, 1971, 1974) show less variability in the behaviour of the concrete panels. The general pattern of behaviour is, however, similar, and equivalent diagonal strut is again the approximate model.

Only in infill panels of reinforced concrete with adequate reinforcement tied into the bounding frame or continuous with the reinforcement of adjacent infill panels will a state approximating to uniform shear arise as a result of a racking deformation. In such cases the shear stiffness of the infill panels may be calculated simply on the basis of the vertical cross-sectional area of the infill panel and a shear modulus equal to 40% of the normal elastic modulus.

Steel infill panels are not used at present, but their use as partitions to limit sidesway in multistorey steel-frame buildings has been advocated and guidance on their treatment can be found in Bryan and Davies (1976).

Based on test and non-linear finite element analysis, a uniform plastic analysis for infilled frames with three types of interface conditions is proposed by Liauw and Kwan (1985), in which the stress redistribution towards collapse and the conditions at the infill-frame interface are taken into account. The theory is applicable to single and multistorey infilled frames. Design recommendations for multistorey infilled frames are given by them.

It appears from the above review that the equivalent diagonal strut representation of the infills is an effective tool in traditional analysis of infilled frames. However, little is known about the contribution of various types of infills on the integral structure-soil interaction behaviour. While the contribution of various types of infill to the stiffness of framed buildings is recognised, orthotropic materials such as brickwork and blockwork are the most widely used in the construction of infills. The influence of such infills on the interaction of framed structures and their supporting soil appears to remain uninvestigated.

1.4 ESSENTIAL FEATURES OF STRUCTURE-SOIL INTERACTION PROBLEM

The following are the main features of a realistic interaction problem:

1. The problem is three-dimensional in nature and this should be given proper consideration.
2. The mechanical behaviour of the soil is non-linear and therefore an acceptable stress-strain representation is essential.
3. Soil is heterogeneous. This nature of the soil must therefore be considered in an interactive approach.
4. The initial state of stress caused by the body forces influence the mechanical behaviour of the soil. Thus the stiffness and the strength of soil increase with depth.
5. The redistribution of stresses within the soil and the structure takes place due to creation of local tensile failure zones within the soil. The resulting change in mechanical behaviour of soil must be catered for in an interaction analysis.
6. The redistribution of stresses due to tensile separations at the interface of the structure and the soil must not be overlooked either.

7. A treatment of the complete structure, the foundation and the soil as an integral system for the analysis is essential.

8. Engineering structures are often irregular, complex and large. An interaction method should be flexible, capable of including irregularities that are obvious at the beginning of the analysis or may develop later. The method should be versatile and economical.

9. Framed buildings often have infill panels that contribute to the stiffness of the frame and share the load. Such infills are orthotropic and their contribution should be duly accounted for in a realistic interaction analysis of such buildings.

1.5 OBJECTIVES OF PRESENT RESEARCH

The principal objectives of the research are:

1. To develop a finite element computer program for the non-linear analysis of orthotropic wall infilled three-dimensional frames with foundation and soil as an integral system.

2. To analyse the above system under different loading conditions.

3. To investigate the contribution of infills on the stress distribution and deformation characteristics of the structure-soil systems for various building plan configurations.

4. To ascertain the changes in behaviour of the frames, both bare and infilled, due to the inclusion of soil in the system over the traditionally considered fixed base analysis.

1.6 SCOPE OF THE WORK

Orthotropic infills may contribute substantially to influence the overall load-deformation behaviour of building frames and the distribution of stress throughout the structure and the foundation. Proper consideration for infill in an interaction analysis would result in a better understanding of the structure-soil interaction phenomenon of such structures. The influence of building plan configuration on the load-deformation behaviour of structure-soil systems is also likely to be significant, specially for lateral loads. The study of structure-soil interaction for buildings of various plan arrangements would also lead to a better understanding of the fundamental interaction phenomenon. The problem is three-dimensional and the soil behaviour is essentially nonlinear. The tensile strength of soil is negligible which results in tensile failures at the foundation-soil interface and within the soil mass. This introduces a further nonlinearity in the problem.

All the above features of the problem can be efficiently handled by a suitable finite element program. A comprehensive program incorporating various types of finite elements to represent the different components of structure and soil in a three dimensional system is reported in this thesis. The program automatically caters for material nonlinearity and nonlinearity due to the development and propagation of cracks and tension separations. The analytical aspects of the method including the development of an orthotropic plate element are described in Chapter 2.

The finite element program considers the structure, the foundation and the soil as an integral system and tackles the non-linear analysis by an incremental technique. The problem is formidable and would ordinarily be beyond the storage capacity and calculating speed of most computers. Novel techniques for the efficient storage of the various matrices, efficient method of solution of simultaneous equations and implementation o an automatic crack propagation scheme are included in the features of the program. These result in an efficient utilization of storage and time and make the program viable for computers of even the moderate size. The features of the computer program are described in Chapter 3.

Once the program is implemented, it can be used as a tool to investigate various structure-soil interaction problems. A planned scheme of analyses of various structures with different plan configurations and having frames with orthotropic infills were undertaken. The analyses are described in Chapter 4. The results are critically examined.

and discussed in Chapter 5. Such diverse but interrelated parameters as deflections, bending moments, soil stresses, wall stresses and crack propagation are examined in detail.

The conclusions made from the study are presented in Chapter 6. The chapter also recommends avenues of future work in this and related fields. Finally, a description of the finite elements used is given in the Appendix.

Chapter 2

ANALYTICAL TREATMENT OF THE INTERACTION PROBLEM

2.1 INTRODUCTION

A completely unyielding foundation exists only as a hypothesis for the simple analysis of structures. A relatively unyielding foundation is provided by sound hard bed rock, but the realization of such a rigid form of support is generally expensive if rock is not near the surface. Since most structures are directly underlain by compressible ground, structure-soil interaction is an inevitable phenomenon.

The essential features of the structure-soil interaction problem have been described in Art. 1.4. Material nonlinearity of the soil is represented by the so called spline functions and followed by an incremental technique. Nonlinearity due to tension separation and crack propagation in a three dimensional structure-soil system is accounted for by an automatic procedure of double joint numbering. The infill walls of framed buildings being orthotropic are represented by orthotropic plate finite elements. The methods of handling nonlinearity due to material behaviour and crack propagation together with the formulation of an orthotropic plate element are described in the following sections.

2.2 SPLINE FUNCTION REPRESENTATION OF NON-LINEAR SOIL PROPERTIES

The analysis of a structure resting on soil by the finite element method requires an explicit representation of the soil properties. At each stage of loading, properties like E, ν and G may be non-linear, but should be kept uniquely defined because the stiffness matrix of the individual elements must be constructed explicitly before the analysis can proceed.

It is, therefore necessary to convert the sample test results to smooth and representative functions of sufficient accuracy so that the finite element analysis gives acceptable results. This is particularly needed when an incremental analysis is carried out and the soil properties are defined by more than one graph. In this section a method to represent the non-linear soil behaviour is presented. This makes use of the highly efficient spline function. While the mathematics involved in the derivation of these functions is advanced, they are originated from the draughman's spline which is a strip used to draw smooth graphs of variable curvature.

A non-linear elasticity model has been used successfully by many authors where the dependency of the state of stress on time and on the history of loading is excluded. Thus in this approach the state of stress is assumed to be a function of the state of strain only. Utilizing this approach here, the stress-strain relationship is assumed to consist of a series of elastic steps. The laws of elasticity are,therefore, applicable in each of these steps. The formulation of the laws of elasticity in a three-dimensional state is facilitated by the use of octahedral stress components. The octahedral stress approach has been used successfully by Girija Vallabhan and Reese (1968), to describe stress-deformation behaviour of soils, and by Cunnel (1974) and Girija Vallabhan and Jain (1972), to perform finite element analyses of soils in conjunction with triaxial test results. While it is possible to determine all the octahedral parameters under arbitrary conditions by using sophisticated and expensive laboratory testing, the triaxial test results can be utilized effectively to develop the octahedral parameters.

Mathematical formulation of spline function is presented in detail by Rahman (1978). The versatility and flexibility of the cubic spline function make it readily applicable to describe the τ_{oct} - γ_{oct} curves in Fig. 2.1. The curves in this figure describe the stress-strain properties of the soil used during the analyses reported in this thesis. Each value is for a particular initial value of octahedral normal stress, σ_{octi} and each set of data requires a different spline formulation. Some form of interpolation is necessary to predict the τ_{oct} - γ_{oct} behaviour for an intermediate value of σ_{octi}. Desai (1971), for instance, suggested the establishment of a number of secondary splines between the tangent slopes and σ_{octi} for various values of stress and strain. It is also possible to formulate a bicubic spline in a three-dimensional space of τ_{oct}, γ_{oct} and σ_{octi}, Desai (1972). Trial solutions revealed that variation of the tangent slope at a particular strain level between two

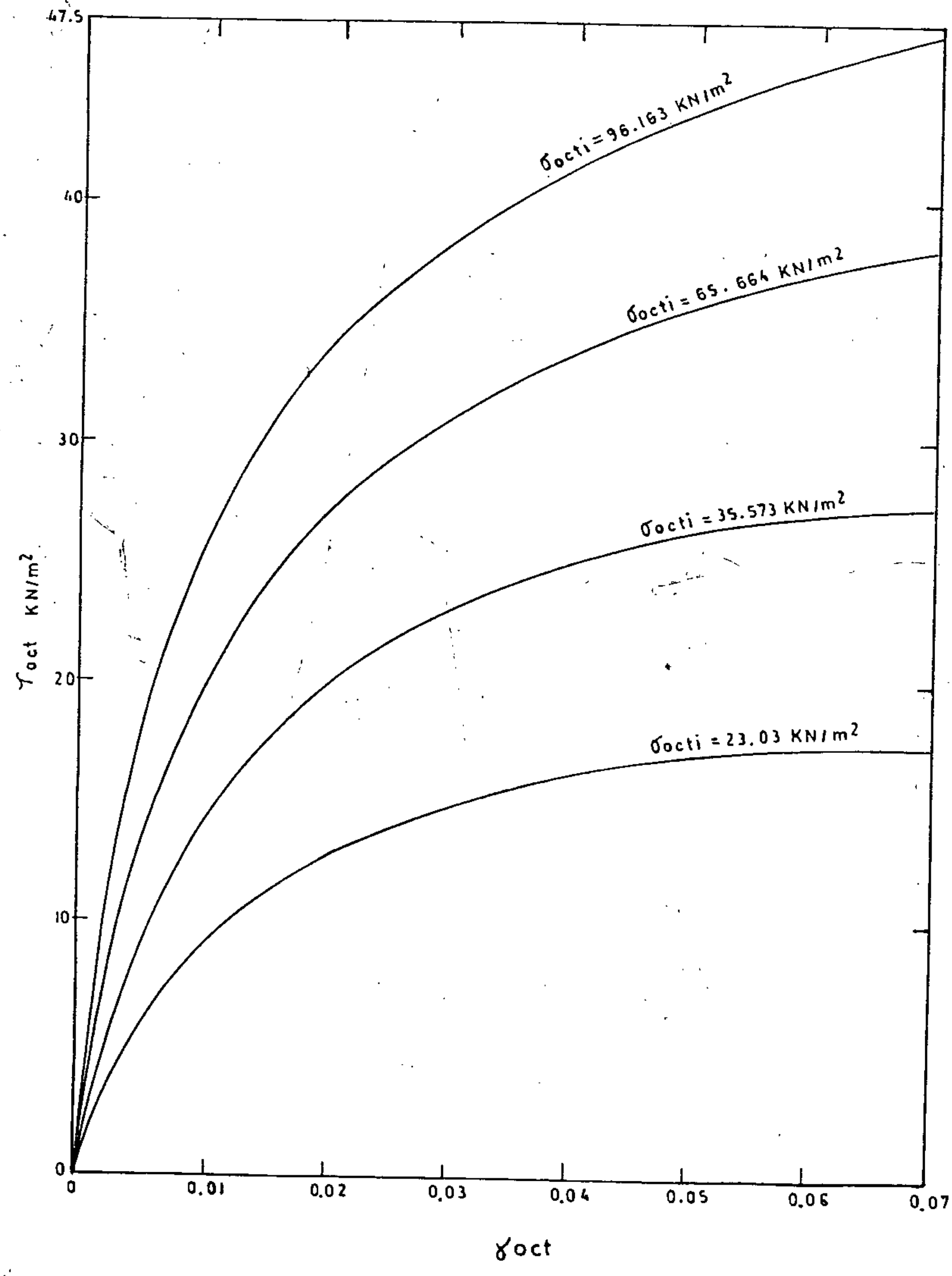

FIGURE 2.1 τ_{oct} - γ_{oct} CURVES OF SOIL USED IN THE ANALYSES.

consecutive values of σ_{octi} was not far from linear. It was decided therefore, to use a linear interpolation at any strain level to find the shear modulus for an intermediate value of σ_{octi}.

2.3 THE NON-LINEAR ANALYSIS TECHNIQUE

The interaction analysis of a structure resting on soil can be carried out by the finite element approach. In that case the soil is represented by three dimensional solid elements. The element should be so chosen that it can conveniently and economically be included in a finite element program for solving large problems.

The properties of soil are non-linear and, therefore, the analysis using the three dimensional solid elements for soil must take account of this. A method of analysis, which follows the complete load deflection history of the structure as well as the non-linear stress-strain path of soil elements is described in this section.

2.3.1 Selection of Solid Element

The finite element approach can be useful only if it can deal with large structures using existing computers with their limited capacity. Even then the cost of the analysis must be low. These aims can be achieved without any loss of accuracy provided that the stiffness matrix of a solid element is prepared and programmed in explicit form.

The isoparametric concept of finite element formulation offers a virtually unlimited choice of shape and order of elements, but elements used to represent soil need not be of an irregular shape. The essence of the concept is that the same interpolation functions used to determine the field displacements from their nodal values are used to determine the co-ordinates of any point in the element from the nodal co-ordinates, these functions are called 'shape functions', as they completely define the element shape. A suitable choice of these functions can define any element with arbitrary shape.

The eight noded isoparametric haxahedral element shown in Fig. 2.2a was used by Majid and Cunnel (1976). The weakness of such an element is that it has to be formulated, starting from the shape function and following the entire process of constructing the matrix $\underline{B}$ and $\underline{D}$ in the integral $\underline{K} = \int_V \underline{B}^T \underline{D} \underline{B} \, dv$ in every step of the analysis. Furthermore the integration has to be carried out numerically. The difficulty increases especially when there are a large number of different element sizes. The stiffness matrix for each element has to be constructed separately. The transformation of the local co-ordinates of each element to the global system is also an integral part of the analysis using isoparametric elements, and adds to the computer time. For these reasons, in the non-linear analysis of large structures, it was discovered that the use of isoparametric elements became very uneconomical.

Since the fictitious boundary plans of the soil elements can be selected in a flexible manner, the computer time can be reduced considerably by developing a fixed shape rectangular parallelopiped element. The rectangular parallelopiped element shown in Fig. 2.2b is a special case of the arbitrarily shaped isoparametric element in Fig. 2.2a. The two linear elements in Fig. 2.2 are defined by the same set of shape functions. They also satisfy the same conditions of continuity and convergence. Therefore, the same degree of accuracy is obtained by using either of them. However, the rectangular parallelopiped element of Fig. 2.2b is superior because its stiffness matrix can be prepared once and for all and programmed in terms of simple and explicit expressions. Before writing the computer program, the integration involved are performed manually and, therefore, the stiffness matrix is obtained uniquely. In fact, the finite element mesh can be designed in such a way that the various solid elements can be grouped into a few elements of the same size. It is only necessary to construct the stiffness matrix of each group once. Later, as the material properties of these elements change, their stiffness matrices need not be constructed again but merely updated. Likewise, explicit expressions for strains and stresses within the element are obtained once and then used repeatedly during the entire process of the non-linear analysis. Thus a considerable reduction in computer time can be achieved by

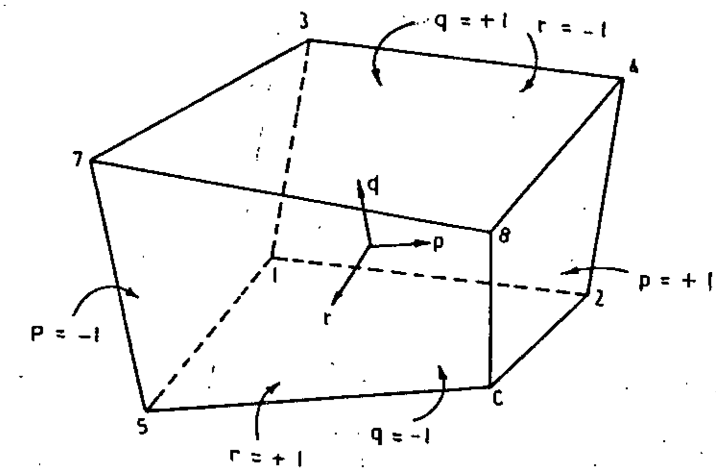

(a) Linear isoparametric hexahedral element.

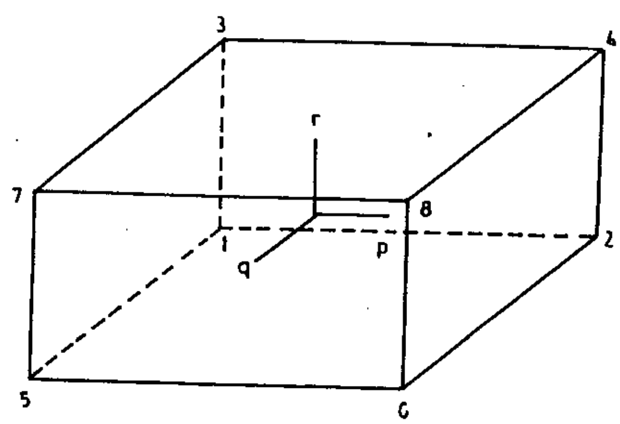

(b) Isoparametric rectangular parallelopiped element.

FIGURE 2.2 EIGHT NODED LINEAR HEXAHEDRAL ELEMENTS.

using the rectangular parallelopiped solid element to represent the soil under a structure. An important feature of this element is that its local axes can easily be made to coincide with the global axes, and, therefore, no co-ordinate transformation is required. While the displacement functions of the parallelopiped element are given in the texts, e.g. Coates et. al. (1972), the stiffness matrix of this element was derived explicitly by Rahman (1978) and utilized in a finite element analysis of structure-soil interaction.

2.3.2 The Incremental Method

The rectangular parallelopiped element is used extensively in this thesis to represent the soil under a structure and an incremental method of analysis is adopted for analysing the non-linear behaviour of soil. The non-linear three dimensional soil properties are expressed in terms of curves of octahedral shear stress and octahedral shear strain. Solid elements representing the soil under a structure have different values of initial octahedral normal stress. This influences their stress-strain behaviour under subsequent loading. Let the τ_{oct} - γ_{oct} curve shown in Fig. 2.3b represent the stress-strain properties of a particular solid element.

In the incremental method of analysis, the total load on the structure is divided into a number of small increments.

The system of load-displacement relationship, $\{\underline{L}\}$ = $[\underline{K}(L, x)]$ $\{\underline{x}\}$ (Rahman, 1978) is solved repeatedly with each of these incremental loads. The stiffness matrix is obtained each time by substituting the values of the shear modulus, G, that corresponds to the current level of the octahedral shear strain in each element.

Initially at any depth h, σ_{octi} is taken approximately as γh. With σ_{octi} known, initial tangent shear modulus, G_o for each element is calculated from a spline function representation of the τ_{oct} - γ_{oct} curve in Fig. 2.3b. This is used to construct the initial stiffness matrix, $\underline{K}_o$, Fig. 2.3a. A small increment of load ΔL_1 is supplied and the resulting displacements Δx_1 are obtained by solving the equation:

$$\{\Delta\underline{L}\}_1 = \underline{K}_o \{\Delta\underline{X}\}_1 \qquad 2.1$$

The increment of strain due to this increment of load are calculated from:

$$\{\Delta\underline{\varepsilon}\}_1 = \underline{B} \{\Delta\underline{X}\}_1 \qquad 2.2$$

The incremental stresses are calculated from the incremental strains as:

$$\{\Delta\underline{\sigma}\}_1 = \underline{D}_o \{\Delta\underline{\varepsilon}\}_1 \qquad 2.3$$

The elastic properties matrix $\underline{D}_o$ is obtained by using the initial shear moduli, G_o, of each element. For the solid element whose τ_{oct} - γ_{oct} curve is represented by Fig.2.3b, the increments of the octahedral shear stress and the octahedral shear strain due to the load ΔL_1 is $\delta\tau_{oct1}$ and $\delta\gamma_{oct1}$ respectively. These represent the point A' on the figure. The point on the load-deflection diagram of Fig.2.3a obtained after application of the first incremental load, ΔL_1, is a'. Point A corresponds to the strain $\delta\gamma_{oct1}$ on the actual τ_{oct} - γ_{oct} curve in Fig. 2.3b. The amount AA' is thus the error in the theoretical τ_{oct} of this element. The corresponding error in the load-deflection diagram is the amount aa' in Fig. 2.3a.

The tangent slope of the τ_{oct} - γ_{oct} curve at point A is evaluated by the spline functions. The value G_1, thus obtained, gives the tangent shear modulus of the element at the current level of γ_{oct}. These new values of the shear modulus for each element are substituted in to the stiffness matrix to obtain a new matrix. A further increment of load ΔL_2 is now applied and the structure and soil are reanalysed with this new stiffness matrix. Such analysis gives a new set of displacements Δx_2 for the increment of load ΔL_2 alone. With this increment, the increments of the strains and stresses are obtained. The corresponding increments in τ_{oct} and γ_{oct} in the single element are $\delta\tau_{oct2}$ and $\delta\gamma_{oct2}$ respectively. The total octahedral shear strain is obtained as the sum of $\delta\gamma_{oct1}$ and $\delta\gamma_{oct2}$ and the tangent shear modulus

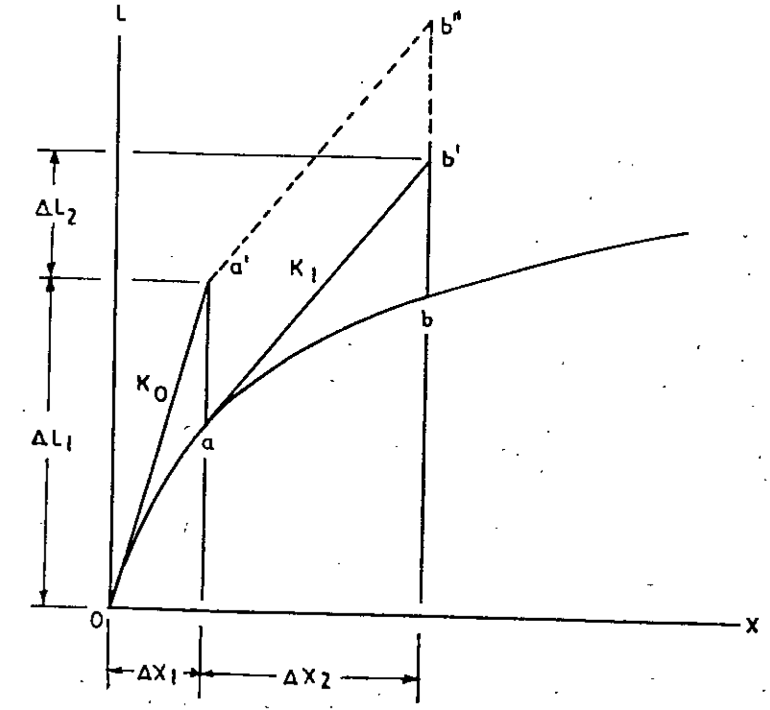

(a) Load - deflection diagram

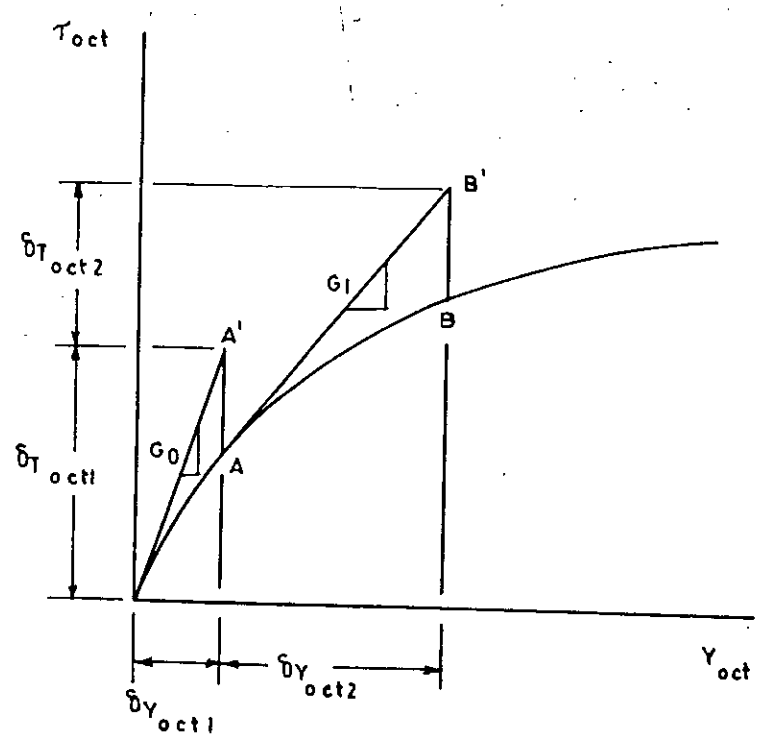

(b) Stress - strain diagram of an element.

FIGURE 2.3 INCREMENTAL ANALYSIS SCHEME.

at point B on the τ_{oct} - γ_{oct} curve corresponding to the current total γ_{oct} is obtained. This defines the stiffness matrix for the next increment of the load. The procedure is repeated for successive increments of load until all the loads have been applied.

In general, the incremental analysis number j is performed with the incremental load $\{\Delta \underline{L}\}_j$ and with the tangent stiffness matrix $[\underline{K}]_{j-1}$ corresponding to the shear moduli values at the end of the last increment. The displacements, the strains and stresses are successively accumulated to give the current state of these values.

2.4 TENSION SEPARATION AND PROPAGATION OF CRACK

In a complete system of structure, its foundation and the supporting soil, non-linearity due to cracks and/or separation is possible. Separation may occur in any zone where the tensile stresses exceed the tensile strength of the material. This may be either within the soil mass or at the interface between the soil and the foundation.

As the soil is weak in tension, stress redistribution occurs due to unsightly separations in the soil mass. However, such a separation within the mass of cohesionless soils, is expected to be filled up by the neighbouring body of soil. This causes a complete redistribution of stresses as well as the actual material.

In some circumstances, the changed geometry of the system, due to cracks, may on subsequent loading, result in relaxation of the stresses in the cracked zone. This may cause the crack to close again. On the other hand, new cracks may develop elsewhere in the system. Some of these may widen, bifurcate, extend in length or change direction. All these indicate a continuous change within the system until either equilibrium has been restored or failure is reached.

Appreciation of tensile weakness in the foundation materials has been shown by many research workers in the past. More recently finite element technique has been applied to take account of cracking in the physical systems. Majid and Al-Hashimi (1976) pointed out that a crack does not change the material properties. It only introduces a physical separation of the two parts of the material on either side. Majid and Al-Hashimi's method was used for two dimensional problems. The separation was carried out by first introducing initially inactive joints to be associated with every active joint. These were then activated each time a crack occured by separating the elements on one side of the crack from the parent joint and rejoining them to the new joint. An incremental technique was used to follow the crack propagation upto and including failure.

Based on the above approach, Rahman (1978) developed a tension separation scheme applicable to non-linear three dimensional interaction problems. This generalization offers the possibility of initiation, extension, bifurcation, widening and closure of any pattern of cracks in the finite element mesh and is easily programmable for an automatic crack propagation analysis. Rahman's generalized scheme, a brief description of which is outlined below, has been utilized in the present analysis.

2.4.1 Method of Introducing a Separation

The essence of the method is to assign two numbers to each joint in the finite element mesh that is likely to suffer a tension separation. The joints are disconnected when such a separation is indicated. This takes place either within the soil mass or between a wall or a slab and the adjacent soil. The disconnection physically introduces a gap between adjacent elements meeting at that joint.

In Fig. 2.4a, I is a general joint in a three dimensional finite element mesh, which is considered to be likely to suffer a tensile stress. Joint N has initially no degree of freedom and is simply a dummy joint associated with the active joint I. Joint N will not take part in the finite element analysis as long as the tensile stress in a direction normal to the plane ABCD does not exceed the tensile strength of the material. As soon asthe stress exceeds this limiting value, a separation at I in a direction normal to the plane ABCD is introduced as illustrated

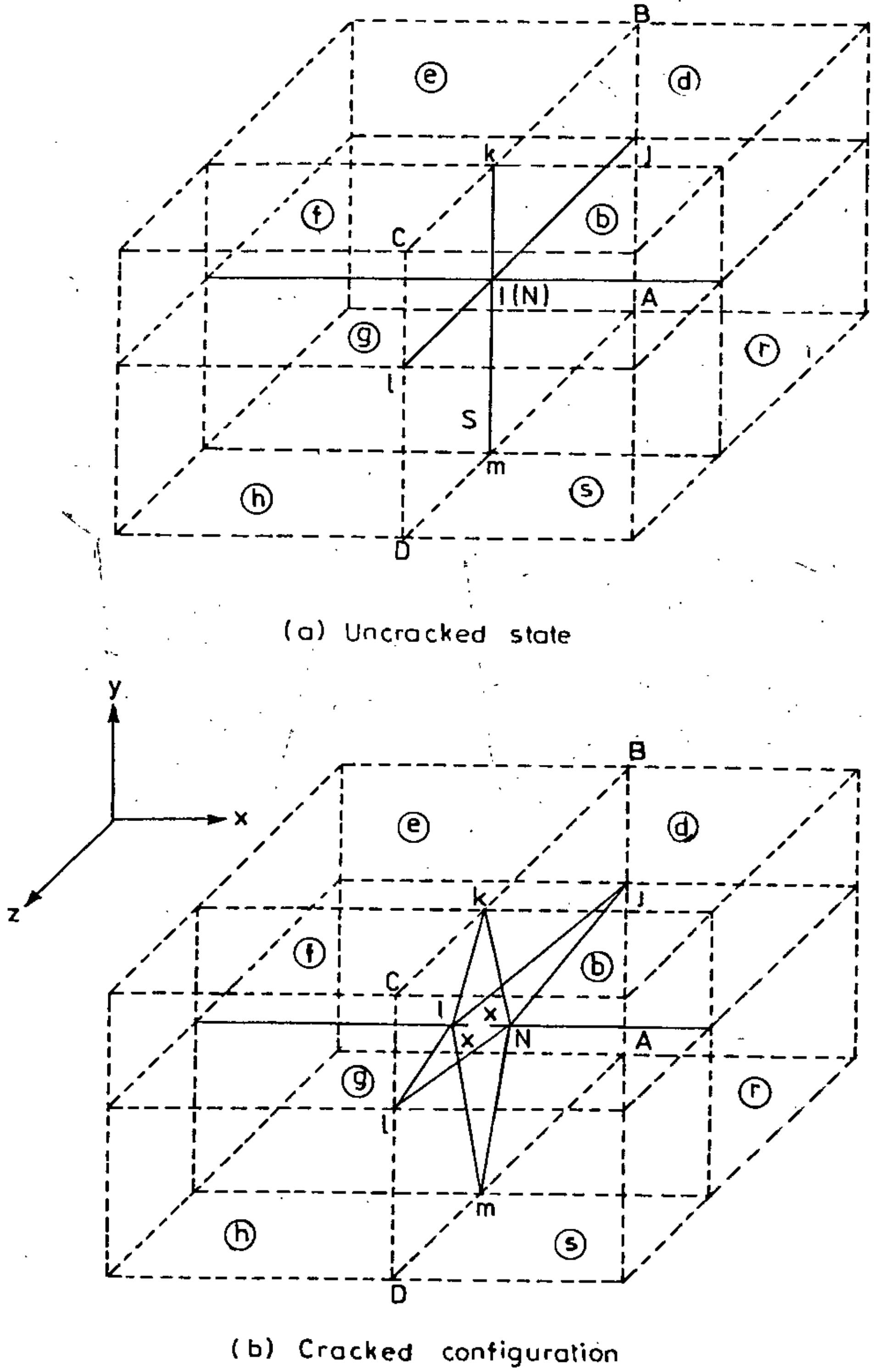

FIGURE 2.4 A GENERAL TENSION SEPARATION.

in Fig. 2.4b. During subsequent loading of the system, joint N is brought into action in the finite element analysis. This is done by introducing new rows and new columns in the stiffness matrix to correspond to the degree of freedom of joint N.

2.4.2 Types of Crack

In the previous section the method of tension separation was described for a general joint which was surrounded on all sides by eight rectangular parallelopiped solid elements. The same technique can be extended to joints at the interface between a plate or a member and solid element.

To tackle all the different cases of separation, they are classified into five different groups. Each joint that is likely to suffer a separation is given an index number indicating the type of separation expected. The various types of cracks are shown in Fig. 2.5 and described below.

Crack Type 1: These joints are connected to plates and/or space members with rectangular parallelopiped solid elements on both sides of the plate or member, as shown in Fig. 2.5a. They are allowed to separate in the vertical direction only. The resulting cavity is thus horizontal. The two configurations are determined by testing the sense of the vertical displacement of the joint when a type 1 crack is indicated there.

Crack Type 2 (Fig. 2.5b): This case is similar to Type 1 except that the solid elements are present on one side of a plate or member. The separation takes place in a vertical direction by disconnecting the solid element from the parent joint I and attaching them to the dummy joint N.

Crack Type 3 (Fig. 2.5c): This case is similar to Type 2 except the plates and the members are vertical and separation takes place in the horizontal direction.

Crack Type 4 (Fig. 2.5d): In this case the joint is surrounded by solid elements only. The separation is free to occur in any direction, depending on the relative magnitudes of the normal tensile stresses.

Crack Type 5 (Fig. 2.5e): This is for a joint on the boundary of the soil in contact with rigid plane such as rock and also for a joint on the plane of symmetry, on one side of which only the body is analysed. No dummy joint is needed to tackle such a crack. These joints would normally have freedom of in-plane movements only, the out of plane degree of freedom being restrained. When a tensile separation, out of plane, takes place, the restriction on the out of plane degree of freedom is lifted. The separation can take place in two directions at the intersection of two boundary planes and in all directions at a corner.

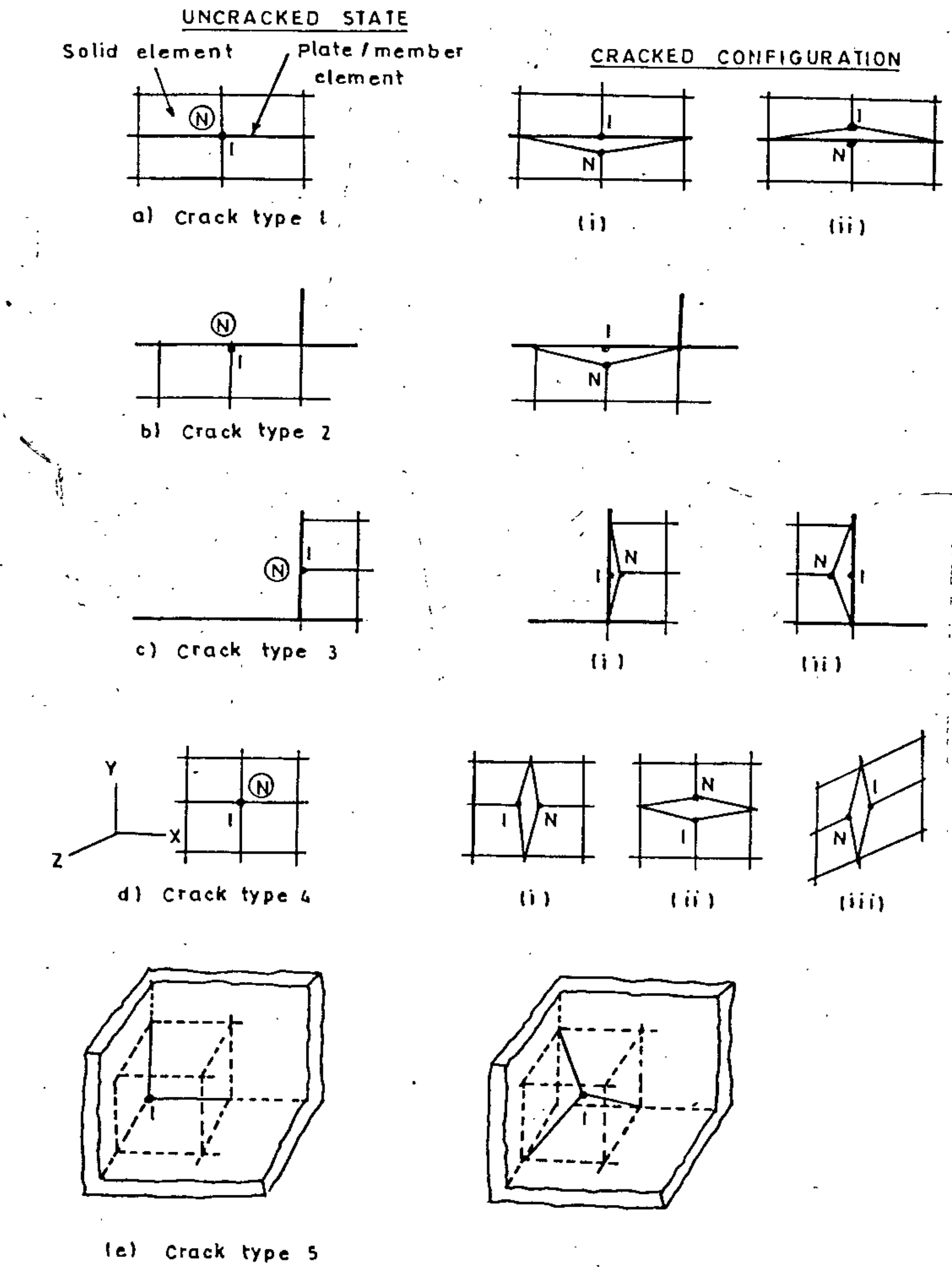

I = Parent joint, N = Dummy joint

FIGURE 2.5 TYPES OF CRACKS.

2.4.3 Procedure for Crack Propagation Analysis

For the determination, initiation, propagation and closure of cracks satisfactorily, an initial knowledge of zones where cracks may develop is necessary. The problem may first be analysed without any crack and the directions and positions of the tensile stresses are determined. The finite element mesh may then be redesigned if necessary. The joints and mesh are renumbered and is then analysed by the non-linear incremental procedure with facilities of crack propagation.

Initially the mesh is uncracked and the analysis starts in the normal way. Once a crack is detected at a point, the elements on either side of the crack are separated by activating the dummy joint. At this stage the crack width is zero and both the parent and the dummy joints have the same values of co-ordinates and displacements. Further loading will cause these joints to displace relative to each other. The crack width is given by the relative displacement of the joints. If the joints displace towards each other and overlap, the crack is closed. This is done by simply rejoining the elements to their parent joint. As the loading progresses new cracks develop elsewhere in the mesh in both the horizontal and the vertical directions. A crack may also increase in length by the separation of more joints along the crack. Thus the system becomes less and less stiff and the stresses alter continuously.

2.5 ORTHOTROPIC INFILLS OF FRAMES

Nonisotropic or anisotropic materials display direction-dependent properties. Simplest among them are those in which the material properties differ in two mutually perpendicular directions. A material so described is orthotropic. A number of manufactured materials are approximated as orthotropic. Examples include corrugated and rolled metal sheet, fillers in sandwich plate construction, plywood, fibre reinforced composites, reinforced concrete, and grid work. Brickwork is known to be an anisotropic material, the treatment of which requires, in general, twenty one independent elastic constants. However, if brick walls are to be treated as a two dimensional problem, the central plane of the wall must be a plane of symmetry of the material structure. If, in addition, the planes parallel and perpendicular to the bed joint are assumed to be planes of material symmetry, brickwork in walls may be reduced to an orthotropic material with the orthogonal planes of material symmetry coinciding with the sides of a brick. Thus the total number of independent elastic parameters may be reduced to four.

From the discussion on analysis of infill frames presented in Chapter 1, the wide use of brick walls as infill of building frames is quite evident. Hence the brick infill walls or the other materials discussed above when used as infill of frames need to be treated as orthotropic material for a more rigorous analysis. The finite element formulation of the orthotropic infill walls for inclusion in a general finite element treatment of the structure-foundation-soil interaction problem follows.

2.5.1 Basic Relationships and Determination of Elastic Constants

Solution of the bending problem of orthotropic plates requires formulation of Hooke's law as

$$\sigma_x = \frac{E'_x}{1-\nu_x\nu_y}(\varepsilon_x+\nu_y\varepsilon_y)$$

$$\sigma_y = \frac{E'_y}{1-\nu_x\nu_y}(\varepsilon_y+\nu_x\varepsilon_x) \qquad 2.4$$

$$\tau_{xy} = G\gamma_{xy}$$

Here ν_x, ν_y and E'_x, E'_y are the effective Poisson's ratios and effective modulii of elasticity respectively. Subscripts x and y relate to the directions. xy plane coincides with the midplane of the plate and z-axis is normal to this plane as shown in Fig. 2.6. G is the shear modulus of elasticity for the orthotropic material. σ_x, σ_y are normal stresses along x and y directions and τ_{xy} is the shearing stress. ε_x, ε_y and γ_{xy} are the corresponding linear strains and shearing strain. Introducing notations

$$E_x = \frac{E'_x}{1-\nu_x\nu_y} \qquad 2.5$$

$$E_y = \frac{E_y'}{1-\nu_x\nu_y}$$

$$E_{xy} = \frac{E_x'\nu_y}{1-\nu_x\nu_y} = \frac{E_y'\nu_x}{1-\nu_x\nu_y} \qquad 2.5$$

the Hooke's law represented by Eq. 2.4 may be expressed as

$$\sigma_x = E_x\varepsilon_x + E_{xy}\varepsilon_y$$

$$\sigma_y = E_y\varepsilon_y + E_{xy}\varepsilon_x \qquad 2.6$$

$$\tau_{xy} = G\gamma_{xy}$$

The strain-displacement relations are based upon purely geometrical considerations and remain unchanged for orthotropic plates. Hence for a plate element shown in Fig. 2.6 with displacement w in the z-direction these are

$$\varepsilon_x = -Z\frac{\partial^2 w}{\partial x^2}$$

$$\varepsilon_y = -Z\frac{\partial^2 w}{\partial y^2} \qquad 2.7$$

$$\gamma_{xy} = -2Z\frac{\partial^2 w}{\partial x\partial y}$$

The stresses are obtained by introducing Eq. 2.7 in to Eq. 2.6:

$$\sigma_x = -Z(E_x \frac{\partial^2 w}{\partial x^2} + E_{xy} \frac{\partial^2 w}{\partial y^2})$$

$$\sigma_y = -Z(E_y \frac{\partial^2 w}{\partial y^2} + E_{xy} \frac{\partial^2 w}{\partial x^2}) \qquad 2.8$$

$$\tau_{xy} = -2GZ \frac{\partial^2 w}{\partial x \partial y}$$

The stress resultants per unit length producing bending moments about both x and y axes and twisting moments are derived from

$$\begin{Bmatrix} M_x \\ M_y \\ M_{xy} \end{Bmatrix} = \int_{-t/2}^{t/2} \begin{Bmatrix} \sigma_x \\ \sigma_y \\ \tau_{xy} \end{Bmatrix} Z\, dz \qquad 2.9$$

Inserting Eq. 2.8 into Eq.2.9

$$M_x = -(D_x \frac{\partial^2 w}{\partial x^2} + D_1 \frac{\partial^2 w}{\partial y^2})$$

$$M_y = -(D_y \frac{\partial^2 w}{\partial y^2} + D_1 \frac{\partial^2 w}{\partial x^2}) \qquad 2.10$$

$$M_{xy} = -2 D_{xy} \frac{\partial^2 w}{\partial x \partial y}$$

where

$$D_x = \frac{E_x t^3}{12} = \frac{E_x' t^3}{12(1-\nu_x\nu_y)}$$

$$D_y = \frac{E_y t^3}{12} = \frac{E_y' t^3}{12(1-\nu_x\nu_y)} \qquad 2.11$$

$$D_1 = \frac{E_{xy} t^3}{12} = \frac{E_x' \nu_y t^3}{12(1-\nu_x\nu_y)}$$

$$D_{xy} = \frac{G t^3}{12}$$

The expressions for D_x, D_y, D_1 and D_{xy} represent the flexural rigidities and the torsional rigidity of an orthotropic plate respectively. Practical considerations often lead to assumptions, with regard to material properties, resulting in approximate expressions for the elastic constants. The orthotropic plate modulii and Poisson's ratios E_x', E_y', ν_x, ν_y and G may be obtained by tension and shear tests, as in the case of isotropic materials and the plate rigidities are then calculated from Eq. 2.11. However, analytical techniques may as well be employed for the approximate determination of the elastic constants.

In brickwork, the elastic moduli and Poisson's ratios parallel and perpendicular to bed joint can be determined experimentally by loading samples of brickwork along these two directions. The experimental determination of shear modulus G is, however, more involved. It can therefore be derived analytically by considering the deformation of an element subjected to pure shear as shown in Fig. 2.7. It should be noted that brickwork in infill walls will be assumed to behave linear elastically in the present analysis. The element in Fig. 2.7b is cut out from that in Fig. 2.7a by planes inclined at 45^o to the x and y axes. Equilibrium requires that the only stress on the sides of Fig. 2.7b is a shear stress τ equal in magnitude to the normal stress σ in Fig. 2.7a.

From the geometry of triangle obc and its deformed shape ob'c' in Fig. 2.7c:

$$\frac{oc'}{ob'} = \tan\left(\frac{\pi}{4} - \frac{\gamma}{2}\right) = \frac{oc + oc\varepsilon_x}{ob + ob\varepsilon_y} \qquad 2.12$$

where γ is the shear strain and ε_x and ε_y are normal strains. Since γ is small and oc = ob,

$$\tan\left(\frac{\pi}{4} - \frac{\gamma}{2}\right) = \frac{\tan\frac{\pi}{4} - \tan\frac{\gamma}{2}}{1+\tan\frac{\pi}{4}\tan\frac{\gamma}{2}} = \frac{1 - \frac{\gamma}{2}}{1 + \frac{\gamma}{2}} = \frac{1 + \varepsilon_x}{1 + \varepsilon_y} \qquad 2.13$$

From the generalized Hooke's law given by Eq. 2.4 and also using Eq. 2.5 the following relations are obtained.

$$\varepsilon_x = -\frac{\sigma}{E'_x} - \frac{\nu_y\sigma}{E'_y} = -\sigma\left(\frac{1}{E'_x} + \frac{\nu_y}{E'_y}\right) \qquad 2.14$$

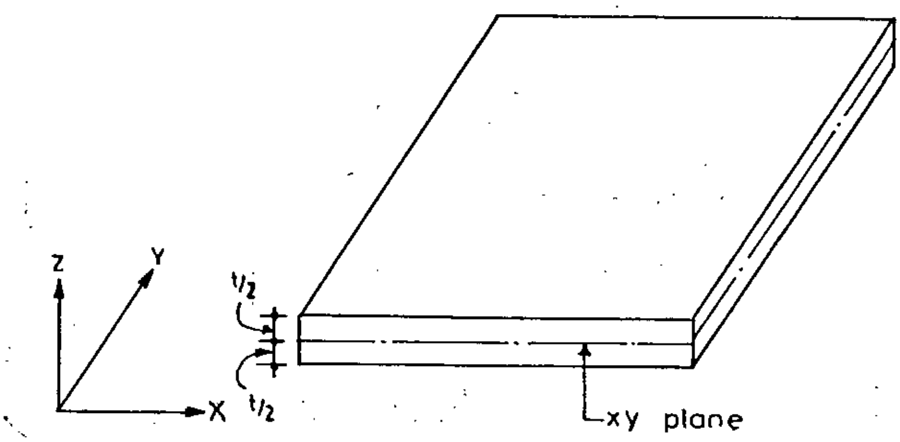

FIGURE 2.6 A RECTANGULAR PLATE.

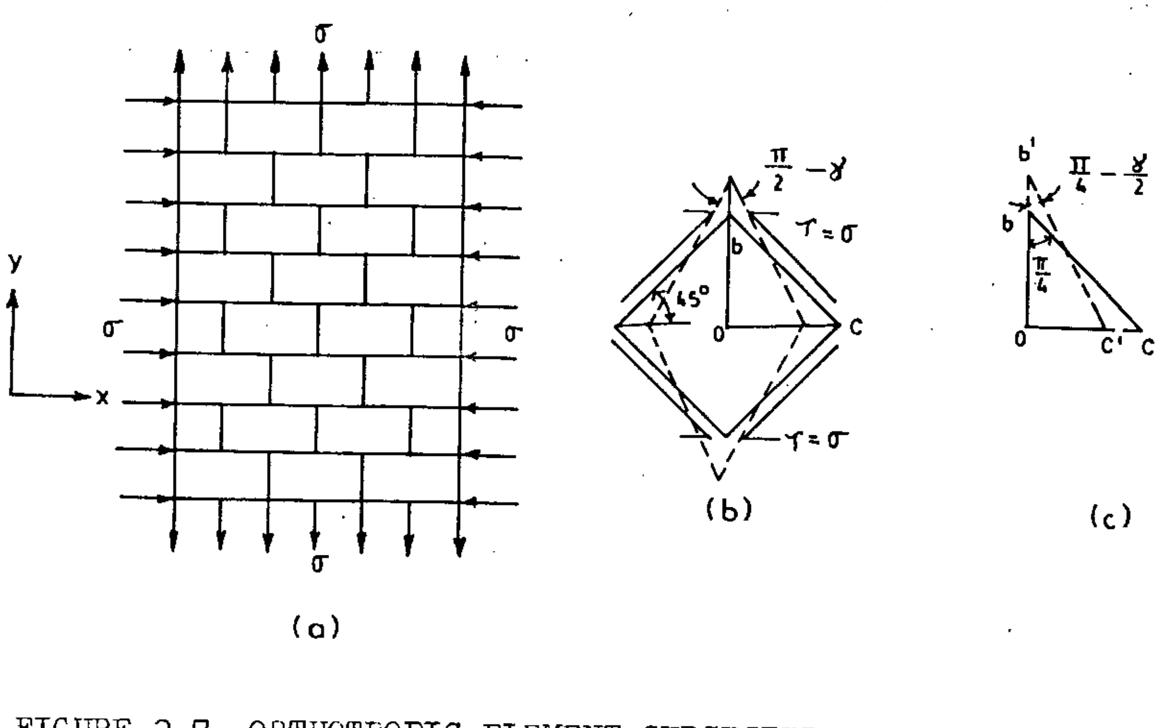

FIGURE 2.7 ORTHOTROPIC ELEMENT SUBJECTED TO PURE SHEAR.

$$\varepsilon_y = \frac{\sigma}{E'_y} + \frac{\nu_x \sigma}{E'_x} = \sigma\left(\frac{1}{E'_y} + \frac{\nu_x}{E'_x}\right) \qquad 2.15$$

In the above, $\sigma_x = -\sigma$ and $\sigma_y = \sigma$ have been substituted in conformity with Fig. 2.7a. Now the strain energies in the two statically equivalent elements of Fig. 2.7a and Fig. 2.7b should be equal. Strain energy per unit volume in Fig. 2.7a is

$$U_1 = \frac{1}{2}\sigma_x\varepsilon_x + \frac{1}{2}\sigma_y\varepsilon_y \qquad 2.16$$

Employing Eq. 2.14 and Eq. 2.15

$$U_1 = \frac{1}{2}\sigma^2\left(\frac{1}{E'_x} + \frac{\nu_y}{E'_y}\right) + \frac{1}{2}\sigma^2\left(\frac{1}{E'_y} + \frac{\nu_x}{E'_x}\right)$$

$$= \frac{1}{2}\sigma^2\,\frac{E'_x(1+\nu_y) + E'_y(1+\nu_x)}{E'_x E'_y} \qquad 2.17$$

strain energy per unit volume in Fig. 2.7b is:

$$U_2 = \frac{1}{2}\tau\gamma = \frac{1}{2}\sigma\frac{\sigma}{G} = \frac{1}{2}\frac{\sigma^2}{G} \qquad 2.18$$

Equating U_1 and U_2 from Eq. 2.17 and Eq. 2.18:

$$\frac{1}{2}\frac{\sigma^2}{G} = \frac{1}{2}\sigma^2\,\frac{E'_x(1+\nu_y)+E'_y(1+\nu_x)}{E'_x E'_y} \qquad 2.19$$

Therefore,

$$G = \frac{E'_x\, E'_y}{E'_x(1+\nu_y)+E'_y(1+\nu_x)} \qquad 2.20$$

2.5.2 Finite Element Formulation: Stiffness Matrix for Orthotropic Wall Element

If three dimensional structures under arbitrary load conditions are to be analyzed using orthotropic wall elements both inplane and bending load carrying capacity for the elements should be provided. In the analysis of three dimensional structures, therefore, the inplane and the bending stiffnesses have to be combined accordingly. The process of combination should be in accordance with the following observations:

i) For small displacements, the inplane (membrane) and bending stiffness are uncoupled. In otherwords the displacements prescribed for 'inplane' forces do not affect the bending deformations and vice-versa.

ii) The inplane rotation θ_z (rotation about the local z-axis) is not necessary for a single element. However, θ_z and its conjugate force M_z have to be considered in the analysis by including appropriate number of zeroes to obtain the element stiffness matrix for the purpose of assembling several elements.

Before the stiffness combination procedure is presented, the independent element stiffness matrices for a plane stress and a plate bending element of orthotropic material will be derived in explicit forms. In problems of plane stress the displacement field is uniquely given by the u and v displacements in directions of the cartesian, orthogonal x and y axes. The only strains and stresses those have to be considered are the three components in the x-y plane. All other components of stress are zero by definition and therefore give no contribution to internal work.

Fig. 2.8 shows the typical rectangular plane stress element considered, with nodes 1,2,3 and 4 numbered as per given scheme. The origin of the local co-ordinates is chosen at node 1, while their directions are parallel to the element boundaries. The dimensions of the element are a and b along x and y directions respectively. Each node of the element is given two translational degrees of freedom u,v in x and y directions respectively. The displacement functions of the element are well documented and can be expressed as

$$u = \alpha_1 + \alpha_2 x + \alpha_3 y + \alpha_4 xy \qquad 2.21a$$

$$v = \alpha_5 + \alpha_6 x + \alpha_7 y + \alpha_8 xy \qquad 2.21b$$

The above functions automatically guarantee continuity of displacements with adjacent elements because displacements vary linearly along any side of the rectangle and, with identical displacement imposed at the nodes, the same displacement will clearly exist all along an interface.

The values of the constants α_1, α_2, α_3 .... α_8 in Eq. 2.21 can be expressed in terms of the nodal displacements

u_1, v_1, u_2, v_2 .... u_4, v_4. This is achieved by substituting the values of the co-ordinates of each node in turn in Eq.2.21 and solving for α_1, α_2 .... α_8. Thus, at node 1, $x = y = 0$ and $u = u_1$. Substituting these values in Eq. 2.21a

$$\alpha_1 = u_1 \qquad 2.22a$$

Similarly, at node 2, $x = a$, $y = 0$ and $u = u_2$, and therefore

$$u_2 = \alpha_1 + \alpha_2 a = u_1 + \alpha_2 a$$

and

$$\alpha_2 = \frac{1}{a}(u_2 - u_1) \qquad 2.22b$$

Proceeding in the same manner and substituting the co-ordinates of nodes 3,4 in turn in Eq. 2.21a, the following values of α are obtained

$$\alpha_3 = \frac{1}{b}(u_3 - u_1) \qquad 2.22c$$

$$\alpha_4 = \frac{1}{ab}(u_1 - u_2 - u_3 + u_4) \qquad 2.22d$$

Similar expressions for α_5,.... α_8 can be obtained by substituting the nodal co-ordinates in Eq. 2.21b. The solutions of α_5, ... α_8 are given by replacing u_1, u_2 etc. by v_1, v_2 etc. in Eq. 2.22a, Eq. 2.22b, Eq. 2.22c, Eq. 2.22d respectively. Thus the following relationship is obtained

$$\{\underline{\alpha}\}_{ps} = \underline{C}^{-1}_{ps} \; \{\underline{X}\}_{ps} \qquad 2.23$$

where, $\{\underline{\alpha}\}_{ps} = \{\alpha_1 \alpha_2 \alpha_3 \alpha_4 \alpha_5 \alpha_6 \alpha_7 \alpha_8\}$

$$\{\underline{X}\}_{ps} = \{u_1\ v_1\ u_2\ v_2\ u_3\ v_3\ u_4\ v_4\}$$

and $\underline{C}_{ps}^{-1}$ is an 8x8 matrix containing constant terms of the element dimensions a and b only.

The strain vector $\{\underline{\varepsilon}\}_{ps}$ is obtained by utilizing the strain-displacement relationships. By performing the appropriate partial differentiations of the displacement of Eq. 2.21, the following relationship is obtained.

$$\{\underline{\varepsilon}\}_{ps} = \begin{bmatrix} \varepsilon_x \\ \varepsilon_y \\ \gamma_{xy} \end{bmatrix}_{ps} = \begin{bmatrix} \frac{\partial u}{\partial x} \\ \frac{\partial v}{\partial y} \\ \frac{\partial u}{\partial y} + \frac{\partial v}{\partial x} \end{bmatrix}_{ps} = \underline{A}_{ps}\ \{\underline{\alpha}\}_{ps} \qquad 2.24$$

where $\underline{A}_{ps}$ is a 3x8 matrix containing terms of x and y only. Substituting for $\{\underline{\alpha}\}_{ps}$ from Eq. 2.23 into Eq. 2.24,

$$\{\underline{\varepsilon}\}_{ps} = \underline{A}_{ps}\ \underline{C}_{ps}^{-1}\ \{\underline{X}\}_{ps} = \underline{B}_{ps}\ \{\underline{X}\}_{ps} \qquad 2.25$$

the 3x8 matrix $\underline{B}_{ps}$ is obtained by performing the matrix multiplication $\underline{A}_{ps}\ \underline{C}_{ps}^{-1}$. The elements of this matrix are given below explicitly:

$$b_{1,1} = -\ b_{1,3} = b_{3,2} = -b_{3,4} = \frac{Y}{ab} - \frac{1}{a}$$

$$b_{1,5} = -\ b_{1,7} = b_{3,6} = -\ b_{3,8} = -\frac{Y}{ab}$$

$$b_{2,2} = -b_{2,6} = b_{3,1} = -b_{3,5} = \frac{x}{ab} - \frac{1}{b}$$

$$b_{2,4} = -b_{2,8} = b_{3,3} = -b_{3,7} = -\frac{x}{ab}$$

All the other elements of $\underline{B}_{ps}$ are zero.

The stress-strain relationship is given by:

$$\{\underline{\sigma}\}_{ps} = \underline{D}_{ps} \{\underline{\varepsilon}\}_{ps} \qquad 2.26$$

The elastic properties matrix $\underline{D}_{ps}$, in plane stress analysis for orthotropic material, is given by

$$\underline{D}_{ps} = \begin{bmatrix} E_x & E_{xy} & 0 \\ E_{xy} & E_y & 0 \\ 0 & 0 & G \end{bmatrix} \qquad 2.27$$

E_x, E_y and E_{xy} are given by expressions 2.5 and shear modulus G for brickwork may be calculated from Eq. 2.20.

Finally, the stiffness matrix of the plane stress element of orthotropic material is obtained from

$$\underline{K}_{ps} = t \int_0^b \int_0^a \underline{B}_{ps}^T \underline{D}_{ps} \underline{B}_{ps} \, dxdy \qquad 2.28$$

where t is the constant thickness of the element. Performing the matrix multiplication in Eq. 2.28 and carrying out the integration as indicated for each term of the product, the stiffness matrix is explicitly obtained. The stiffness matrix expressions are given below:

$$\underline{K}_{ps} = \begin{bmatrix} \underline{K}_{11}^{ps} & & \text{sym} & \\ \underline{K}_{21}^{ps} & \underline{K}_{22}^{ps} & & \\ \underline{K}_{31}^{ps} & \underline{K}_{32}^{ps} & \underline{K}_{33}^{ps} & \\ \underline{K}_{41}^{ps} & \underline{K}_{42}^{ps} & \underline{K}_{43}^{ps} & \underline{K}_{44}^{ps} \end{bmatrix} \qquad 2.29$$

In which each $\underline{K}_{ij}^{ps}$ is a 2x2 submatrix. The submatrices are written explicitly below:

$$\underline{K}_{11}^{ps} = \underline{K}_{44}^{ps} = \begin{bmatrix} N1+N2 & N3 \\ N3 & N4+N5 \end{bmatrix}$$

$$\underline{K}_{22}^{ps} = \underline{K}_{33}^{ps} = \begin{bmatrix} N1+N2 & -N3 \\ -N3 & N4+N5 \end{bmatrix}$$

$$\underline{K}_{21}^{ps} = \underline{K}_{43}^{ps} = \begin{bmatrix} -N1+.5N2 & -N6 \\ N6 & .5N4-N5 \end{bmatrix}$$

$$\underline{K}_{31}^{ps} = \underline{K}_{42}^{ps} = \begin{bmatrix} .5N1-N2 & N6 \\ -N6 & -N4+.5N5 \end{bmatrix}$$

$$\underline{K}_{32}^{ps} = \begin{bmatrix} -.5N1-.5N2 & N3 \\ N3 & -.5N4-.5N5 \end{bmatrix}$$

$$\underline{K}_{41}^{ps} = \begin{bmatrix} -.5N1-.5N2 & -N3 \\ -N3 & -.5N4-.5N5 \end{bmatrix}$$

where, $N1 = \frac{E_x tb}{3a}$; $N2 = \frac{Gta}{3b}$; $N3 = \frac{t}{4}(E_{xy}+G)$; $N4 = \frac{E_y ta}{3b}$;

$N5 = \frac{Gtb}{3a}$ and $N6 = \frac{t}{4}(E_{xy} - G)$

The stiffness matrix $\underline{K}_{ps}$ is symmetrical. This implies that the submatrices have the relationship

$$\underline{K}^{ps}_{ij} = \underline{K}^{ps^T}_{ji} \quad \text{for } i = 1,2,3,4 \text{ and } j = 1,2,3,4.$$

The stiffness matrix given above is derived with respect to the local co-ordinates shown in Fig. 2.8. A transformation to global axes is therefore necessary and this will be carried out after combining it with the stiffness matrix for the plate bending element which is derived next.

The rectangular element of a plate, the x-y plane coinciding with its midplane, as shown in Fig. 2.9 is considered. The origin of the local co-ordinates is chosen at node 1, while directions of x and y axes are parallel to element boundaries and z is normal to the mid plane. The dimensions of the element remain the same as those of the plane stress element. At each node displacements $\{\underline{X}_n\}_{pb}$ are introduced. These have three components: the first a displacement in the z-direction, w_n, the second a rotation about the x-axis, θ_{xn}, and the third a rotation about the y-axis, θ_{yn}.

The element displacement now is given by the listing of the nodal displacements as

$$\{X\}_{pb} = \{\underline{X}_1 \quad \underline{X}_2 \quad \underline{X}_3 \quad \underline{X}_4\}_{pb} \tag{2.30}$$

where, $\{\underline{X}_n\}_{pb} = \{w_n \quad _{xn} \quad \theta_{yn}\} = \{w_n \ (\frac{\partial w}{\partial y})_n \ (\frac{\partial w}{\partial x})_n\}$

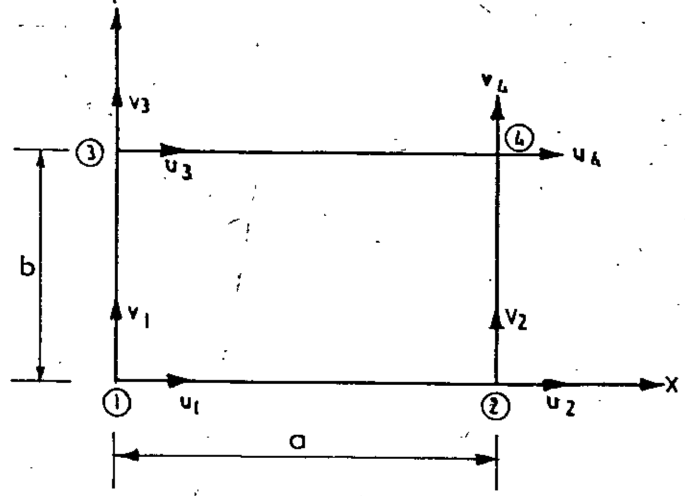

FIGURE 2.8 NOTATIONS FOR THE PLANE STRESS ELEMENT.

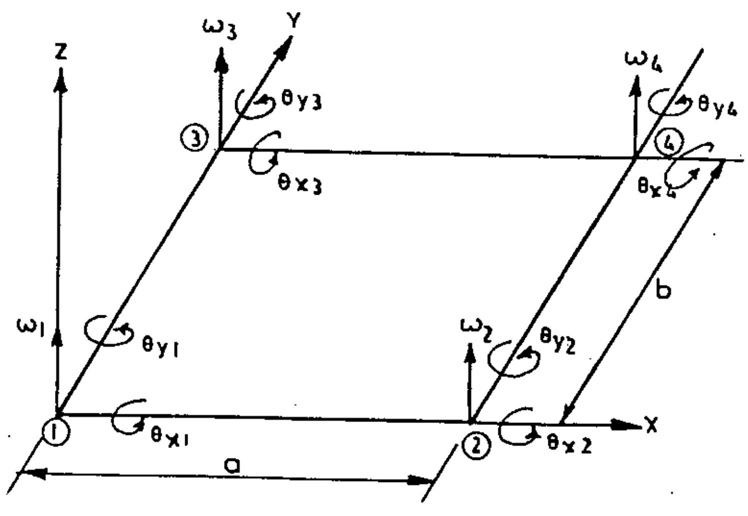

FIGURE 2.9 RECTANGULAR PLATE BENDING ELEMENT.

The following polynomial expression may conveniently be used to define the shape functions in terms of the twelve parameters:

$$W = \alpha_1 + \alpha_2 x + \alpha_3 y + \alpha_4 x^2 + \alpha_5 xy + \alpha_6 y^2 + \alpha_7 x^3 + \alpha_8 x^2 y + \alpha_9 xy^2 + \alpha_{10} y^3 + \alpha_{11} x^3 y + \alpha_{12} xy^3 \qquad 2.31$$

Continuity of w between elements is imposed all along any interface. However, a discontinuity of normal slope will occur at the element boundaries except at the nodes making the function 'non-conforming'. Convergence may still be found, Zienkiewicz (1977), and for practical usage, the use of above non-conforming shape function is quite acceptable.

The constants α_1 to α_{12} can be expressed in terms of the nodal displacements w_1, θ_{x1}, θ_{y1}, ... w_4, θ_{x4}, θ_{y4}. This is achieved by writing down the twelve simultaneous equations linking the values of w and its slopes at the nodes when the co-ordinates take up their appropriate values and then solving for α_1 to α_{12}. Listing all twelve equations in matrix form

$$\{\underline{X}\}_{pb} = \underline{C}_{pb} \quad \{\underline{\alpha}\}_{pb} \qquad 2.32$$

where

$$\{\underline{\alpha}\}_{pb} = \{\alpha_1 \ \alpha_2 \ . \ . \ . \ . \ . \ \alpha_{12}\}$$

$\underline{C}_{pb}$ is a 12x12 matrix containing constant terms of the element dimensions a and b only. Inverting

$$\{\underline{\alpha}\}_{pb} = \underline{C}_{pb}^{-1} \{\underline{X}\}_{pb} \tag{2.33}$$

Refering to Eq. 2.7, a generalized strain-displacement relationship for the finite element analysis can be written as

$$\{\underline{\varepsilon}\}_{pb} = \begin{bmatrix} \varepsilon_x \\ \varepsilon_y \\ \gamma_{xy} \end{bmatrix} = \begin{bmatrix} -\dfrac{\partial^2 w}{\partial x^2} \\ -\dfrac{\partial^2 w}{\partial y^2} \\ -2\dfrac{\partial^2 w}{\partial x \partial y} \end{bmatrix} \tag{2.34}$$

By performing the appropriate partial differentiations of the displacement Eq. 2.31

$$\{\underline{\varepsilon}\}_{pb} = \underline{A}_{pb} \{\underline{\alpha}\}_{pb} \tag{2.35}$$

where $\underline{A}_{pb}$ is a 3x12 matrix containing terms of x, y and Z only. Substituting for $\{\underline{\alpha}\}_{pb}$ from Eq. 2.33 into Eq. 2.35

$$\{\underline{\varepsilon}\}_{pb} = \underline{A}_{pb} \underline{C}_{pb}^{-1} \{\underline{X}\}_{pb} = \underline{B}_{pb} \{\underline{X}\}_{pb} \tag{2.36}$$

The 3x12 matrix $\underline{B}_{pb}$ is obtained by performing the matrix multiplication $\underline{A}_{pb} \underline{C}_{pb}^{-1}$.

Remembering that stresses are in fact the usual bending and twisting moments per unit lengths in x and y directions and refering to Eq. 2.10, the stress-generalized strain relationship may be written as

$$\{\underline{\sigma}\}_{pb} = \begin{Bmatrix} M_x \\ M_y \\ M_{xy} \end{Bmatrix}_{pb} = \underline{D}_{pb} \{\underline{\varepsilon}\}_{pb} \qquad 2.37$$

The elastic properties matrix $\underline{D}_{pb}$ for an orthotropic slab with principal directions of orthotropy coinciding with x and y axes are defined by the four constants D_x, D_y, D_1 and D_{xy} given by Eq. 2.11 and is expressed as

$$\underline{D}_{pb} = \begin{bmatrix} D_x & D_1 & 0 \\ D_1 & D_y & 0 \\ 0 & 0 & D_{xy} \end{bmatrix} \qquad 2.38$$

Finally, the stiffness matrix of the element of constant thickness t is obtained from

$$\underline{K}_{pb} = t \int_0^b \int_0^a \underline{B}_{pb}^T \underline{D}_{pb} \underline{B}_{pb} \, dxdy \qquad 2.39$$

or substituting $\underline{A}_{pb} \underline{C}_{pb}^{-1}$ for $\underline{B}_{pb}$ from Eq. 2.36 in Eq. 2.39

$$\underline{K}_{pb} = \{\underline{C}_{pb}^{-1}\}^T \left(t \int_0^b \int_0^a \underline{A}_{pb}^T \underline{D}_{pb} \underline{A}_{pb} \, dxdy\right) \{\underline{C}_{pb}^{-1}\} \qquad 2.40$$

The terms not containing x and y have been removed from the operation of integrating. The term within the integration sign is multiplied out and integrated explicitly with more ease.

An explicit expression for the stiffness matrix $\underline{K}_{pb}$ has been evaluated for the case of orthotropic material and the result is presented below.

$$\underline{K}_{pb} = \frac{1}{15ab} \times \begin{bmatrix} \underline{K}^{pb}_{11} & \text{Symmetrical} & & \\ \underline{K}^{pb}_{21} & \underline{K}^{pb}_{22} & & \\ \underline{K}^{pb}_{31} & \underline{K}^{pb}_{32} & \underline{K}^{pb}_{33} & \\ \underline{K}^{pb}_{41} & \underline{K}^{pb}_{42} & \underline{K}^{pb}_{43} & \underline{K}^{pb}_{44} \end{bmatrix} \qquad 2.41$$

in which each $\underline{K}^{pb}_{ij}$ is a 3x3 submatrix. The submatrices are written explicitly below:

Introducing the notations

$$X1 = 60 \left(\frac{b^2}{a^2} D_x + \frac{a^2}{b^2} D_y\right) + 30 D_1 + 84 D_{xy}$$

$$X2 = 20 a^2 D_y + 8b^2 D_{xy}$$

$$X3 = 20 b^2 D_x + 8a^2 D_{xy}$$

$$X4 = 30 \frac{a^2}{b} D_y + 15 bD_1 + 6b D_{xy}$$

$$X5 = 30 \frac{b^2}{a} D_x + 15aD_1 + 6a D_{xy}$$

$$X6 = 15 ab D_1$$

$$X7 = -60 \frac{b^2}{a^2} D_x + 30 \frac{a^2}{b^2} D_y - 84 D_{xy} - 30D_1$$

$$X8 = -60\frac{a^2}{b^2}D_y + 30\frac{b^2}{a^2}D_x - 30\,D_1 - 84\,D_{xy}$$

$$X9 = 15\frac{a^2}{b}D_y - 6b\,D_{xy} - 15\,bD_1$$

$$X10 = 30\frac{b^2}{a}D_x + 6a\,D_{xy}$$

$$X11 = 10a^2D_y - 8b^2D_{xy}$$

$$X12 = 10b^2D_x - 2b^2D_{xy}$$

$$X13 = 30\frac{a^2}{b}D_y + 6\,b\,D_{xy}$$

$$X14 = 15\frac{b^2}{a}D_x - 6A\,D_{xy} - 15aD_1$$

$$X15 = 10a^2\,D_y - 2b^2D_{xy}$$

$$X16 = 10b^2D_x - 8a^2D_{xy}$$

$$X17 = -30\left(\frac{b^2}{a^2}D_x + \frac{a^2}{b^2}D_y\right) + 30D_1 + 84\,D_{xy}$$

$$X18 = 15\frac{a^2}{b}D_y - 6b\,D_{xy}$$

$$X19 = 15\frac{b^2}{a}D_x - 6a\,D_{xy}$$

$$X20 = 5\,a^2D_y + 2b^2D_{xy}$$

$$X21 = 5\,b^2D_x + 2a^2D_{xy}$$

the submatrices are

$$\underset{\sim}{K}^{pb}_{11} = \begin{bmatrix} X1 & sym & \\ X4 & X2 & \\ -X5 & -X6 & X3 \end{bmatrix} \quad \underset{\sim}{K}^{pb}_{22} = \begin{bmatrix} X1 & sym & \\ X4 & X2 & \\ X5 & X6 & X3 \end{bmatrix}$$

$$\underline{K}^{pb}_{33} = \begin{bmatrix} X1 & Sym & \\ -X4 & X2 & \\ -X5 & X6 & X3 \end{bmatrix} \qquad \underline{K}^{pb}_{44} = \begin{bmatrix} X1 & Sym & \\ -X4 & X2 & \\ X5 & -X6 & X3 \end{bmatrix}$$

$$\underline{K}^{pb}_{21} = \begin{bmatrix} X7 & X9 & -X10 \\ X9 & X11 & 0 \\ X10 & 0 & X12 \end{bmatrix} \qquad \underline{K}^{pb}_{43} = \begin{bmatrix} X7 & -X9 & -X10 \\ -X9 & X11 & 0 \\ X10 & 0 & X12 \end{bmatrix}$$

$$\underline{K}^{pb}_{31} = \begin{bmatrix} X8 & X13 & -X14 \\ -X13 & X15 & 0 \\ -X14 & 0 & X16 \end{bmatrix} \qquad \underline{K}^{pb}_{42} = \begin{bmatrix} X8 & X13 & X14 \\ -X13 & X15 & 0 \\ X14 & 0 & X16 \end{bmatrix}$$

$$\underline{K}^{pb}_{32} = \begin{bmatrix} X17 & X18 & X12 \\ -X18 & X20 & 0 \\ -X19 & 0 & X21 \end{bmatrix} \qquad \underline{K}^{pb}_{41} = \begin{bmatrix} X17 & X18 & -X12 \\ -X18 & X20 & 0 \\ X19 & 0 & X21 \end{bmatrix}$$

The stiffness matrix $\underline{K}_{pb}$ is symmetrical. This implies again that the submatrices have the relationship

$$\underline{K}^{pb}_{ij} = \underline{K}^{pb\,T}_{ji} \text{ for } i = 1,2,3,4 \text{ and } j = 1,2,3,4$$

The stiffness matrix $\underline{K}_{pb}$ is derived with respect to the local co-ordinates.

It has already been mentioned that for analysis of three dimensional structures under arbitrary load conditions using plate elements, both inplane and bending load carrying capacity for the elements be provided. Now a typical orthotropic wall element subjected simultaneously to 'in plane' and bending actions (Fig. 2.10) is considered.

Considering first the inplane action, the relationship between the nodal displacements and nodal forces can be written as

$$\begin{bmatrix} P_{x1} \\ P_{y1} \\ P_{x2} \\ P_{y2} \\ P_{x3} \\ P_{y3} \\ P_{x4} \\ P_{y4} \end{bmatrix} = \underline{K}_{ps} \begin{bmatrix} u_1 \\ v_1 \\ u_2 \\ v_2 \\ u_3 \\ v_3 \\ u_4 \\ v_4 \end{bmatrix} \qquad 2.42$$

P_{xi} and P_{yi} indicate the components of force at node i ($i = 1,2,3,4$) parallel to the x and y axes respectively. $\underline{K}_{ps}$ has been defined in Eq. 2.29.

Similarly, the relation between the forces and displacements corresponding to the bending of the plate can be written as

$$\begin{bmatrix} P_{z1} \\ M_{x1} \\ M_{y1} \\ P_{z2} \\ M_{x2} \\ M_{y2} \\ P_{z3} \\ M_{x3} \\ M_{y3} \\ P_{z4} \\ M_{x4} \\ M_{y4} \end{bmatrix} = \underline{K}_{pb} \begin{bmatrix} w_1 \\ \theta_{x1} \\ \theta_{y1} \\ w_2 \\ \theta_{x2} \\ \theta_{y2} \\ w_3 \\ \theta_{x3} \\ \theta_{y3} \\ w_4 \\ \theta_{x4} \\ \theta_{y4} \end{bmatrix} \qquad 2.43$$

where P_{zi} indicate the component of force parallel to Z-axis at node i, M_{xi} and M_{yi} represent the generalized forces corresponding to the rotations (generalized displacements) θ_{xi} and θ_{yi} at node $i(i=1,2,3,4)$ respectively. $\underline{K}_{pb}$ is obtained from Eq. 2.41.

$\underline{K}_{ps}$ and $\underline{K}_{pb}$ are subdivided into 2x2 and 3x3 submatrices respectively as shown in Eq. 2.29 and Eq. 2.41. Now, remembering that the inplane and bending stiffnesses are uncoupled, these can be combined to obtain the total stiffness matrix $\underline{K}$ as shown below. For the purpose of assembling several elements, appropriate number of zeroes have been included corresponding to θ_{zi} and its conjugate M_{zi}.

$$
\underset{24\times24}{\underline{K}} =
\begin{bmatrix}
\underset{2\times2}{\underline{K}^{ps}_{11}} & & & & & & & & & & & \\
0 & \underset{3\times3}{S\underline{K}^{pb}_{11}} & & & & & & & \text{Symmetrical} & & & \\
0 & 0 & 0 & & & & & & & & & \\
\underset{2\times2}{\underline{K}^{ps}_{21}} & 0 & 0 & \underset{2\times2}{\underline{K}^{ps}_{22}} & & & & & & & & \\
0 & \underset{3\times3}{S\underline{K}^{pb}_{21}} & 0 & 0 & \underset{3\times3}{S\underline{K}^{pb}_{22}} & & & & & & & \\
0 & 0 & 0 & 0 & 0 & 0 & & & & & & \\
\underset{2\times2}{\underline{K}^{ps}_{31}} & 0 & 0 & \underset{2\times2}{\underline{K}^{ps}_{32}} & 0 & 0 & \underset{2\times2}{\underline{K}^{ps}_{33}} & & & & & \\
0 & \underset{3\times3}{S\underline{K}^{pb}_{31}} & 0 & 0 & \underset{3\times3}{S\underline{K}^{pb}_{32}} & 0 & 0 & \underset{3\times3}{S\underline{K}^{pb}_{33}} & & & & \\
0 & 0 & 0 & 0 & 0 & 0 & 0 & 0 & 0 & & & \\
\underset{2\times2}{\underline{K}^{ps}_{41}} & 0 & 0 & \underset{2\times2}{\underline{K}^{ps}_{42}} & 0 & 0 & \underset{2\times2}{\underline{K}^{ps}_{43}} & 0 & 0 & \underset{2\times2}{\underline{K}^{ps}_{44}} & & \\
0 & \underset{3\times3}{S\underline{K}^{pb}_{41}} & 0 & 0 & \underset{3\times3}{S\underline{K}^{pb}_{42}} & 0 & 0 & \underset{3\times3}{S\underline{K}^{pb}_{43}} & 0 & 0 & \underset{3\times3}{S\underline{K}^{pb}_{44}} & \\
0 & 0 & 0 & 0 & 0 & 0 & 0 & 0 & 0 & 0 & 0 & 0
\end{bmatrix}
\qquad 2.44
$$

In the above, $S = \frac{1}{15ab}$

The stiffness matrix given by Eq. 2.44 is with reference to the local xyz co-ordinate system shown in Fig. 2.10. It is therefore necessary to transform the local stiffness matrices to a common set of global coordinates x'y'z'. The global stiffness matrix of the element can be obtained as

$$\underline{K}^G = \underline{\lambda}^T \ \underline{K} \ \underline{\lambda} \qquad 2.45$$

where the transformation matrix $\underline{\lambda}$, is given by

$$\underset{24\times24}{\underline{\lambda}} = \begin{bmatrix} \underline{\underline{\lambda}} & & & \\ & \underline{\underline{\lambda}} & & \\ & & \underline{\underline{\lambda}} & \\ & & & \underline{\underline{\lambda}} \end{bmatrix} \qquad 2.46$$

and

$$\underset{6\times6}{\underline{\underline{\lambda}}} = \begin{bmatrix} l_x & m_x & n_x & & & \\ l_y & m_y & n_y & & 0 & \\ l_z & m_z & n_z & & & \\ & & & l_x & m_x & n_x \\ & & & l_y & m_y & n_y \\ & 0 & & l_z & m_z & n_z \end{bmatrix} \qquad 2.47$$

Here, l_x, m_x, n_x, for example, denote the set of direction consines of x axis. Thus l_x, m_x and n_x are consines of angles

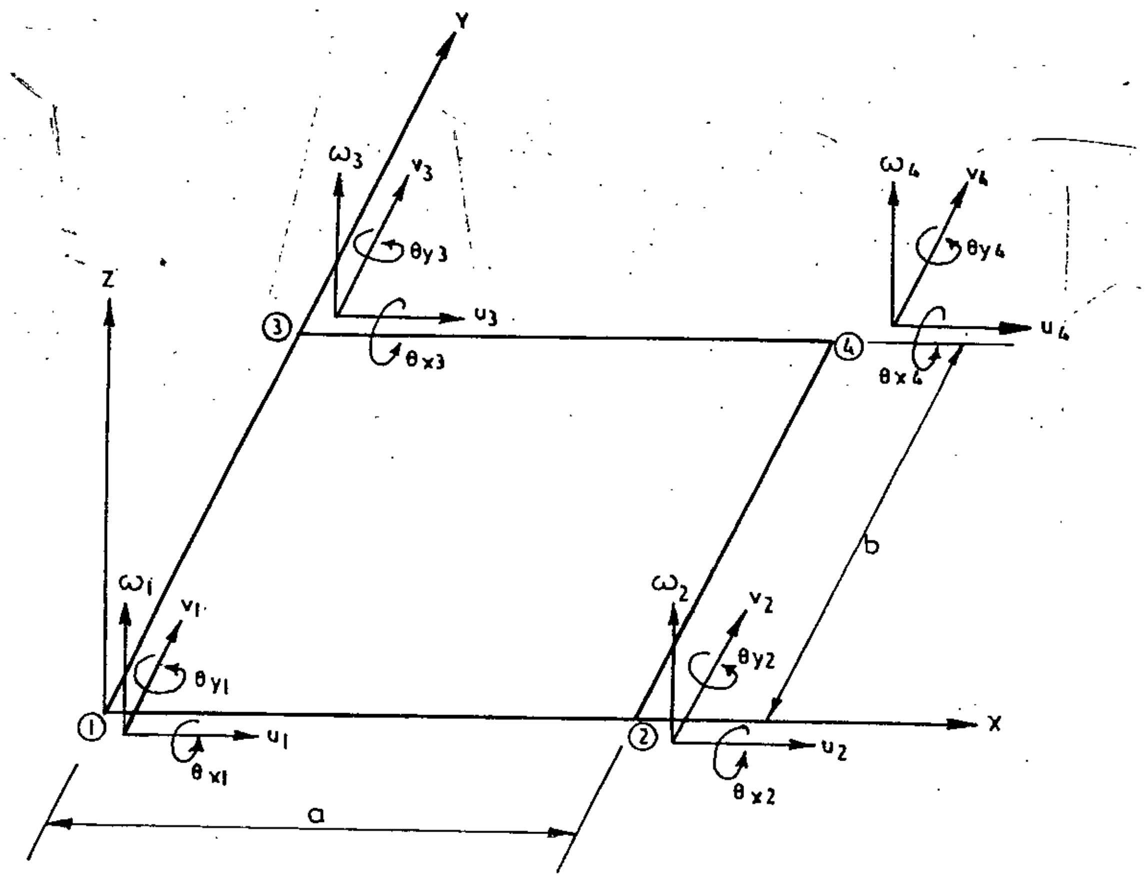

FIGURE 2.10 ORTHOTROPIC WALL ELEMENT SUBJECTED TO INPLANE AND BENDING ACTIONS.

included between x-x', x-y' and x-z' respectively. Similarly, l_y, m_y, n_y are for y and l_z, m_z, n_z are for z axes.

Now the typical 6x6 stiffness submatrices in global coordinates are obtained from their corresponding submatrices in local coordinates by the transformation

$$\underline{K}^G_{ij} = \underline{\lambda}^T \; \underline{K}_{ij} \; \underline{\lambda} \qquad 2.48$$

in which $\underline{K}_{ij}$ is taken from 2.44 and is of the form

$$\underset{6\times6}{\underline{K}_{ij}} = \begin{bmatrix} \underset{2\times2}{\underline{K}^{ps}_{ij}} & 0 & 0 \\ 0 & \underset{3\times3}{5\underline{K}^{pb}_{ij}} & 0 \\ 0 & 0 & 0 \end{bmatrix} \qquad 2.49$$

Elements of stiffness submatrices are calculated first in local co-ordinates, and then stored in a one dimensional array for overall joint stiffness matrix by transforming the elements in global system and transferring to appropriate locations of the array. In the program, submatrices of the lower triangle of the stiffness matrix of any wall element are calculated only to take advantage of symmetry of the element stiffness matrices.

2.5.3 Calculation of the Strains and the Stresses in the Orthotropic Wall Element

Once the vectors of the nodal displacements $\{\underline{X}\}_{ps}$ and $\{\underline{X}\}_{pb}$ are obtained from an analysis, the strains at any point in the element can be calculated from Eq. 2.25 and Eq. 2.36 respectively. This is achieved by substituting the coordinates of the point in the $\underline{B}_{ps}$ and $\underline{B}_{pb}$ matrices already discussed in the previous sub-section. The stresses at the same point are calculated from Eq. 2.26 and Eq. 2.37 by premultiplying the corresponding strain vectors by $\underline{D}_{ps}$ and $\underline{D}_{pb}$ matrices evaluated for that element from Eq. 2.27 and Eq. 2.38 respectively.

It is usual to compute the stresses and the strains at the centroid of the element. Substituting the centroidal coordinates $x = a/2$ and $y = b/2$ in the expressions for $\underline{B}_{ps}$ and $\underline{B}_{pb}$, the matrices can be evaluated at this point.

However, explicit expressions were used in the computer program to calculate strains at the centroid of an element from its nodal displacements already evaluated. Similarly, direct expressions for stresses in terms of the strains were utilized to calculate the stresses at the centroid of an element.

Chapter 3

THE FINITE ELEMENT COMPUTER PROGRAM

3.1 INTRODUCTION

Important aspects of an interactive problem alongwith the methods of considering non-linearity and crack propagation have been described in the preceding chapters. The purpose of this chapter is to describe the development of a finite element program that utilizes these features incorporating orthotropic infill wall elements in an integrated structure-foundation-soil system. The nature of the programs is general and they can be used to analyse large practical structures with orthotropic infills. Special care has been taken to reduce the use of the computer core storage and the execution time. The programs described here are written in FORTRAN and were tested and run on the IBM 4331 computer at the computer centre of Bangladesh University of Engineering and Technology.

The programs were developed around a suite of routines originally developed by Rahman (1978) for the CDC 7600 computer. Special routines for handling direct access backing storage and treating orthotropic wall elements were incorporated by the author.

3.2 THE FINITE ELEMENTS

A total of four different finite elements were included in the programs. These are listed below:

Space frame member elements: These elements, developed by Majid (1972), can take account of the irregularities at the ends of the members in addition to the centre line representation of the frame members. The element is described in Art. A1.1 of Appendix.

Rectangular plate elements: These elements have both in-plane and out of plane forces and displacements. By a suitable selection of the degrees of freedom and the stiffness terms these elements can either be used as plate bending elements or as shear wall elements. These elements were taken from a package developed by Bray (1973). This element is also described in Art. A1.2 of Appendix.

Rectangular orthotropic plate elements: These rectangular elements used to represent the infill walls are capable of taking both inplane and out of plane deformations. The four noded element is formed by combining the stiffnesses of a plane stress element and a plate bending element. The elasticity matrix used was that of an orthotropic material with the directions of orthotropy coinciding with the element sides. The element has been described in Chapter 2.

Rectangular parallelopiped solid elements: This is a regular prismoidal element with eight nodes and a linear variation of displacements between the nodes. Each node of the element can have three translational degrees of froodom. The element has been described in Chapter 2.

For all the above elements the stiffness matrix was formed explicitly in order to save computer time. Explicit expressions were also developed and used for the determination of stresses and forces etc.

3.3 GENERAL FEATURES OF THE COMPUTER PROGRAM

The non-linear analysis is performed by the incremental method described in Chapter 2, the mechanical properties of the soil being given by an explicit set of $\tau_{oct} - \gamma_{oct}$ curves. Although a suite of routines originally developed by Rahman (1978) for CDC 7600 computer was used as the basic unit, an additional type of element and routines for handling of direct access disc backing storage in IBM 4331 computer were incorporated in the program. Besides, the original routines were recorded in FORTRAN 77 and installed and tested on IBM 4331 prior to their use in the present program. The final program contains about 4030 source statements. The general features of the program are as follows:

(a) reduction of the use of the core storage by selecting an efficient storage scheme of the stiffness matrix.

(b) development of program to utilize the backing storage facilities in IBM 4331 so that only a part of the stiffness matrix is held in the core at a time and the efficiency is not hampered significantly (Rahman, 1978).

(c) development of a routine for computation of stiffness contributions of the orthotropic infills.

(d) construction of the stiffness matrix in two phases in order to isolate the part of it which remains unaltered in successive analyses from that which is changed by contributions of non-linear elements. Details of the technique can be found in Rahman (1978).

(e) construction of stiffness matrix joint by joint to simplify the storage techniques and minimize I/O operations with disc.

(f) utilization of an efficient solution routine ensuring an efficient transfer between the core and the backing store of the stiffness matrix solution blocks (Rahman, 1978).

(g) use of spline function to implement a smooth representation of non-linear soil properties.

(h) computer implementation of the crack propagation method.

3.3.1 Storage of the Stiffness Matrix

The scheme of storage of the stiffness matrix was carefully selected to reduce the use of the core space without an undue increase in the execution time. A variable band width storage scheme suggested by Jennings (1966, 1977) was adopted. In this scheme, only the elements between the first non-zero and the leading diagonal in each row of the lower triangle of the matrix were stored (Fig.3.1). This was achieved by storing the elements in a continuous one dimensional array in a row-by-row sequence. For example, by reducing the number of elements of stiffness matrix to be stored from 4×10^5 to 2×10^5, an economy of atleast 46% of computer mill time is achieved (Rahman, 1978).

3.3.2 Construction of the Stiffness Matrix

In addition to the compact storage scheme just described some program modules were developed to take advantage of the backing storage facilities so that only a part of the stiffness matrix is held in the core at a time. This was attained by opening three working files in the disc backing store. When a part of the stiffness matrix is fully constructed it is written into the backing store. The same area of the core space is then used to construct the next part of the stiffness matrix. To reduce the number of transfers, stiffness matrix $\underline{K}$ was subdivided in such a way as to make its parts independent of each other during the assembly process.

The overall stiffness matrix is constructed in two phases. In the first phase, the matrix is constructed with the contributions from the linear elastic elements only. This incomplete stiffness matrix remains unaltered in the successive analyses. In the second phase of construction,

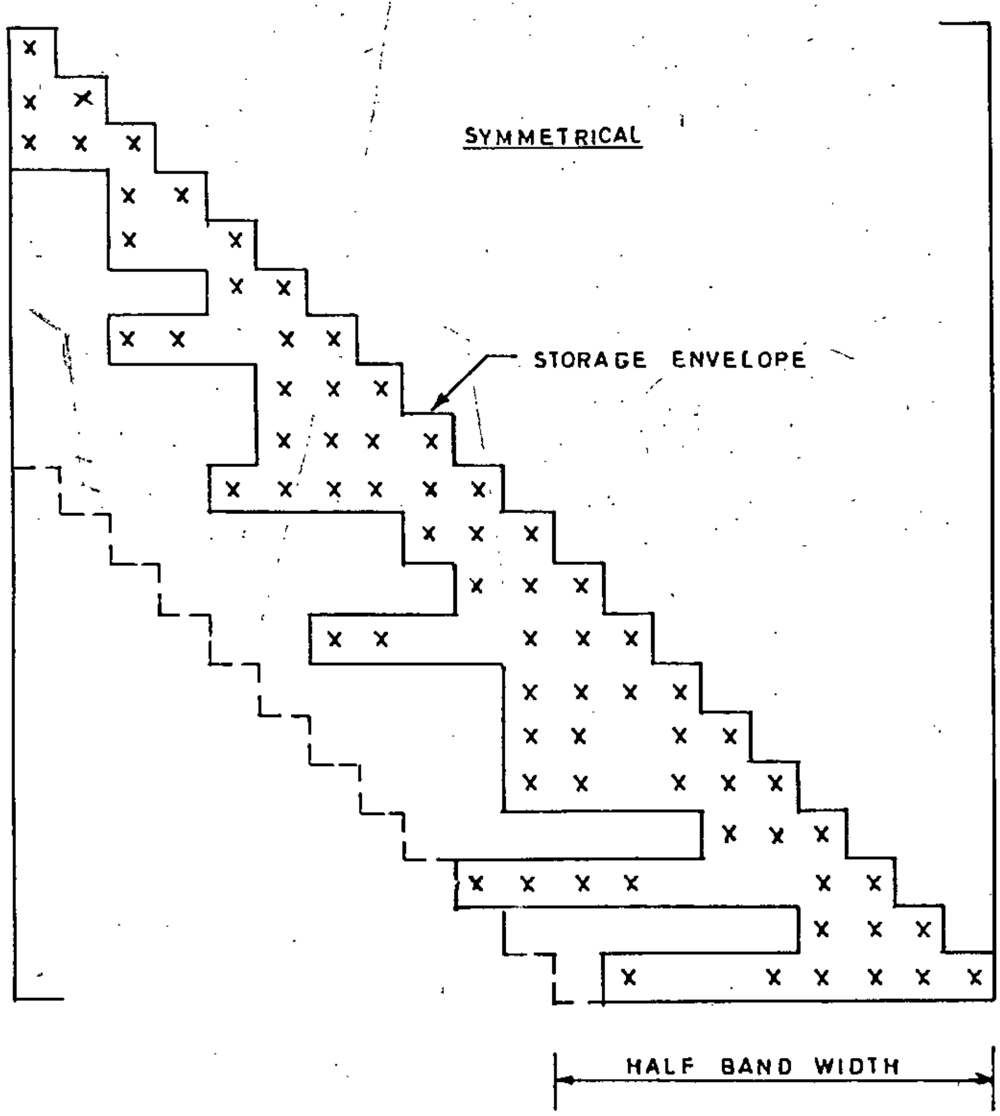

NOTE: EACH X INDICATES A NON-ZERO ELEMENT.

FIGURE 3.1 LAYOUT OF A TYPICAL STIFFNESS MATRIX.

the contributions from the non-linear elements are superimposed on this matrix. In each increment of the load only the second phase of the construction is repeated. However, when new rows and columns are introduced to the stiffness matrix due to the development of a crack, the first phase of the construction has also to be repeated.

3.3.3 The Solution Routine

A program for solution of simultaneous linear equations by Gaussian elimination technique modified to suite the compact storage scheme developed by Rahman (1978) is used in this thesis. The stiffness matrix is divided into a number of segements in such a way that each segement contains a number of complete rows. The direct access backing store file is also divided into fixed length blocks in which each complete segment wholly or partially fills the block. A block size of 1250 elements was used for the problems analysed in this thesis.

The stiffness matrix is divided into the solution blocks in a subroutine CSDIV. In the second phase of the construction, the final stiffness matrix is written into backing store file ready to be solved. A subroutine WRITW was written to transfer the completed part of $\underline{K}$ corresponding to a joint into a pseudo-buffer equal in length to a preselected block size. When the pseudo-buffer is filled, its contents are written into the backing store file ready for solution.

The solution routine uses two scratch arrays to copy two blocks of the stiffness matrix $\underline{K}$ from the backing store into the core. The first, called the active block, is the part of $\underline{K}$ currently being eliminated. The second, called the passive block, corresponds dynamically to the other parts of $\underline{K}$ that are necessary in eliminating the active block. The back substitution process also follows the same block by block sequence in the reverse order.

3.3.4 The Use of Spline Functions

A program was written to formulate the spline functions for a set of τ_{oct} - γ_{oct} curves described in Chapter 2. For any particular set of curves obtained for a given soil, this program is run only once and the output is used repeatedly for all the analyses with this soil. This output consists of the nodal values of τ_{oct}, γ_{oct} and the second derivatives ϕ at each node for each curve.

A subroutine GVALUE is included in the main program to calculate the values of τ_{oct} and G for any value of γ_{oct}. The routine is entered before each increment of the load to obtain the instantaneous shear modulus of each solid element.

3.3.5 The Implementation of Crack Propagation

A method of following the crack propagation and tension separation in a structure-soil system has already been described in Chapter 2. The method is implemented using a subroutine SEPRTN in the general finite element program. The subroutine was originally developed by Rahman (1978) and subsequently edited for installation in IBM 4331 computer by the author. A call is made to the subroutine, after each increment of load, to detect any new separation or the closure of any existing crack. The subroutine prints out a running history of the propagation of any crack and automatically takes measures for modification of the stiffness matrix in the subsequent increments of load.

3.3.6 The Contribution of Orthotropic Infills

The explicit derivation of the stiffness matrix of the orthotropic infill walls has been described in Chapter 2. The contributions of the stiffness terms of the wall elements to the overall stiffness matrix are computed in the first phase of the construction of this matrix by using a subroutine ORTHPL. The direction cosines of the rectangular elements are calculated by calling a subroutine ORTHDC. A subroutine ORTWRT forms and writes away stiffness terms of orthotropic elements in the appropriate locations of the overall stiffness matrix. A block diagram of this procedure is given in Fig.3.2.

Stresses and moments per unit length at the centre of gravity of each orthotropic wall element are calculated with the help of two subroutines ORTDBT and ORTSTR.

3.4 THE STRUCTURE OF THE COMPUTER PROGRAM

The general structure-soil interaction finite element program was developed by a logical combination of some thirty seven subroutines spreading over about 4030 Fortran source statements. The subroutines can be grouped into four categories depending on the functions they perform. These are: (i) control routines, (ii) ancillary routines, (iii) element routines, and (iv) speciality routines.

The control routines perform such functions as the overall management of the data and control of the incremental analysis process. The main segment of the program reads and generates the nodal coordinates and element connectivity. It also initiates the non-linear analysis by generating initial values of the non-linear elastic parameters. Another routine in this group performs the task of assembling the global stiffness matrix in each increment of the load. A third routine controls the incremental procedure by summing the displacements and stresses etc. and by altering the non-linear elastic properties of the material.

Ancillary routines are used by subroutines of the other groups for performing various computational chores. These include transfer of data to and from the backing store in fixed length blocks, division of the stiffness matrix into solution blocks, reconstruction of the load vector in each increment, calculation of elastic moduli from the spline functions and so on.

The element subroutines formulate each type of finite element used in the program. They evaluate the element stiffness matrices and calculate the stresses, the strains, the forces and the moments.

Two speciality subroutines perform the solution of simultaneous equations and the control of crack propagation process. The solution routine utilizes the Gaussian elimination method coupled with the compact storage scheme. The stiffness matrix is eliminated block by block reading as necessary the appropriate active blocks and their corresponding passive blocks from the backing store. The crack propagation subroutine incorporates an automatic procedure of detection, initiation, propagation, closure and bifurcation of cracks in the finite element mesh. The physical changes in the mesh due to changes in the crack configuration are automatically catered for by activating and inactivating dummy joints and altering the connectivity matrix accordingly.

The subroutines are combined in the program during linkage editing to form an executable module. A grossly simplified flowchart of the complete program is shown in Fig. 3.3.

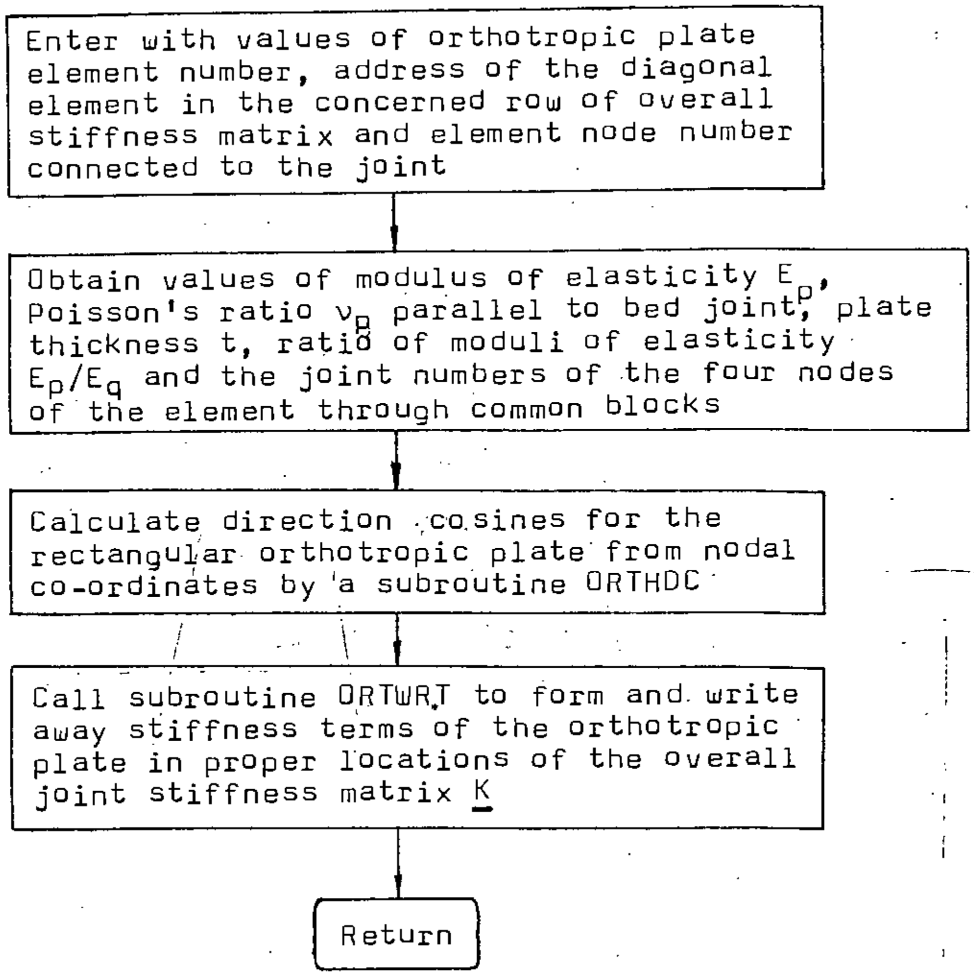

FIGURE 3.2 BLOCK DIAGRAM OF SUBROUTINE ORTHPL.

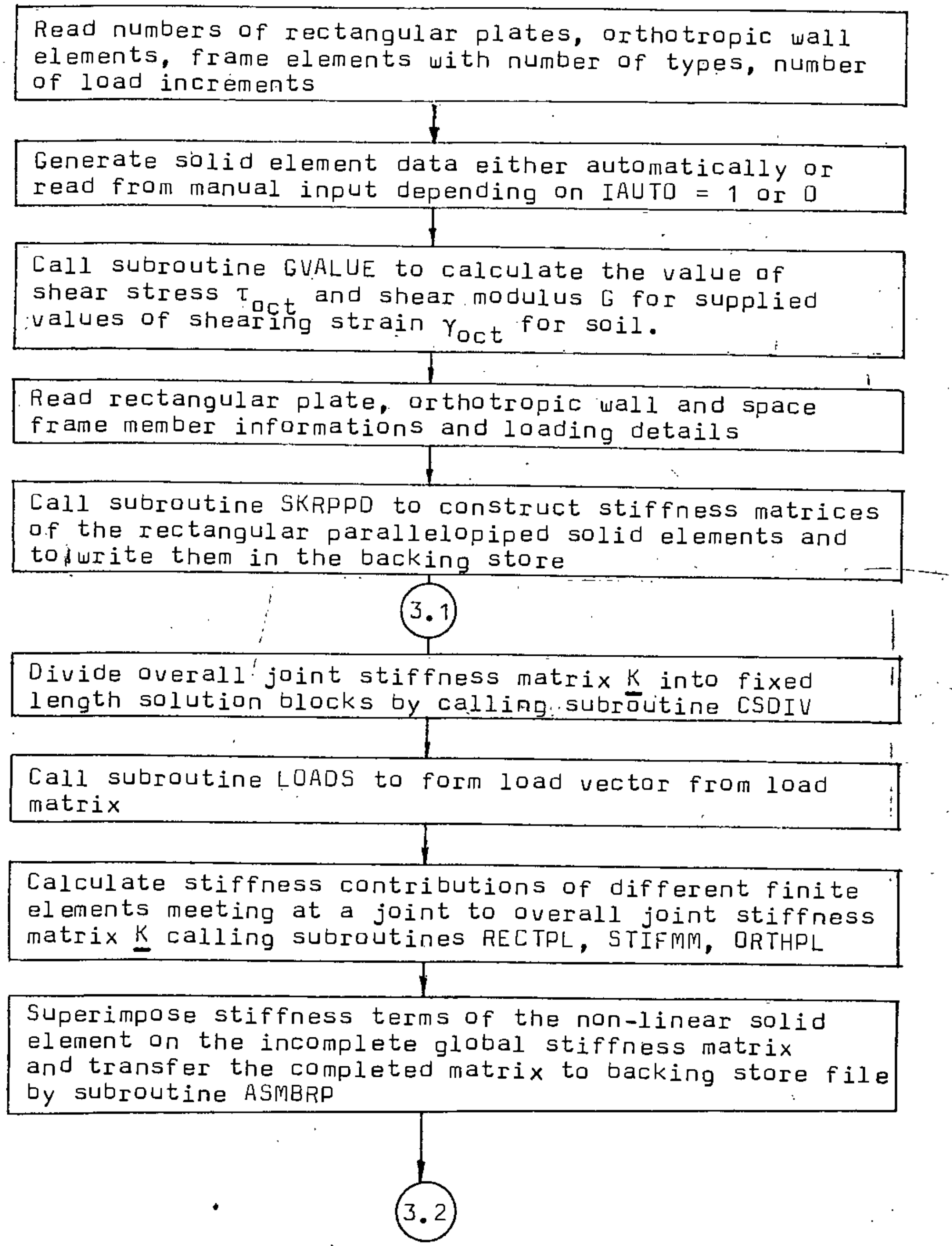

FIGURE 3.3 SIMPLIFIED FLOWCHART OF THE COMPUTER PROGRAM.

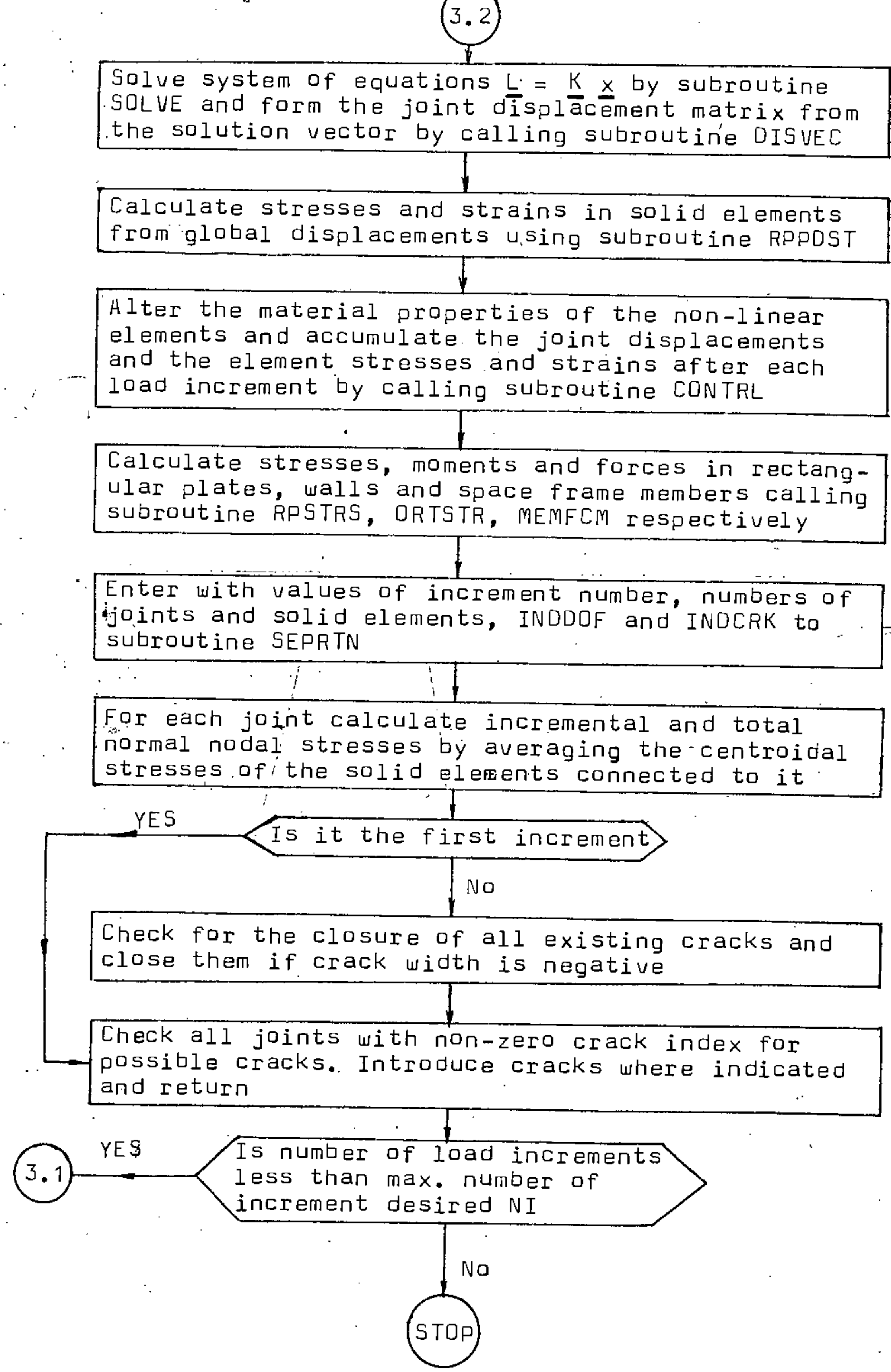

FIGURE 3.3 SIMPLIFIED FLOWCHART OF THE COMPUTER PROGRAM. (CONTINUED)

Chapter 4

INTERACTION ANALYSES OF FRAMED STRUCTURES

4.1 INTRODUCTION

In the preceding chapters the method of analysing an integrated structure-foundation-soil system with frames having orthotropic infills have been described. The finite element computer program developed for this purpose can now be utilized for analysing orthotropic infilled three-dimensional framed structures resting on soil.

In order to study the interaction behaviour and to examine the influence of various parameters on such behaviour, a series of analyses on typical structures were carried out. This chapter describes the structures selected for analysis, their properties, loadings and the finite element representation.

4.2 STRUCTURE WITH SYMMETRIC PLAN CONFIGURATION

The first structure analysed was a five storied framed building with rectangular plan configuration, as shown in Fig. 4.1. It consisted of 5 frames at 7 m intervals, each spanning 7 m in the transverse direction. The frames were connected together in the longitudinal direction by a system of beams. The space frame thus formed had slabs at each floor level. The building rested on a 0.3048 m thick raft foundation. For a general case the frame panels had orthotropic wall infills. The soil strata included in the finite element analysis had a maximum depth of 8 m below the superstructure. The horizontal extent of the soil mass was taken as 42 m x 63 m. It was assumed that the soil mass was supported by rigid permeable boundary on all sides excepting the top. The boundary nodes of the soil mass were free to slide over the boundary but were prevented from displacements normal to the boundary.

The finite element mesh for the integrated structure-soil system is illustrated in Fig. 4.1. The mesh for the superstructure along with the raft foundation is shown in Fig. 4.2 for a better view. The beams and the columns were all prismatic members. The cross-sectional area for all such members was 0.0929 m^2 and the second moment of area about both the major and the minor axes was 7.19×10^{-4} m^4. There was a total of 115 space frame elements. The roof and floor slabs were divided into 20 plate elements of 0.127 m thickness each. The raft consisted of 4 plate elements. Upto 65 orthotropic wall elements were considered to account for the infill walls. This corresponded to the case when all the panel areas bounded by the beams and the columns contained infill walls. The wall thickness was taken to be 0.127 m. The depth d of the soil was varied between 4 m and 8 m for various analyses. Each time the pattern and the number of divisions in the vertical direction were kept the same. A total of 160 rectangular parallelopiped elements represented the soil mass. The structure-foundation-

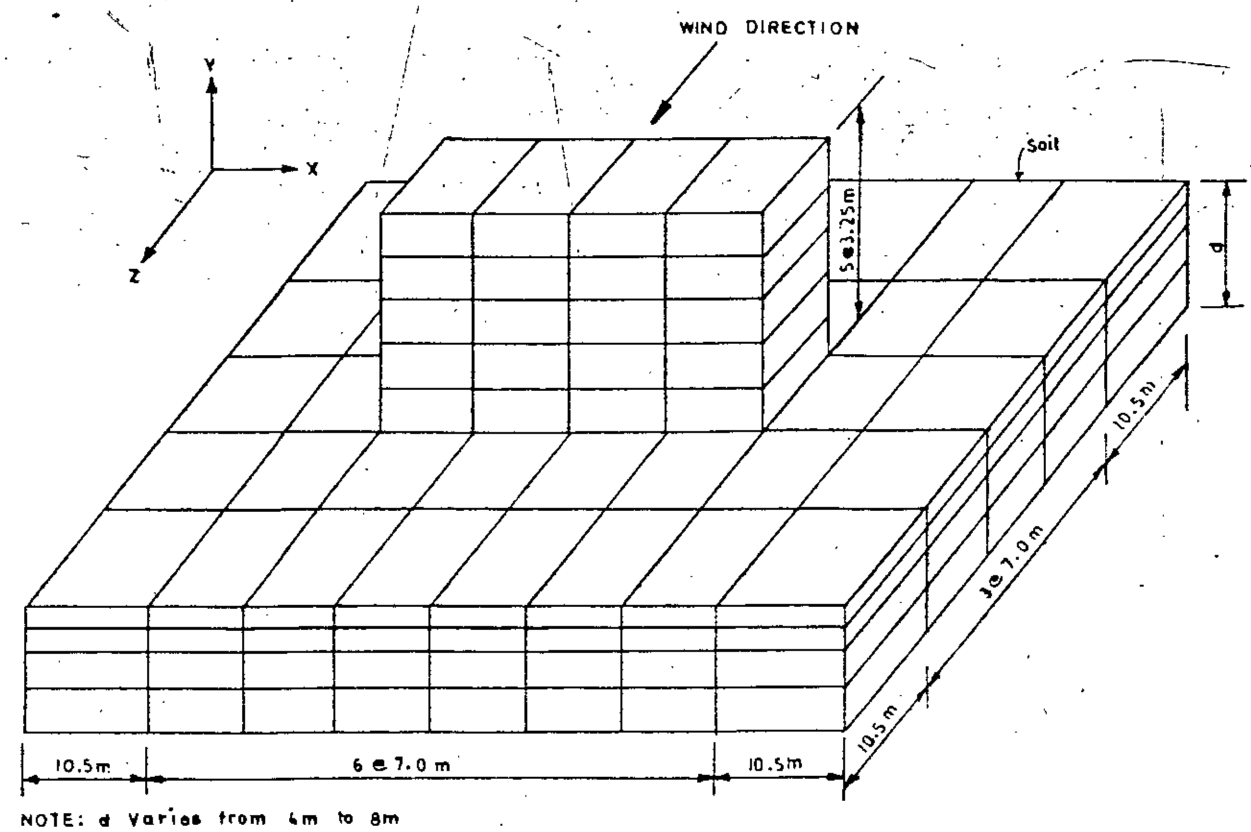

FIGURE 4.1 THE 5-STOREY SPACE STRUCTURE.

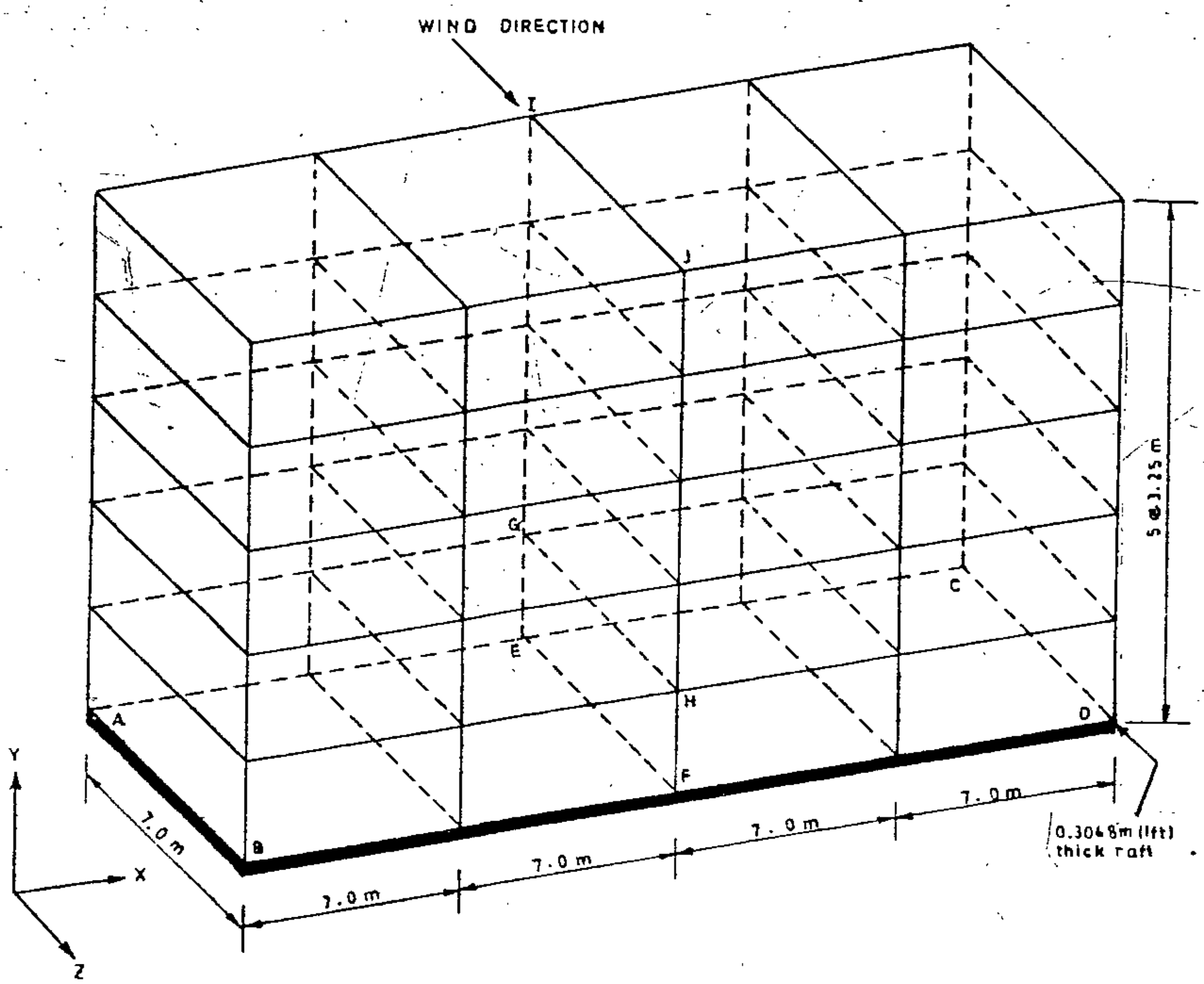

FIGURE 4.2 THE FINITE ELEMENT MESH OF 5-STOREY SPACE STRUCTURE AND MAT FOUNDATION.

soil integrated model thus consisted of 340 joints, 24 plates, 160 solid elements, 65 orthotropic wall elements, and 115 space frame members with 936 unknown degrees of freedom.

A total of 11 analyses were performed. The direction of wind loading was always perpendicular to one of the wider faces. The following four analyses were carried out for each of the two loading cases, viz. simultaneous action of vertical and lateral loads (load case 1) and independent action of the vertical load alone (load case 2):

(a) A fixed base analysis of bare frame with no soil.

(b) The same as analysis (a) but orthotropic infill walls with openings are included. The openings were accounted for by using reduced values of elastic moduli as suggested by Thorburn (1978).

(c) The analysis in the absence of infill of the complete structure, the foundation, and the soil, with the depth of soil taken as 8 m.

(d) The same as (c) but orthotropic infill walls with openings are taken into consideration.

The remaining three analyses were performed for load case 1 only. These are:

(e) The analysis of the complete structure, the foundation and 8 m deep soil having orthotropic infill walls without openings. To represent this case, normal values of moduli of elasticity of walls were taken.

(f) The same as (c) but with 6 m deep soil.

(g) The same as (c) but with 4 m deep soil.

Henceforth identification numbers such as 1a, 1b, etc. will be used to indicate the above described analyses for load case 1 and 2a, 2b etc. for load case 2. Thus for example, analysis 1f will mean analysis in the absence of infills of the complete structure, the foundation and the soil, with the depth of the soil taken as 6 m, when the structure is subjected to the action of vertical and lateral loads.

4.3 STRUCTURE WITH ASYMMETRIC PLAN CONFIGURATION

Additional elements were included in the structure described in the preceding article to obtain a T-shaped plan configuration. This introduced an eccentricity in the plan. The structure is illustrated in Fig. 4.3. It consisted of 5 frames at 7 m intervals. Three of these frames had a single span of 7 m and each of the remaining two had three 7 m spans. The number of storeys were three. A space frame was obtained by linking the above plane frames by beams in the longitudinal direction. As before a system of slabs were considered at each floor level and the frame panels had orthotropic wall infills. The structure rested on a 0.3048 m thick raft lying on a 8 m thick soil layer. The longitudinal extent of the soil was 63 m and the lateral extent was 42 m. A rigid permeable boundary enclosed the soil mass on all sides excepting the top. The boundary nodes of the soil mass were free to slide over the rigid boundary but were prevented from displacements normal to the boundary.

The finite element mesh for the integrated structure-soil system is shown in Fig. 4.3 whereas Fig. 4.4 illustrates the finite element mesh for the superstructure along with the raft foundation. The mesh for the soil remains exactly the same as that for rectangular plan structure shown in Fig. 4.1. Column and beam sections were taken the same as those described in Art. 4.2. The total number of space frame elements was 99. The roof and floor slabs consisted of 18 plate elements. The raft was divided into 6 plate elements and the infill walls were represented by 57 orthotropic wall elements. The slab, raft and wall thicknesses remained the same as those described in Art. 4.2 and the soil thickness was 8 m for various analyses. The integrated structure-foundation-soil model consisted of 350 joints, 24 plates, 160 solid elements, 57 orthotropic wall elements, and 99 space frame members with 900 unknown degrees of freedom.

A total of 8 analyses were performed. Four of the analyses were done for load case 1 and the rest exactly identical analyses corresponded to load case 2. The analyses for any of the load cases are:

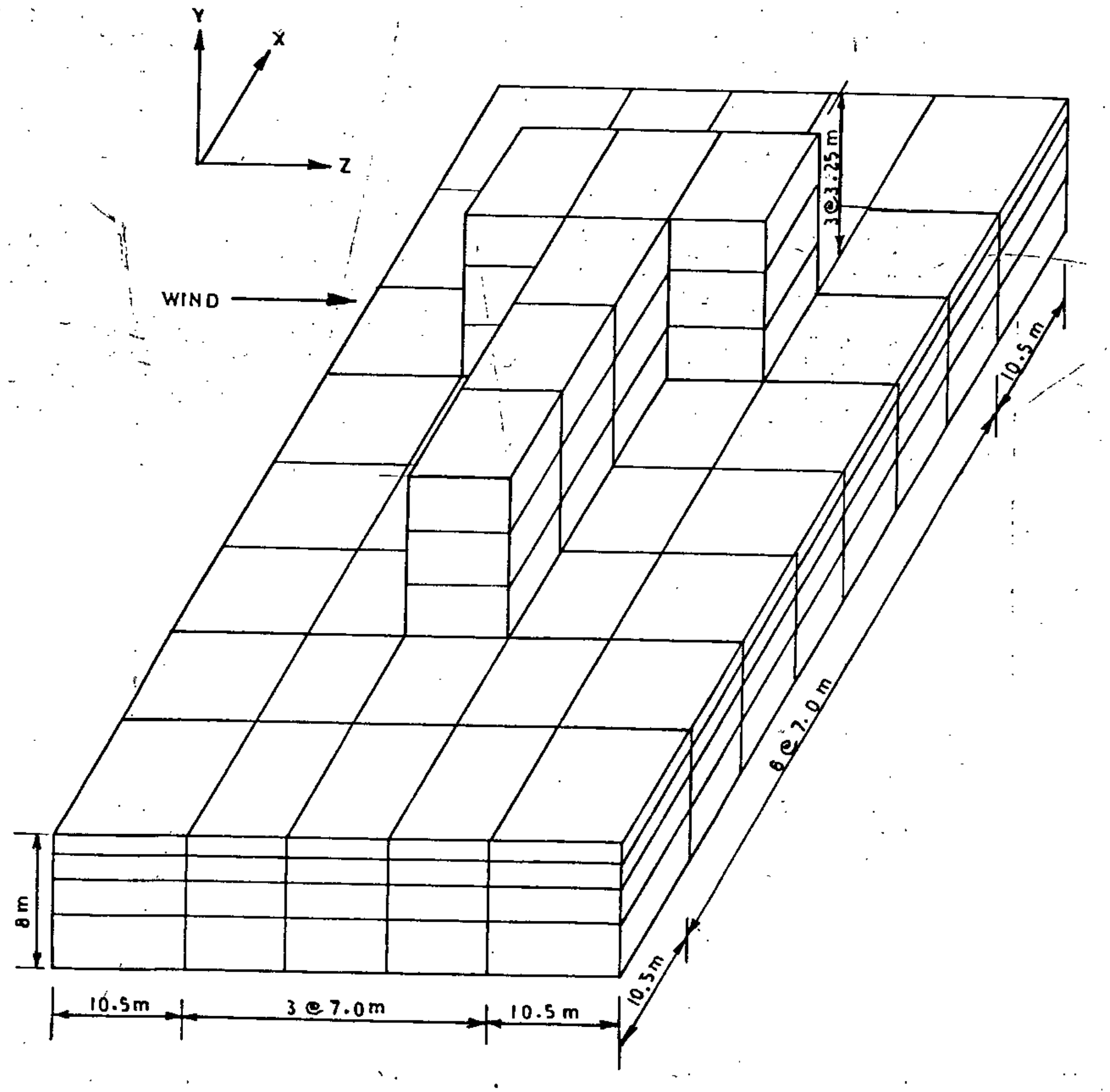

FIGURE 4.3 THE 3-STOREY SPACE STRUCTURE.

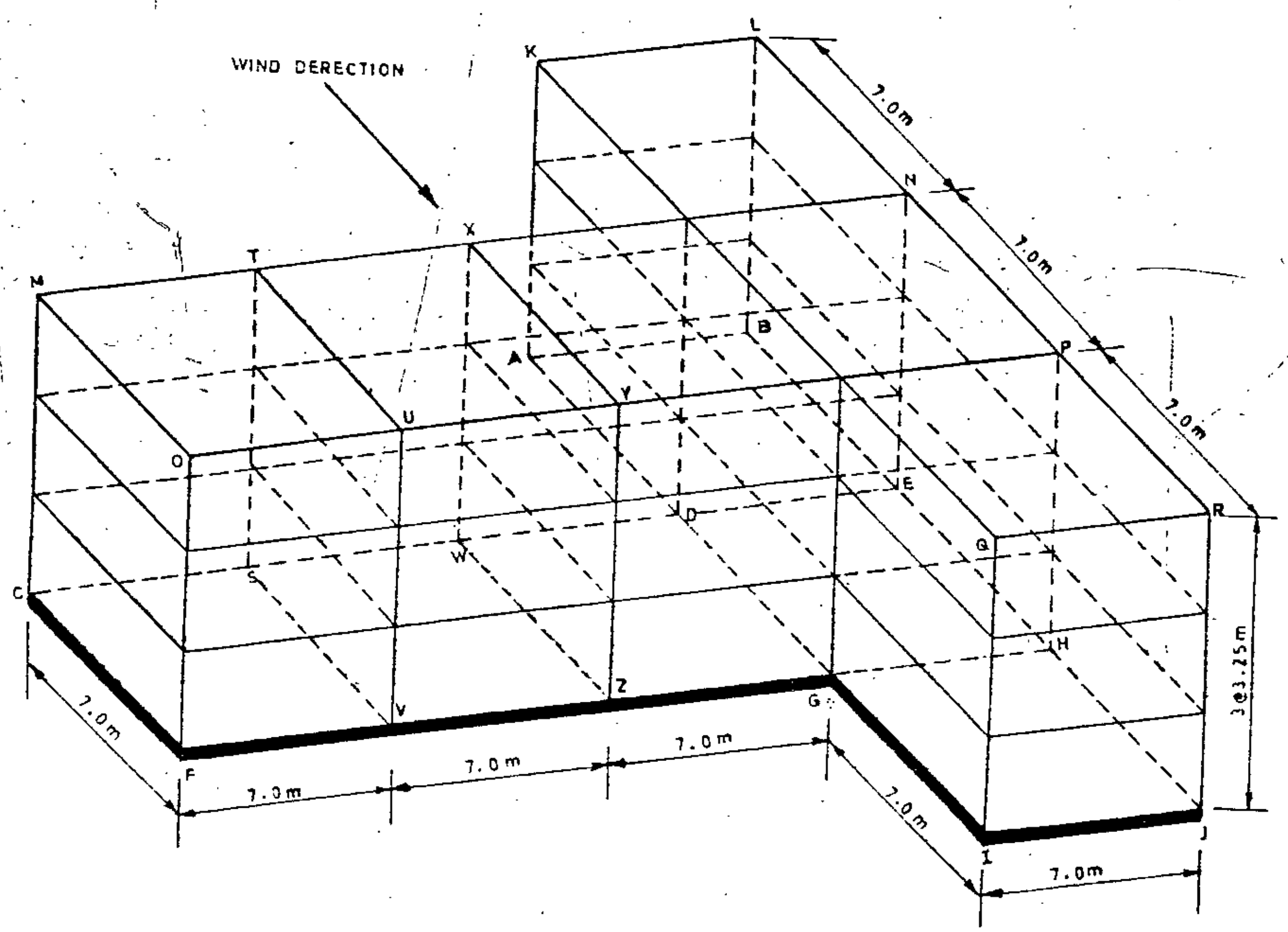

FIGURE 4.4 THE FINITE ELEMENT MESH OF 3-STOREY SPACE STRUCTURE AND MAT FOUNDATION.

(h) A fixed base analysis of bare frame with no soil.

(i) The same as (h) with orthotropic wall infills having openings.

(j) The analysis, in absence of infills, of the complete structure, the foundation and the soil.

(k) The same as (j) with orthotrqpic infill walls having openings.

As before, identification number 2h will mean, for example, a fixed base analysis of bare frame of T-plan structure with no soil under the action of load case 2. All other cases will be identified in an identical fashion in future discussions.

4.4 LOADING ON THE STRUCTURES

The 5-storey and the 3-storey three dimensional structures in Fig. 4.1 and Fig. 4.3 respectively were subjected to both vertical and wind loads. The vertical load receives contribution from dead weight of the structure and live load. The dead load was taken as 3.35 kN/m^2 on each floor of the building. The live load, for a residential private apartment house, taken from the recommendations of the American Standards Association publication, was 1.92 kN/m^2. These vertical loads on the floor were applied as concentrated forces at the joints.

The wind forces recommended in CP3 (Chapter V, Part 2, 1972) depend on the location, topography, building size and height, ground roughness and building life. The code gives a variable wind pressure distribution along the height of the building with the maximum at the top reducing towards the bottom. Basic wind speed defined as 3 second gust speed to be exceeded on the average once in 50 years was taken as 62.58 m/sec, Choudhury (1975), for location Dhaka. Although the value seems to be over estimated, it was considered satisfactory for the present analysis purpose in absence of more precise data. The wind pressure distribution in the buildings was calculated for Dhaka city approximating the topography factor equal to 1.0, ground roughness equal to 3 and assuming class B building size. The resulting wind pressure distribution is shown in Fig. 4.5. This pressure was applied as concentrated horizontal forces at the joints on the windward face of the building.

4.5 MATERIAL PROPERTIES

For all the analyses the material for the frame members, the floor slabs and the mat foundation was assumed to be reinforced concrete. The modulus of elasticity E and Poisson's ratio ν were taken to be 2.2×10^7 kN/m^2 and 0.15 respectively.

The orthotropic infills were assumed to have material properties of brick walls. Thus the modulus of elasticity

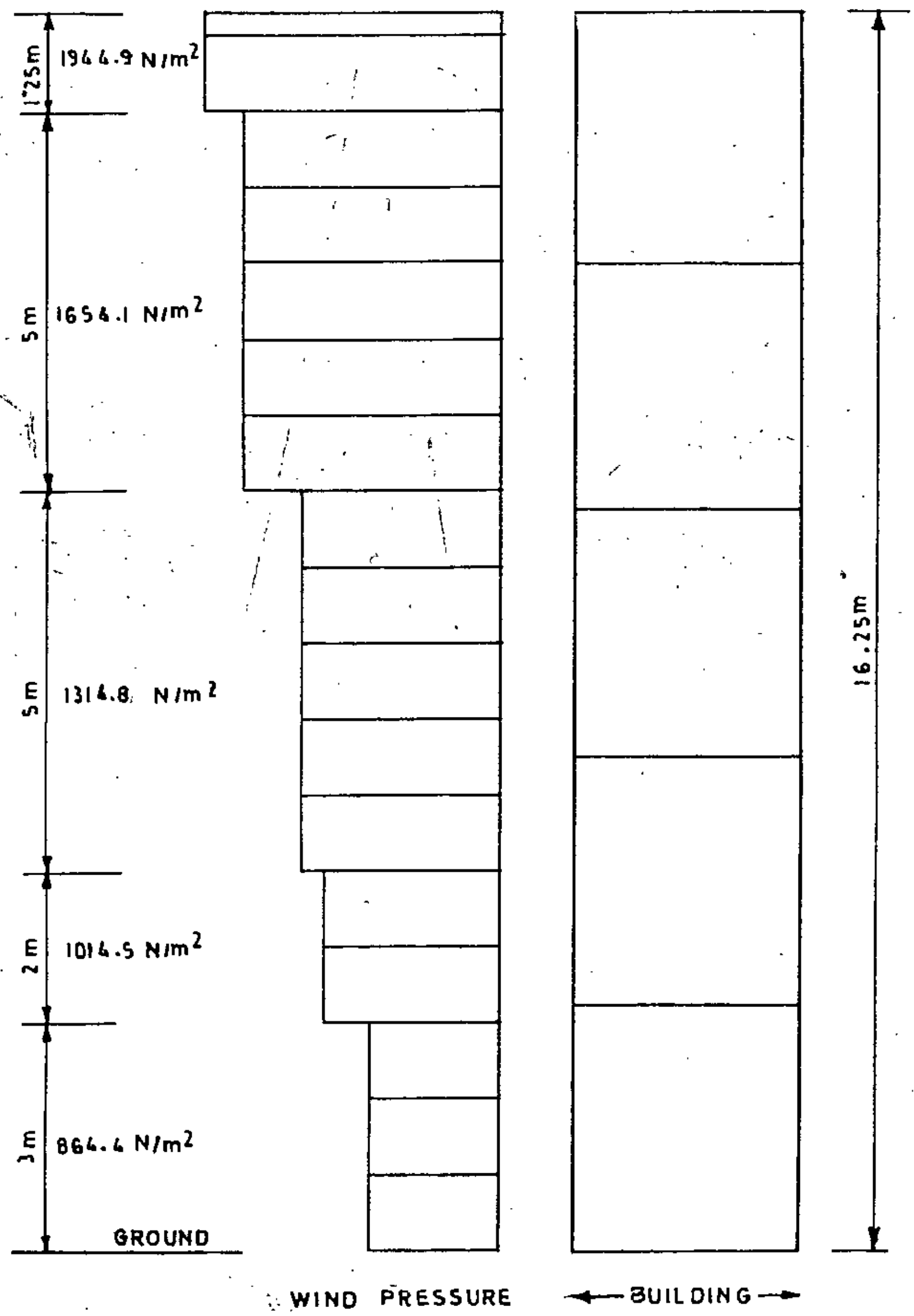

FIGURE 4.5 WIND PRESSURE ON THE FRAME.

parallel to bed joint E_p and the corresponding Poisson's ratio ν_p were taken to be 6×10^6 kN/m^2 and 0.15 respectively. The ratio of the modulus of elasticity E_p parallel to the bed joint to the modulus E_q perpendicular to it was approximated to 1.4. It is worth noting that from considerations of possible presence of openings in the infill walls, the moduli of elasticity were halved where it was necessary.

Soil properties were to be obtained from unconsolidated undrained test. In the analyses to be followed, the soil properties were obtained from the set of octahedral shear stress and octahedral shear strain curves shown in Fig. 2.1. For properties of soil with σ_{octi} values not coinciding with the values indicated in the curves, suitable interpolation or extrapolation schemes were used.

Although the curves shown in Fig. 2.1 are tentative, they represent a set of practical values of soil properties. These were utilized in the absence of test results for a particular type of soil lying below the superstructure and the foundation. For all the analyses Poisson's ratio of soil was taken to be 0.33.

Chapter 5

DISCUSSION ON RESULTS

5.1 INTRODUCTION

As mentioned earlier, a total of 19 analyses, 11 for a structure with symmetric plan configuration and 8 for a structure with asymmetric plan configuration, were performed. Results of these analyses are presented and critically examined in this chapter in graphical and tabular form. Different analysis cases are indicated by the nomenclature introduced and explained in the Chapter 4. Thus the analyses are numbered 1e, 1h etc. without further explanation. It should be recalled, however, that cases with letters a to g relate to structures with symmetric plan configuration and those with h to k to structures with asymmetric plan configuration. Numbers 1 and 2 preceding these letters denote action of vertical plus lateral load and vertical load alone respectively.

In some of the figures presented, the term load increment factor with notation λ has been used. This factor indicates the ratio of the actual load applied to the structure and the maximum value of load upto which it will be increased. The term gradient of relative displacement used in this chapter will mean the ratio of the difference in displacements of two points to the distance between them.

5.2 THE DEFLECTIONS OF THE STRUCTURE AND THE RAFT

5.2.1 Sway of the Structure

Sway at different floor levels of the central frame for analysis cases 1a, 1b, 1c, 1d and 1e has been shown in Fig. 5.1 for maximum values of loads given in Art. 4.4. The curves for cases 1a and 1b show no sway at the base. This is because the analyses assume a fixed base without any soil contribution. The remaining curves which represent interactive analyses of the structure and the soil show certain amount of lateral displacements at the base. Curves for bare frame analyses (cases 1a and 1c) clearly indicate the double curvature nature of the deflected shape over the structure height. In the remaining curves for infilled structure this nature is not prominent.

Comparing curves 1b with 1a and 1d with 1c, it may be observed that the sway is highly diminished in the presence of infilled walls and this applies to both fixed base and interactive analyses. Thus the top sway are 1/117, 1/4851, 1/62 and 1/140 respectively for case 1a, 1b, 1c and 1d and the reduction in sway due to the presence of infill walls is 97.59% for fixed base and 55.72% for interactive analysis. The actual contribution of infill walls to the increase of lateral stiffness of a building is thus much less than the apparent increase exhibited by the conventional fixed base analysis.

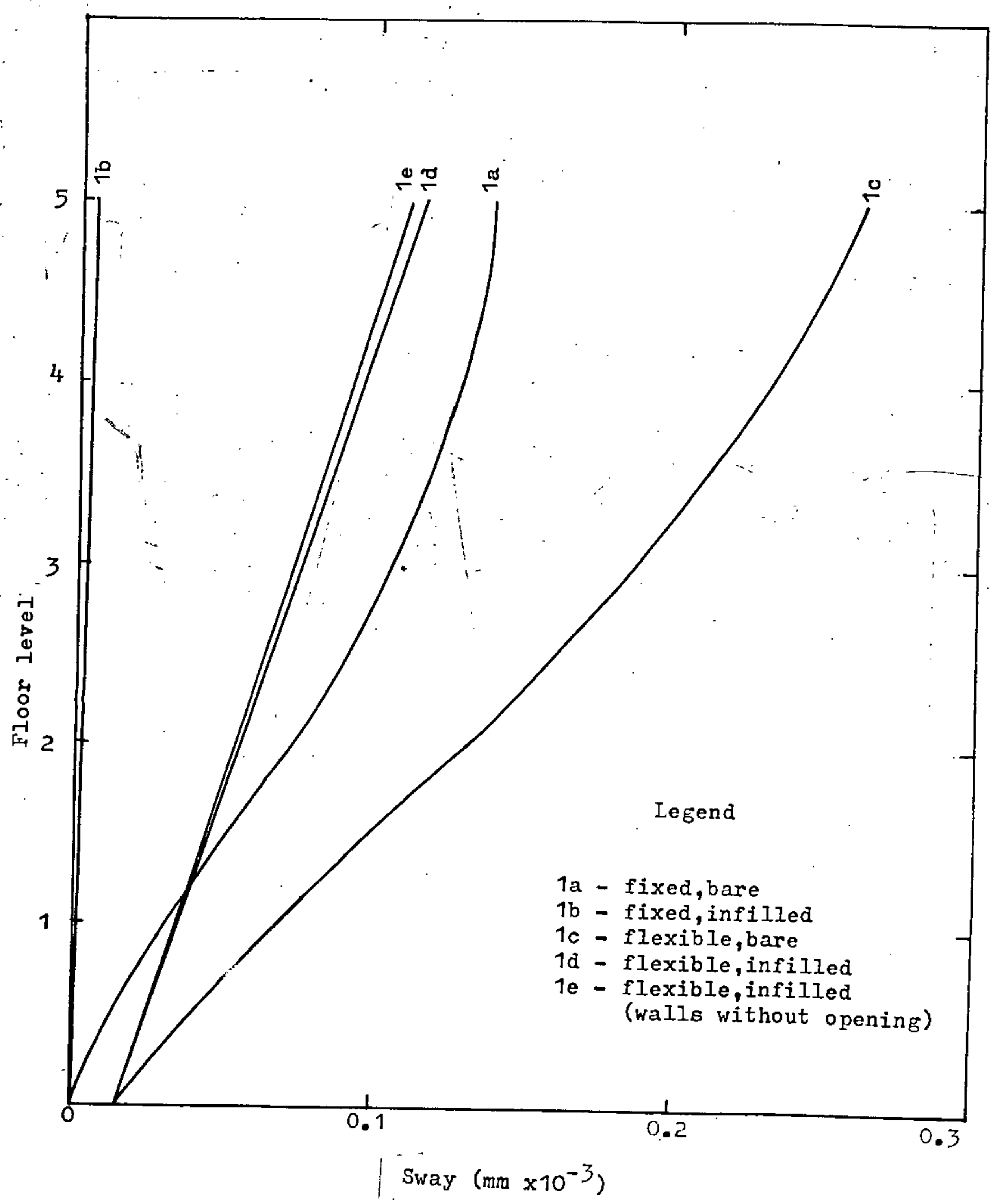

FIGURE 5.1 SWAY AT DIFFERENT FLOOR LEVELS OF THE INTERNAL FRAME OF STRUCTURE WITH SYMMETRIC PLAN.

When sway for case 1c is compared with that of case 1a, it is found that in the absence of infill walls soil increases the top sway 1.885 times. When sway for case 1d is compared with that of 1b, it is found that in the presence of infill walls soil increases the top sway 34.62 times. It becomes clear that the inclusion of soil in the analysis is more important in the case of highly stiff infilled frames than in more flexible bare frames.

Curves of Fig. 5.2 show the variation of the top sway of the central frame against the load increment factor λ for analysis cases indicated along the curves. As may be expected, the maximum top sway occurs in the case of bare frame-soil interactive analysis (case 1c). The minimum is observed for fixed base analysis of orthotropic wall infilled frame (case 1b) and it is 1.28% of the maximum sway. The other analysis cases give intermediate values for top sway. From the comparison of curves for infilled frame analyses (cases 1b and 1d) with bare frame analyses (cases 1a and 1c), it is confirmed that throughout the loading history the percentage reduction in sway due to the presence of infill walls is much less significant in a flexible base analysis than in a conventional fixed base analysis.

Comparison among curves for cases 1e and 1d (Fig. 5.1) reveals that openings in the infill walls do not change the sway values significantly, when the conventional approach of opening consideration is employed (i.e by halving the wall

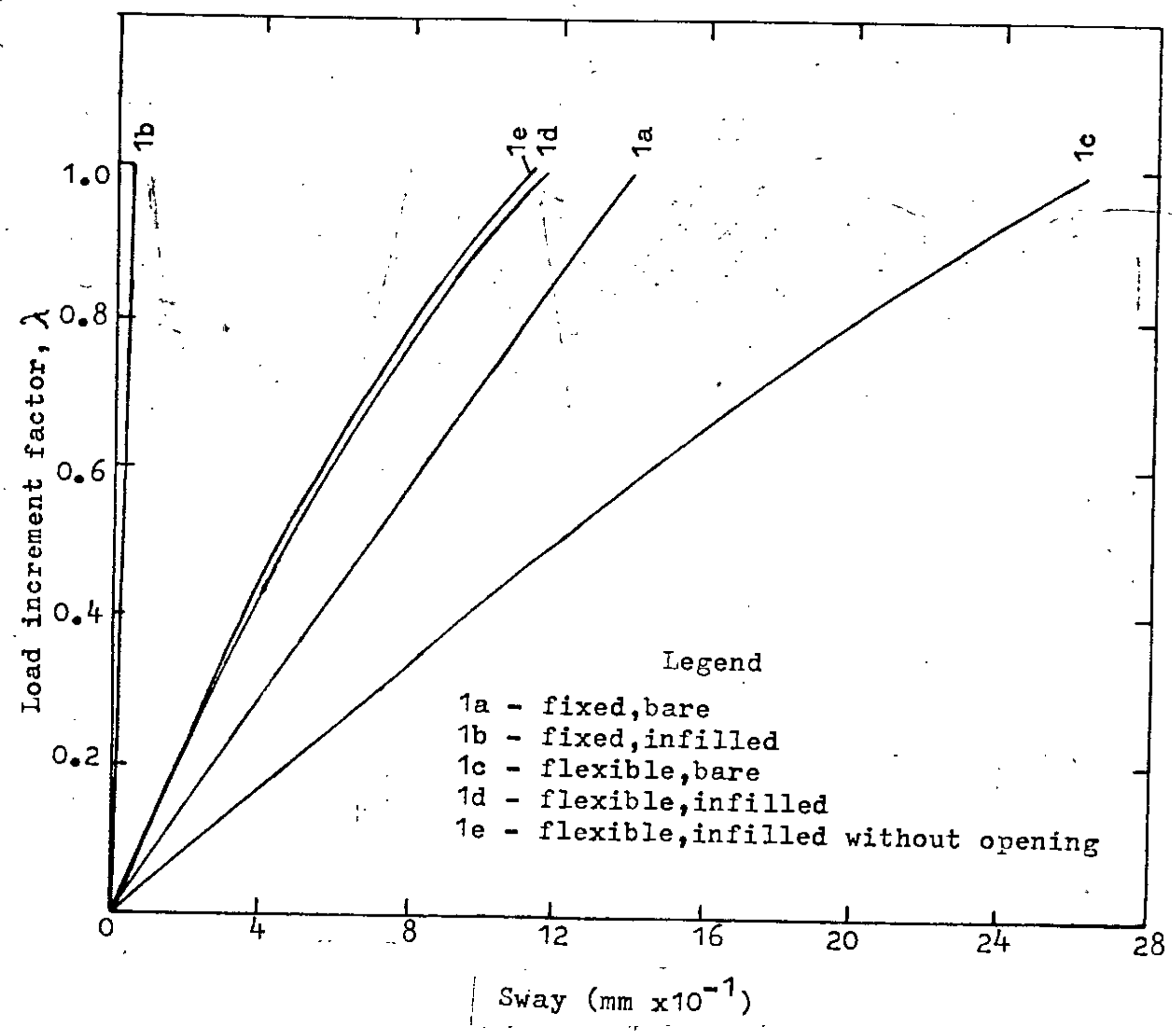

FIGURE 5.2 LOAD-TOP SWAY DIAGRAM OF THE INTERNAL FRAME OF STRUCTURE WITH SYMMETRIC PLAN.

stiffness) and the reduction is 4.31% for top sway. However, this reduction at the top is more significant than at the base. Comparing curves for cases 1e and 1d of Fig. 5.2, it is observed that the openings in the infill walls do not contribute much towards the increase of top sway at any load level. Therefore, it is indicated that openings in infill walls increase the structure sway only marginally when their effect is accounted for by the conventional approach.

Sway of the external frame CMOF (Fig. 4.4) of T-plan structure at different floor levels has been plotted for analysis cases 1h, 1i, 1j and 1k as shown in Fig. 5.3. Comparing curves 1i with 1h and 1k with 1j, it is found that the top sway diminishes by 98.2% and 81.13% due to infills for fixed base and flexible base analyses respectively. When compared to the corresponding percentage reductions (97.59% and 55.72%) obtained for rectangular plan, it is demonstrated that the real increase in resistance to sway due to the presence of infill walls is higher in the T-plan configuration. This is considered to be due to the inherent lateral stiffness of the exterior frame contributed by the adjacent interior frames which are much stiffer.

Comparing sway for cases 1j and 1k with those for 1h and 1i (Fig. 5.3) respectively, the top sway in the absence of infills increases 1.53 times and in the presence of infills 16.13 times due to interactive analyses. The

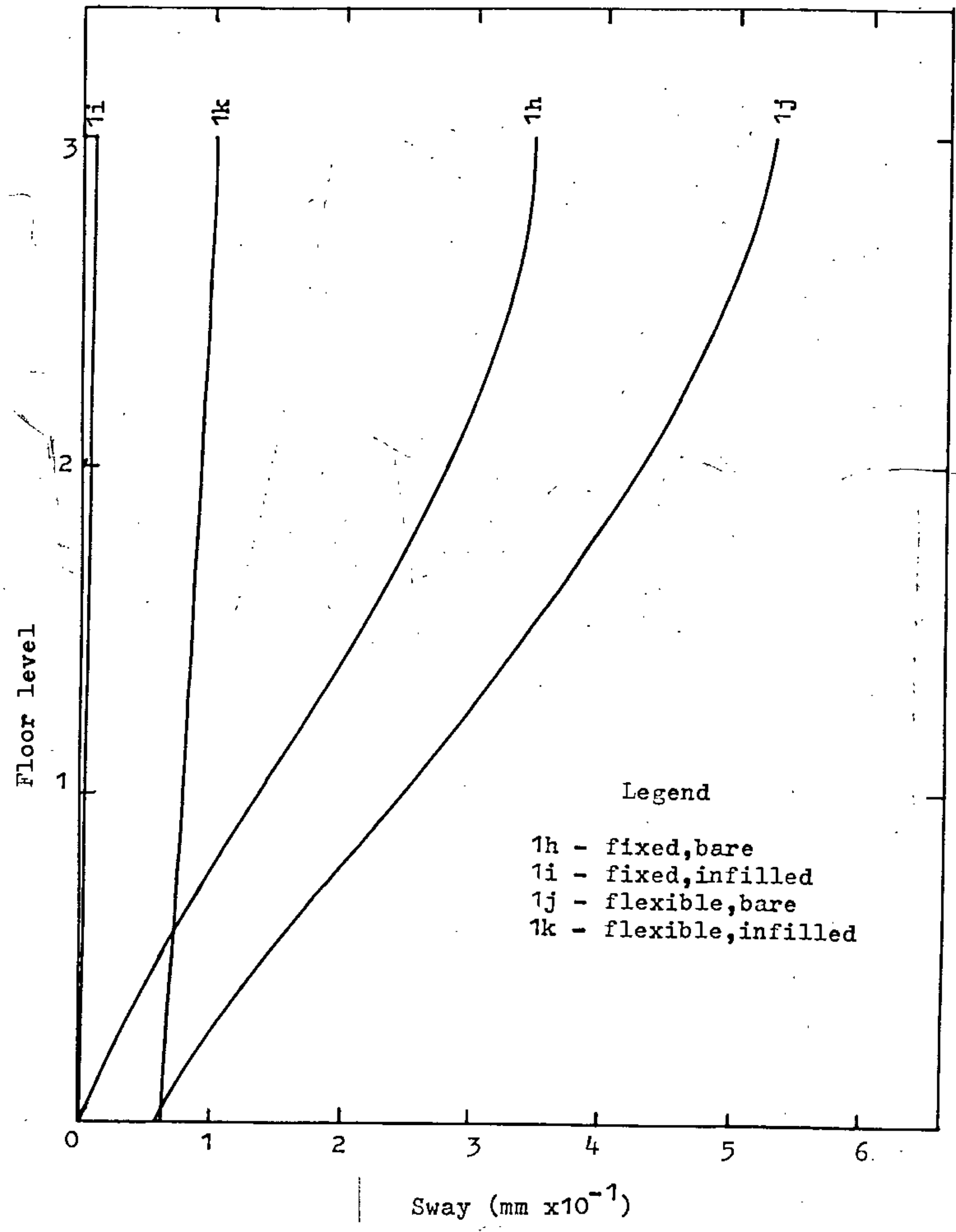

FIGURE 5.3 SWAY AT DIFFERENT FLOOR LEVELS OF THE EXTERNAL FRAME OF STRUCTURE WITH ASYMMETRIC PLAN CONFIGURATION.

corresponding increases for rectangular plan configuration were higher, 1.885 times and 34.62 times for bare frame analysis and flexible base analysis respectively. This demonstrates the importance of including the soil in analysing structures bare or infilled, and also the importance of selecting inherently stiffer plan configuration.

Sway diagrams in three-dimensions of the T-plan structure at different floor levels are shown in Fig. 5.4. These correspond to analysis cases 1h and 1j for maximum values of the load. It is interesting to note that when moving from external one-bay frame CMOF towards the three-bay frame LNPRJ, the top sway in both of the cases 1h and 1j and the base sway in case 1j gradually decrease. This is considered to be obvious as the T-flange is stiffer than the web in the transverse direction in which the load is acting.

5.2.2 Vertical Deformations of the Structure

Variation in the vertical displacement of point c at the top of the central frame with the load increment factor λ for the first eight analysis cases of the structure with symmetric plan configuration are plotted in Fig. 5.5. Comparison of curves for cases 1b with 1a and 1d with 1c shows that wall infills decrease the vertical deflections for both the fixed base and the interactive analyses. For deflections at maximum load, this reduction is 58.97% for

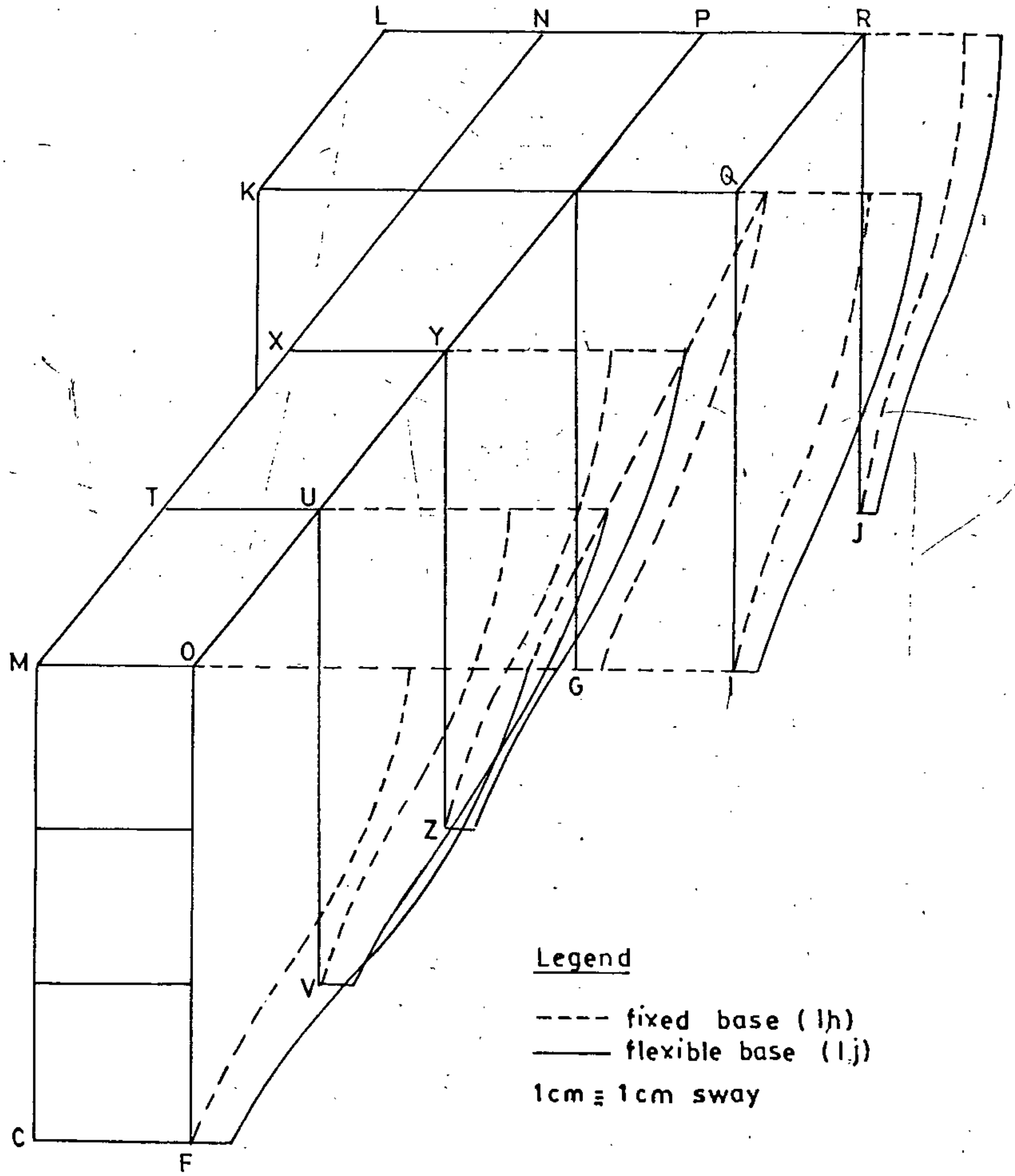

FIGURE 5.4 SWAY DIAGRAM OF THE WHOLE STRUCTURE AT DIFFERENT FLOOR LEVELS FOR ANALYSIS CASES 1h AND 1j.

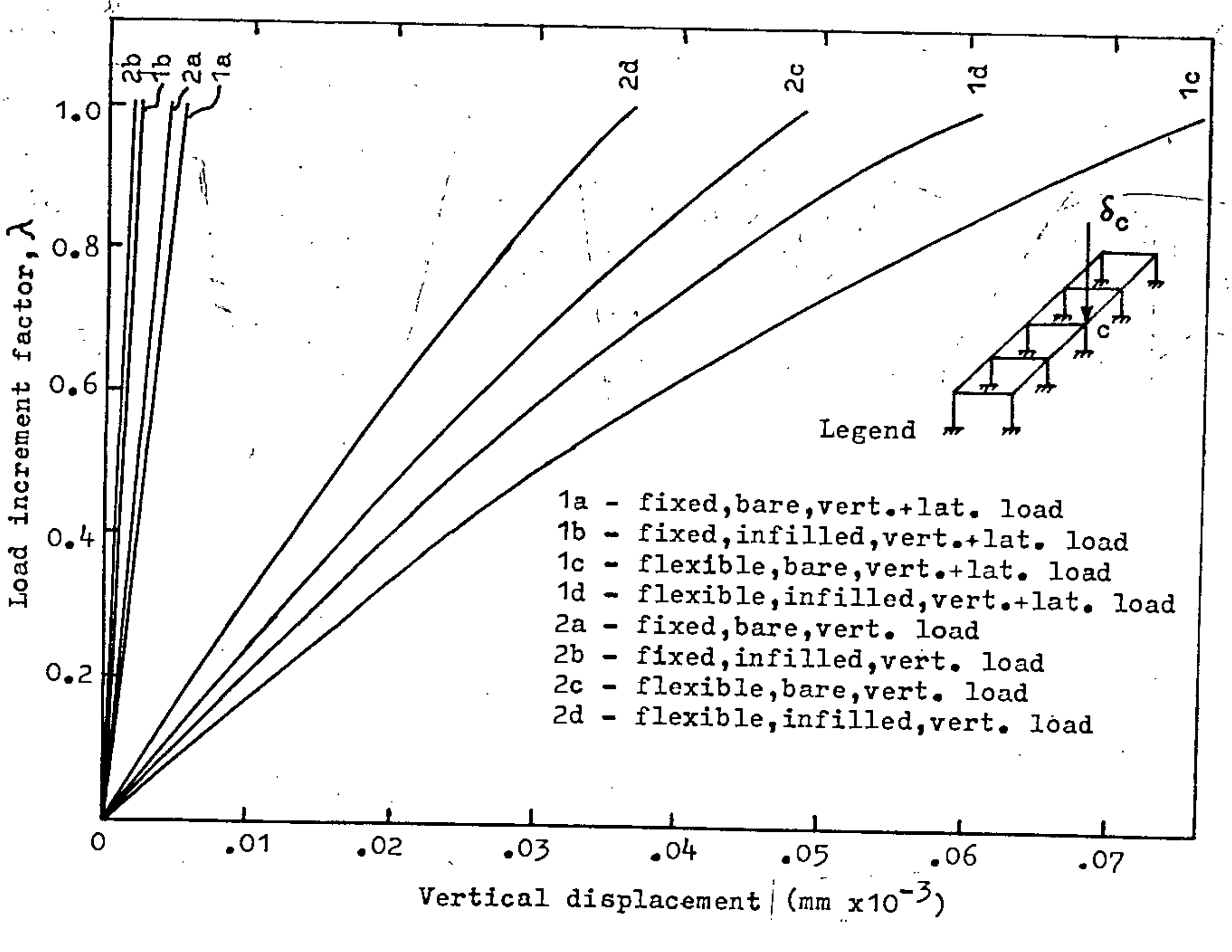

FIGURE 5.5 VERTICAL DISPLACEMENT OF POINT C FOR DIFFERENT ANALYSIS CASES OF STRUCTURE WITH SYMMETRIC PLAN.

fixed base and 20.79% for interactive analyses. It may be noted that the reductions in vertical displacements are much less significant than those in horizontal sway of the same point. This confirms that the fundamental purpose of infill walls, i.e. to increase the frame stiffness against lateral loads, remains significant though perhaps to a lesser extent, when the contribution of soil is accounted for.

The extent of influence of the soil on vertical displacement of point c (Fig. 5.5) in case of bare frame (comparing case 1a with 1c) and in case of infilled frame (comparing case 1b with 1d) is quite considerable. Interactive analysis increases this vertical displacement at maximum load by 14.5 times for bare frame and 28 times for infilled frames.

The influence of soil on vertical displacement of point c (Fig. 5.5) for load case 2 (vertical load acting alone) is identical in nature to that for load case 1 (vertical and lateral load acting simultaneously). Comparison of curves for cases 1a with 2a and 1b with 2b shows that additional lateral load does not increase the vertical deflection much for bare or infilled frames on fixed base. The respective increases are only 20.46% and 22.16%. Similar comparison of curves for interactive analyses shows a considerable increase in the displacement of point c. Comparing curves for cases 1c and 1d with curves for cases 2c and 2d, the computed increases are 56.38% and 65.84% respectively. This increased effect of lateral loads in amplifying vertical displacement is attributable to the displacements of the soil, which can be accounted for only by an interaction analysis.

Curves in Fig. 5.6 illustrate the relative vertical displacements of point C with respect to points A and B at the top of the structure plotted against the load increment factor λ for analysis cases 1c and 1d. For the same cases, the gradients of relative vertical displacements among the points mentioned are plotted against λ in Fig. 5.7. Comparing curves of Fig. 5.7, it is found that the relative displacement of point C with respect to point A exceeds that with respect to point B for both infilled and bare frames. The correspon-ding gradients from Fig. 5.7 give a different picture. The gradient of relative vertical displacement of point C with respect to B exceeds significantly the same gradient of deflection with respect to point A. However, one thing is common in both the figures; orthotropic infills decrease both the relative vertical displacement of a point and the gradient of relative vertical displacements.

5.2.3 Displacements of the Foundation

Displacement for cases 1c, 1d, 2c, and 2d (solid lines) and differential displacement for cases 1c and 1d (dotted lines) of the raft under the central frame of rectangular structure

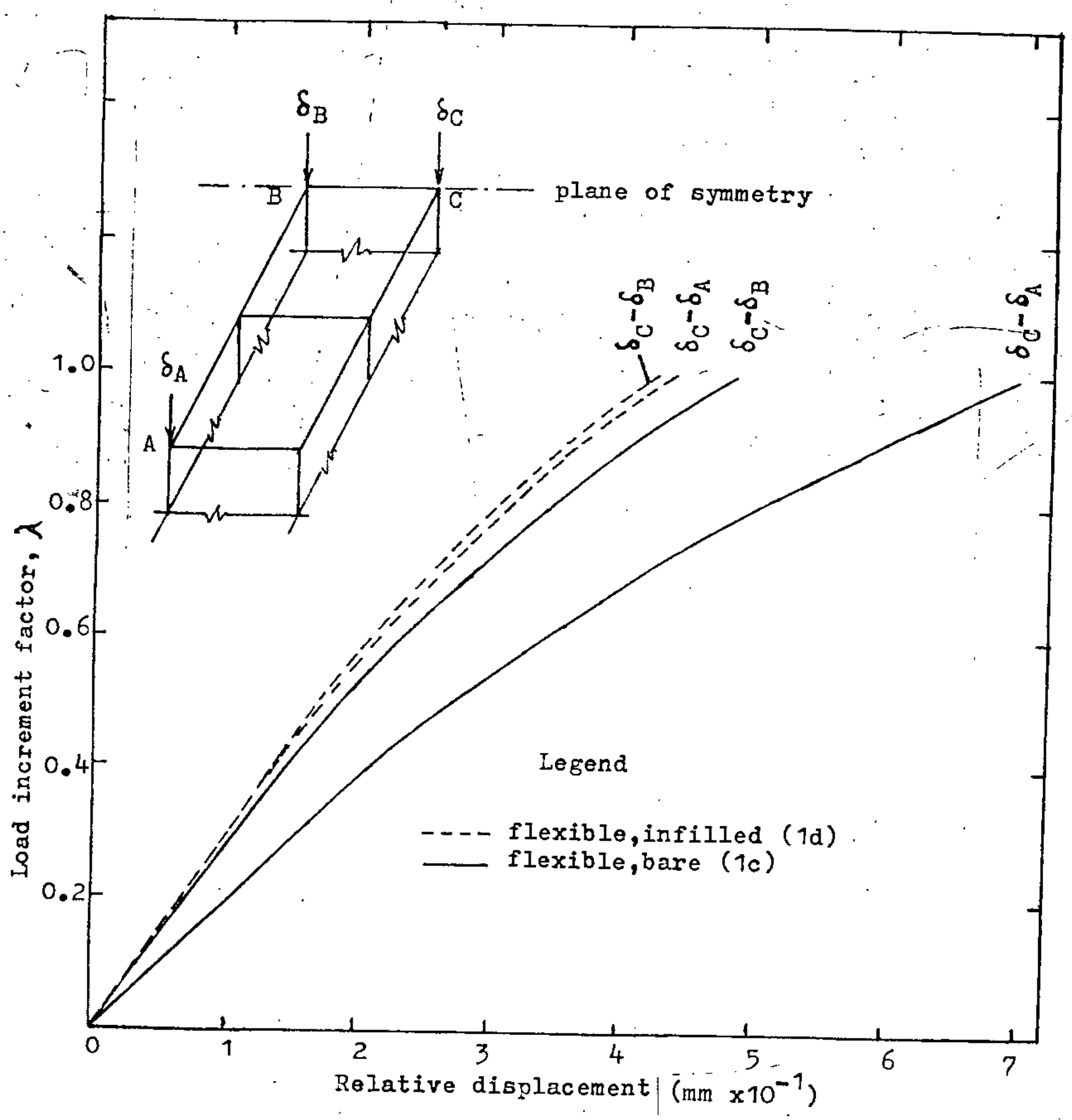

FIGURE 5.6 RELATIVE VERTICAL DEFLECTION OF DIFFERENT POINTSOF STRUCTURE WITH SYMMETRIC PLAN FOR ANALYSIS CASES1c AND 1d.

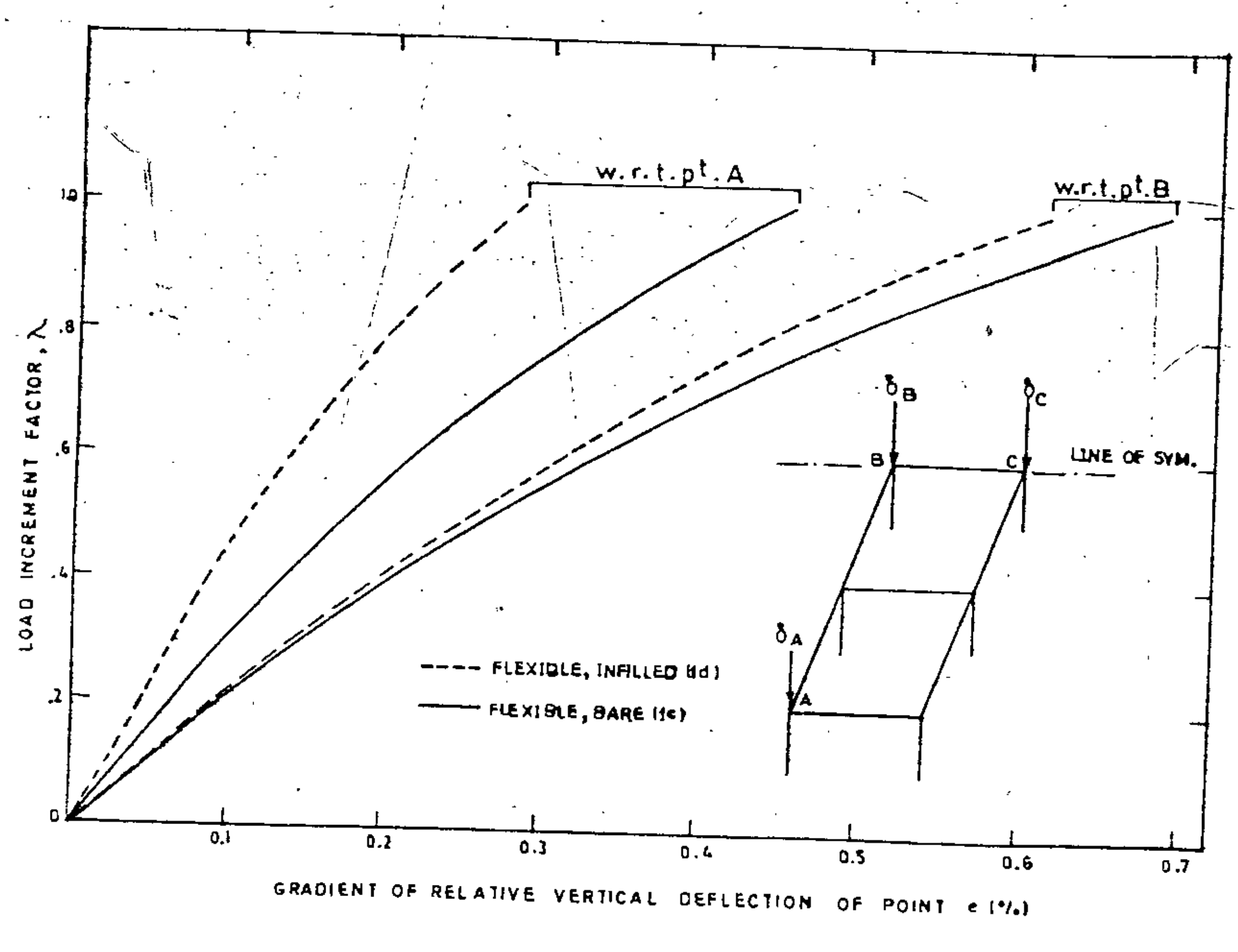

FIGURE 5.7 GRADIENT OF RELATIVE VERTICAL DEFLECTION OF POINT C WITH RESPECT TO POINTS A AND B IN PERCENTAGE FOR CASES 1c and 1d.

are shown in Fig. 5.8 drawn against load increment factor λ. Comparing cases 1c with 1d and 2c with 2d, it is observed that the orthotropic walls reduce the displacement in both the load cases. These reductions are 17.77% and 21.67% respectively. However, as with the vertical displacement of points in the structure, this influence of wall infills on displacement is seen to be less significant compared to that on horizontal sway discussed previously. Superposition of the horizontal wind loading on vertical load increases the displacement both in the presence and in the absence of orthotropic wall infills. This becomes evident from a comparison between the curves for cases 2c and 2d with those for 1c and 1d respectively. Observing displacement and differential displacement curves for cases 1c and 1d, it is apparent that the influence of wall infills on the displacement itself is more pronounced than that on the differential displacement. This observation is significant as it is the differential displacement that induces stresses in the structure.

The variation of displacement with λ for cases 1c, 1f, and 1g is shown in Fig. 5.9. The depth of soil included in the interactive analysis is found to influence the displacement, though not to any significant degree. At maximum load, the displacement obtained by taking 8, 6, and 4 m soils are 70.9 mm, 65.3 mm and 61.1 mm respectively for the rectangular structure. Reducing the soil depth included in the analysis

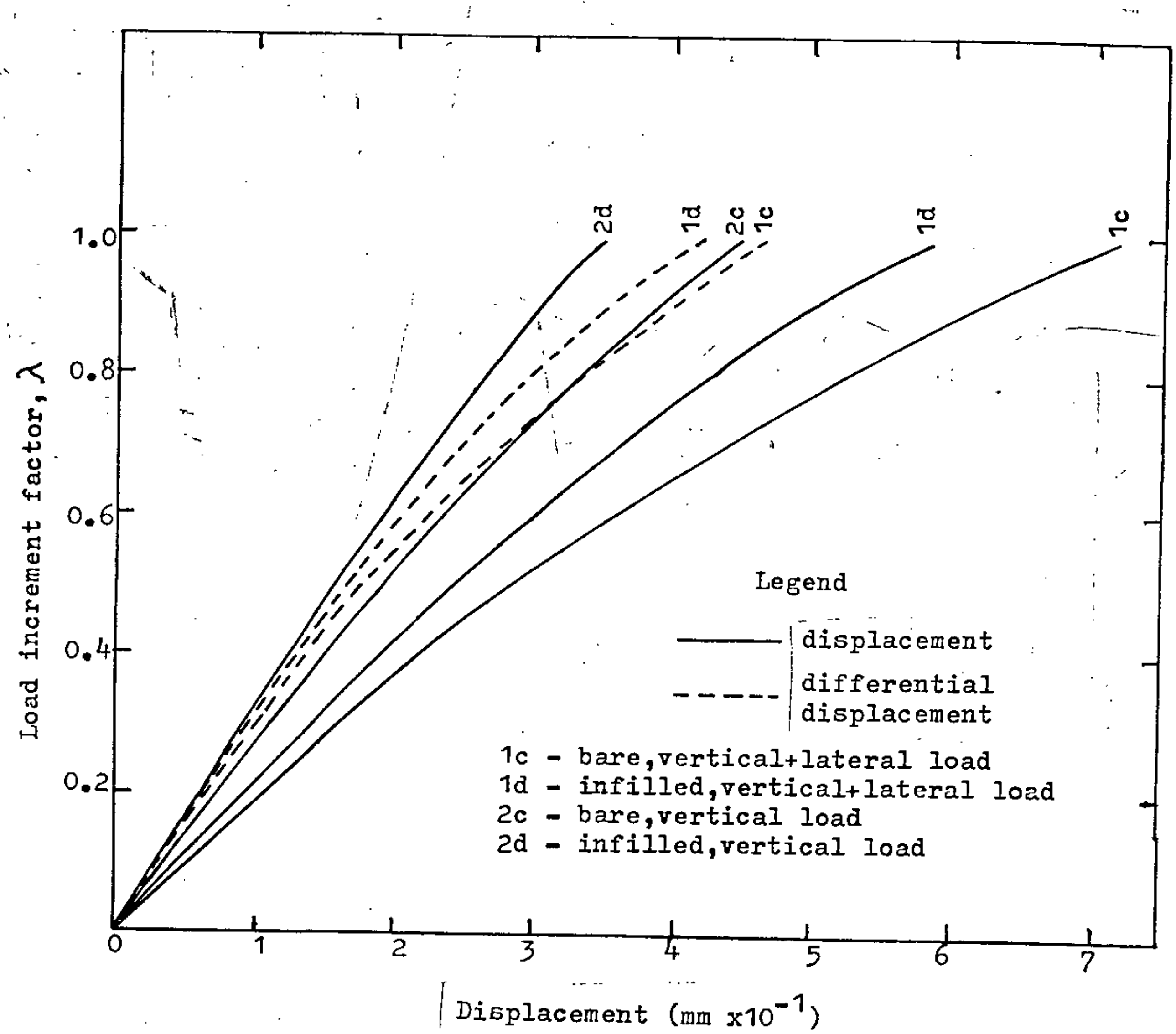

FIGURE 5.8 DISPLACEMENT AND DIFFERENTIAL DISPLACEMENT OF RAFT UNDER INTERNAL FRAME OF STRUCTURE WITH SYMMETRIC PLAN CONFIGURATION FOR DIFFERENT ANALYSIS CASES

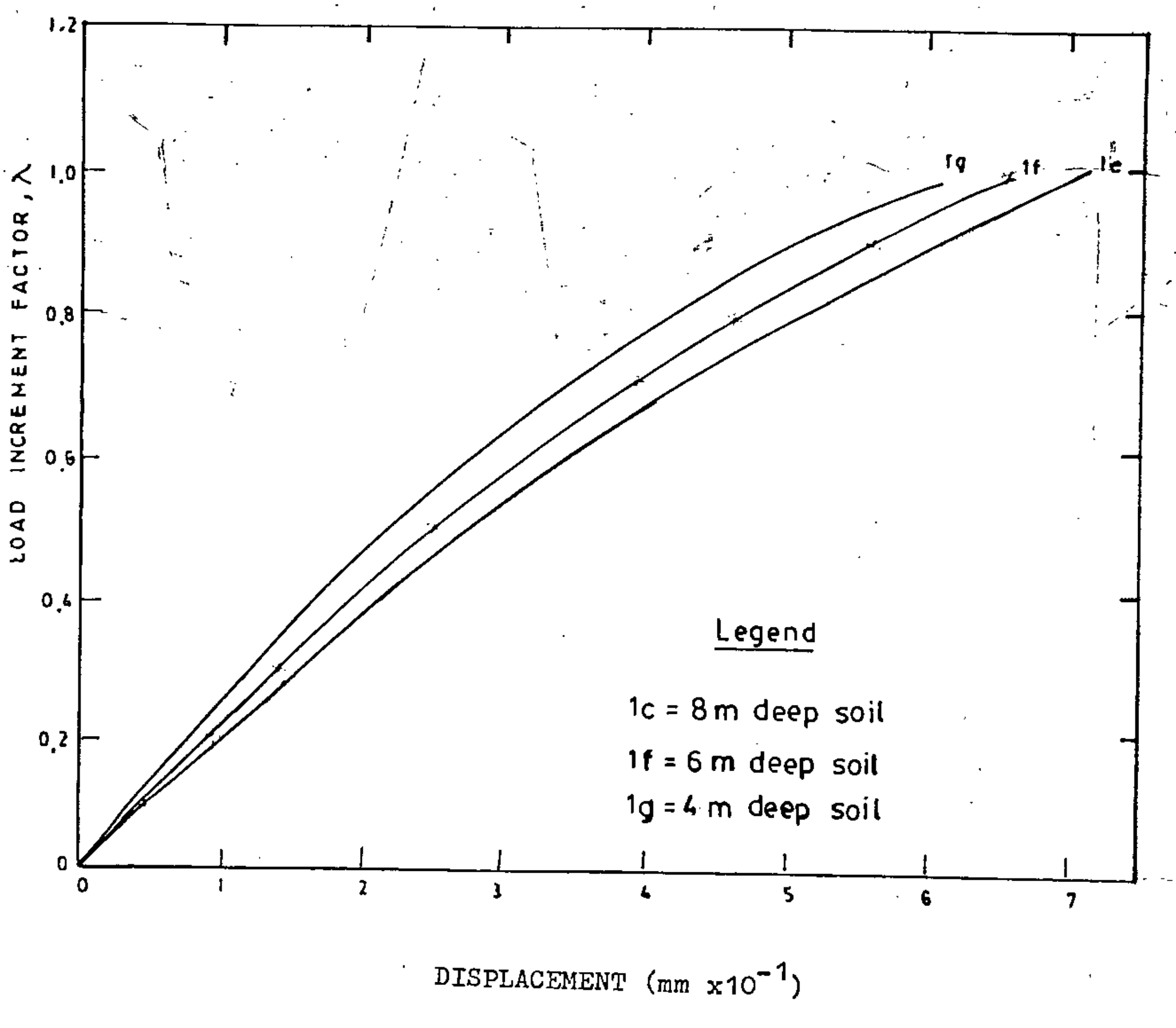

FIGURE 5.9 LOAD-DISPLACEMENT CURVES FOR DIFFERENT SOIL THICKNESSES.

to half reduced the displacement by only 13.8%. This is considered to be due to the fact that soil strains diminish rapidly with depth and that only a moderate depth of soil included in the analysis will suffice for a reasonable interaction analysis.

The variation of top sway of the central frame and the differential displacement under it with the thickness of underlying soil strata is shown in Fig. 5.10. A sudden increase in both the sway and the differential displacement is observed when the soil is included in the analysis. However, the flatness of the upper region of the curves confirms the observation that inclusion of a great depth of soil does not significantly increase the sway or the differential displacement.

The three-dimensional deformation of the raft under the rectangular structure in presence and in absence of wall infills are shown in Fig. 5.11. The deformation is the combined effect of vertical displacement and horizontal displacement. The difference of vertical maximum deflections under the central and exterior frames is negligible (3.39%) for infilled frame and considerable (36.56%) for bare frame. The more pronounced warping of the raft under the bare framed structure indicate that the stiffer infilled frames help distribute the stresses more evenly under the raft.

Displacement under column G and differential displacement between columns D and G of frame AKQI and the same quantities

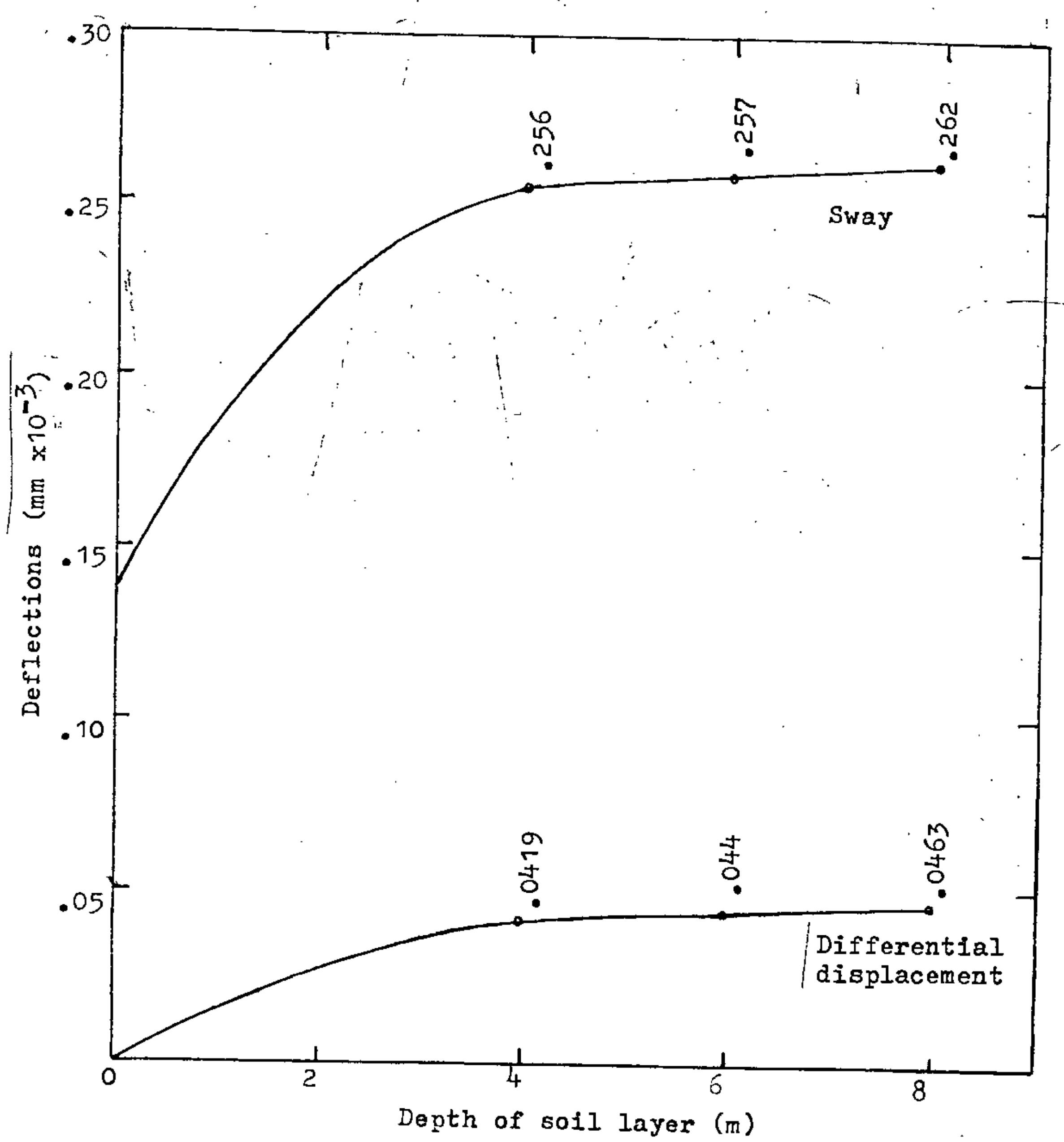

FIGURE 5.10 VARIATION OF SWAY AND DIFFERENTIAL DISPLACEMENT WITH DEPTH OF SOIL FOR A RAFT THICKNESS OF 0.3048 m.

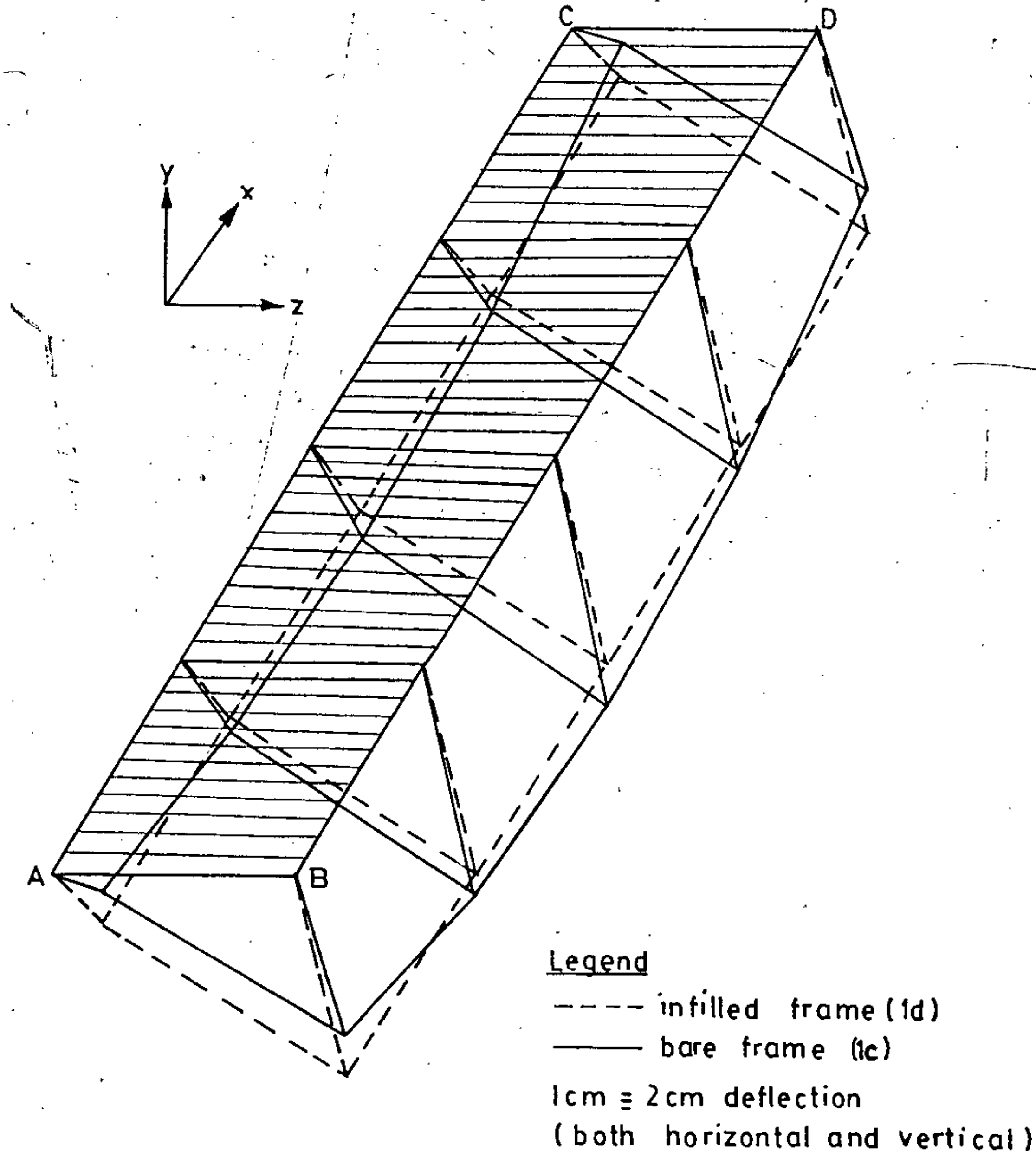

FIGURE 5.11 DEFLECTED SHAPE OF THE RAFT FOR ANALYSIS CASES 1c AND 1d (SHOWING y AND z DEFLECTIONS).

under column OF and between column CM and OF of frame CMOF of the structure with T-plan configuration are plotted against load increment factor λ in Fig. 5.12 for interactive analysis cases (1j and 1k). The displacement under column G of frame AKQI is less when infilled, and the reduction is 27.64% at maximum load with respect to the bare frame. But the differential displacement between the columns D and G under the same frame is more for infilled case, the reduction in the absence of infills being 25% at maximum load. For the external frame CMOF, the picture is the reverse. The displacement under column OF of this frame is less for bare structure, the reduction being 14.43%. The differential displacement, on the other hand, under frame CMOF are much reduced if orthotropic infill walls are present, and the reduction at maximum load is 72.62%. This differential behaviour under the internal and external frame characterizes the T-plan structure and was not noticed in the rectangular structure.

Fig. 5.13 shows the three-dimensional deflected shapes of the raft under T-plan structure for both bare and infilled frames. It is evident in this figure also that for bare structure the maximum displacement occurs under the internal frame AKQI and the minimum under frame CMOF. For the same bare structure the maximum differential displacement between two central columns occurs under exterior frame CMOF and the minimum under internal frame AKQI. The general tendency of

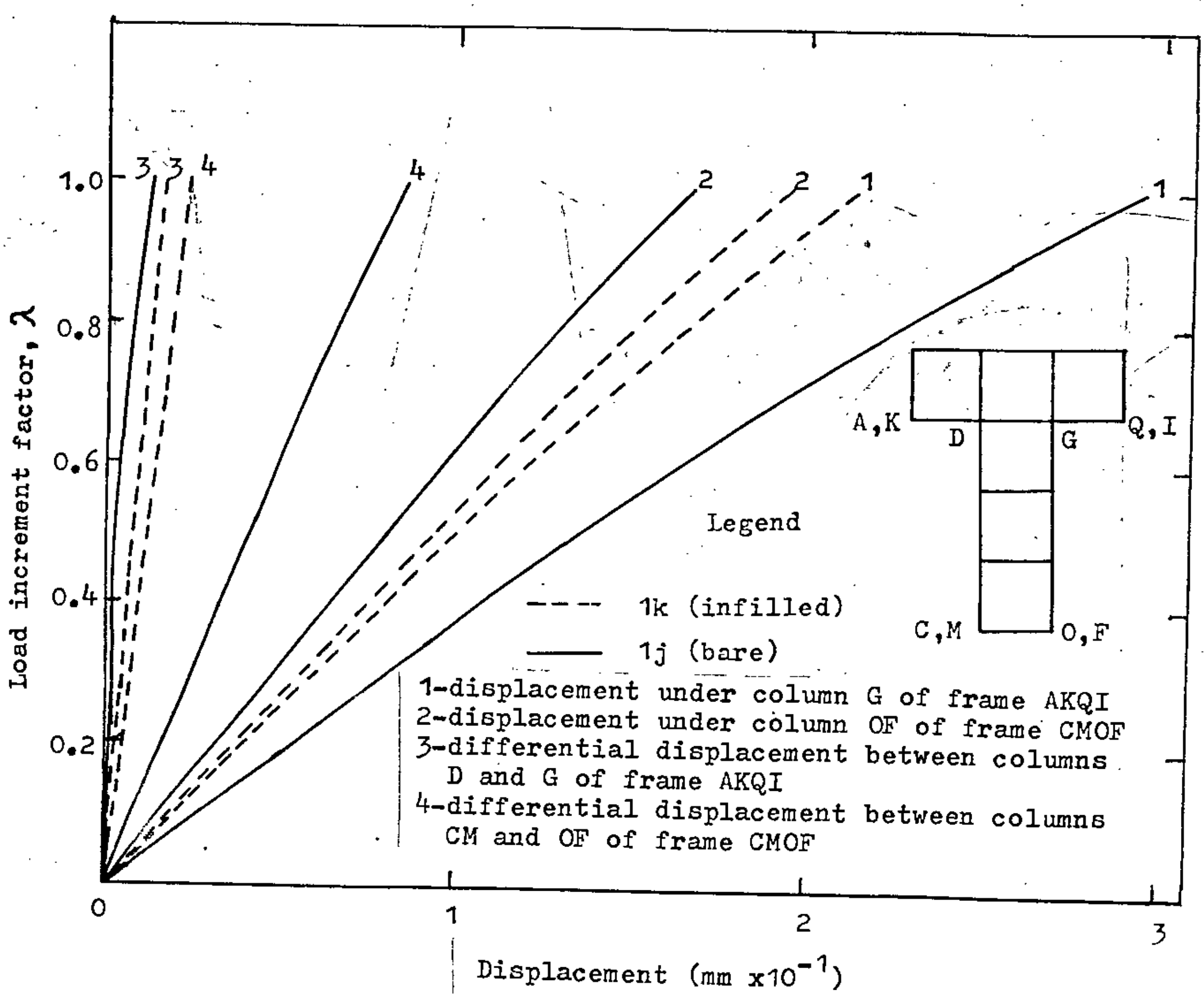

FIGURE 5.12 DISPLACEMENT AND DIFFERENTIAL DISPLACEMENT OF RAFT OF STRUCTURE WITH ASYMMETRIC PLAN CONFIGURATION FOR ANALYSIS CASES 1j AND 1k.

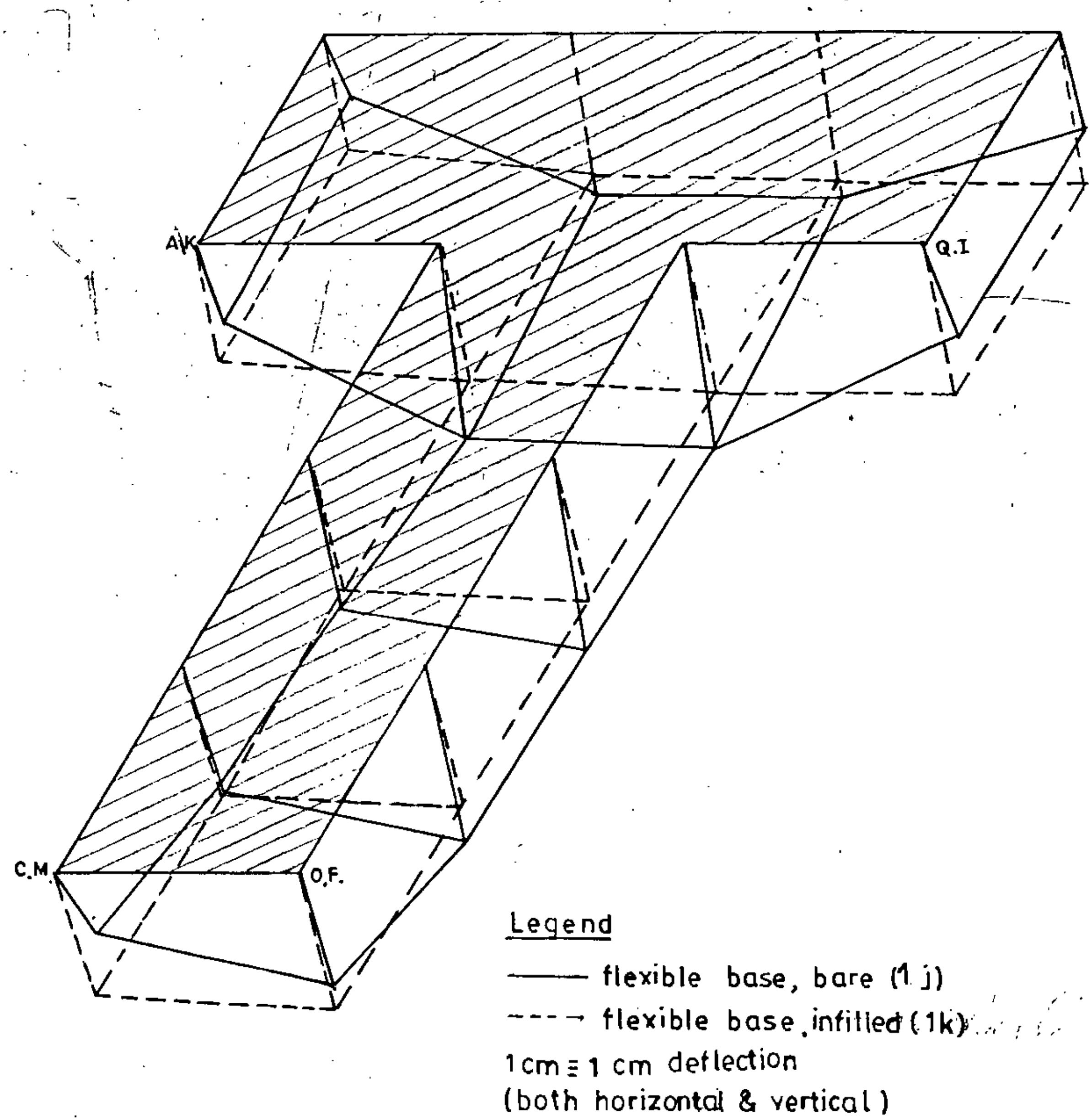

FIGURE 5.13 DEFLECTED SHAPE OF RAFT FOR THE STRUCTURE WITH ASYMMETRIC PLAN CONFIGURATION FOR ANALYSIS CASES 1j AND 1k.

the infill walls to even out the differential displacement of the raft is evident also for T-plan structure as with the rectangular structure.

5.3 BENDING MOMENTS IN FRAMES

The bending moment distribution in the beams of an internal frame of the rectangular structure for bare frame analyses (cases 1a and 1c) are shown in Fig. 5.14a. The same for infilled frame analyses (cases 1b and 1d) are shown in Fig. 5.14b. It is apparent from both the figures that consideration of soil in the interactive analysis has negligible effect on these moment distributions, both qualitatively and quantitatively. Whereas comparing curves of Fig. 5.14b with those of Fig. 5.14a, it is observed that infill walls decrease the beam moments to a very significant degree (98.19% for the bottom floor beam). The signs of the moments, however, remain the same.

Column bending moments for bare frame analysis are shown in Fig. 5.15 and those for infilled frame analysis in Fig. 5.16 for the same frame mentioned above. Soil is again found to have almost no effect on column bending moments. Infill walls, however, as before significantly reduce the column moments (97.8% for bottom column). Therefore, it is evident that the infills in a structure can contribute significantly to reduce the beam and column moments. The reason for the lack of influence of soil on the beam and

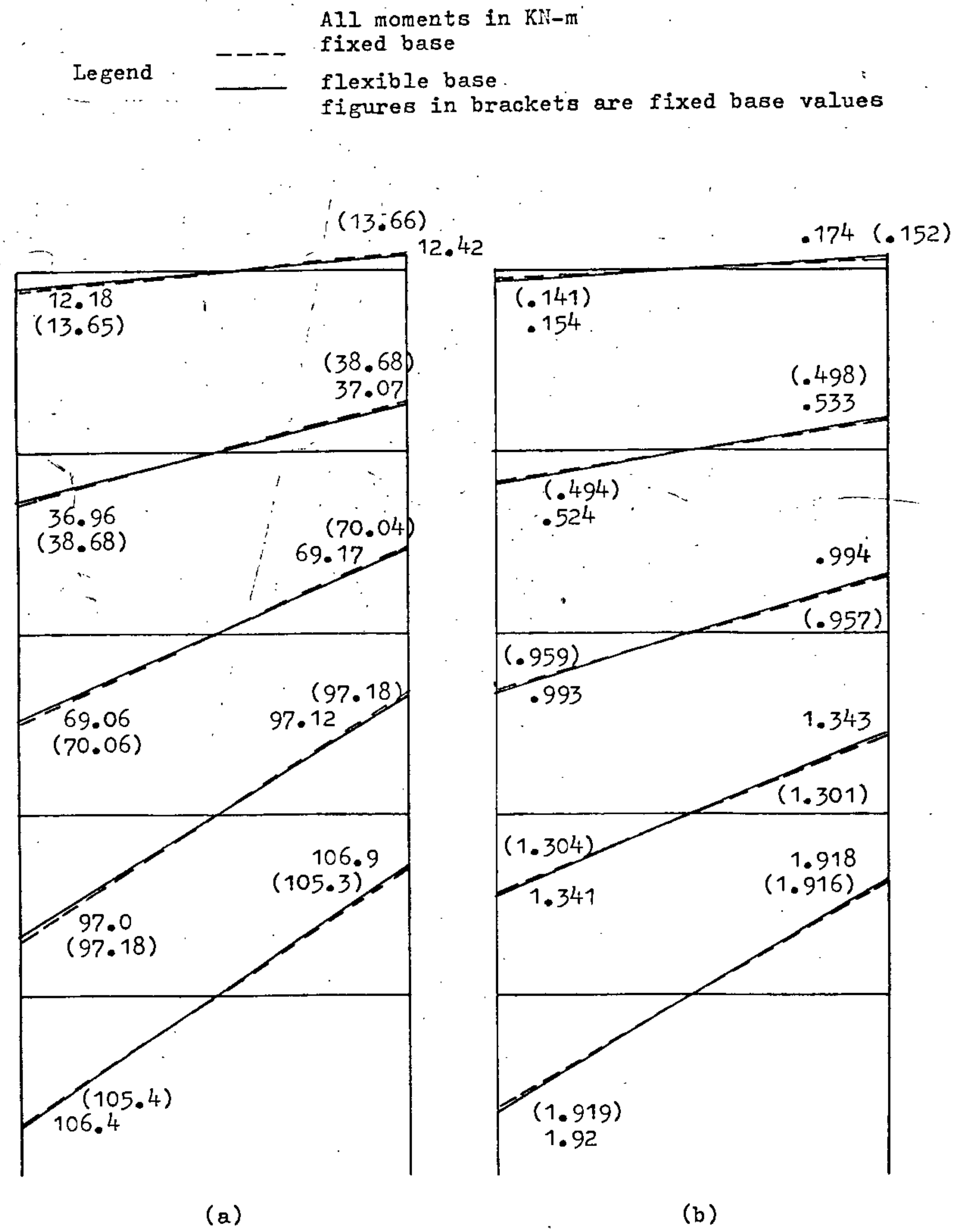

FIGURE 5.14 BEAM BENDING MOMENTS OF THE INTERNAL FRAME (a) ANALYSES 1a AND 1c (b) ANALYSES 1b AND 1d.

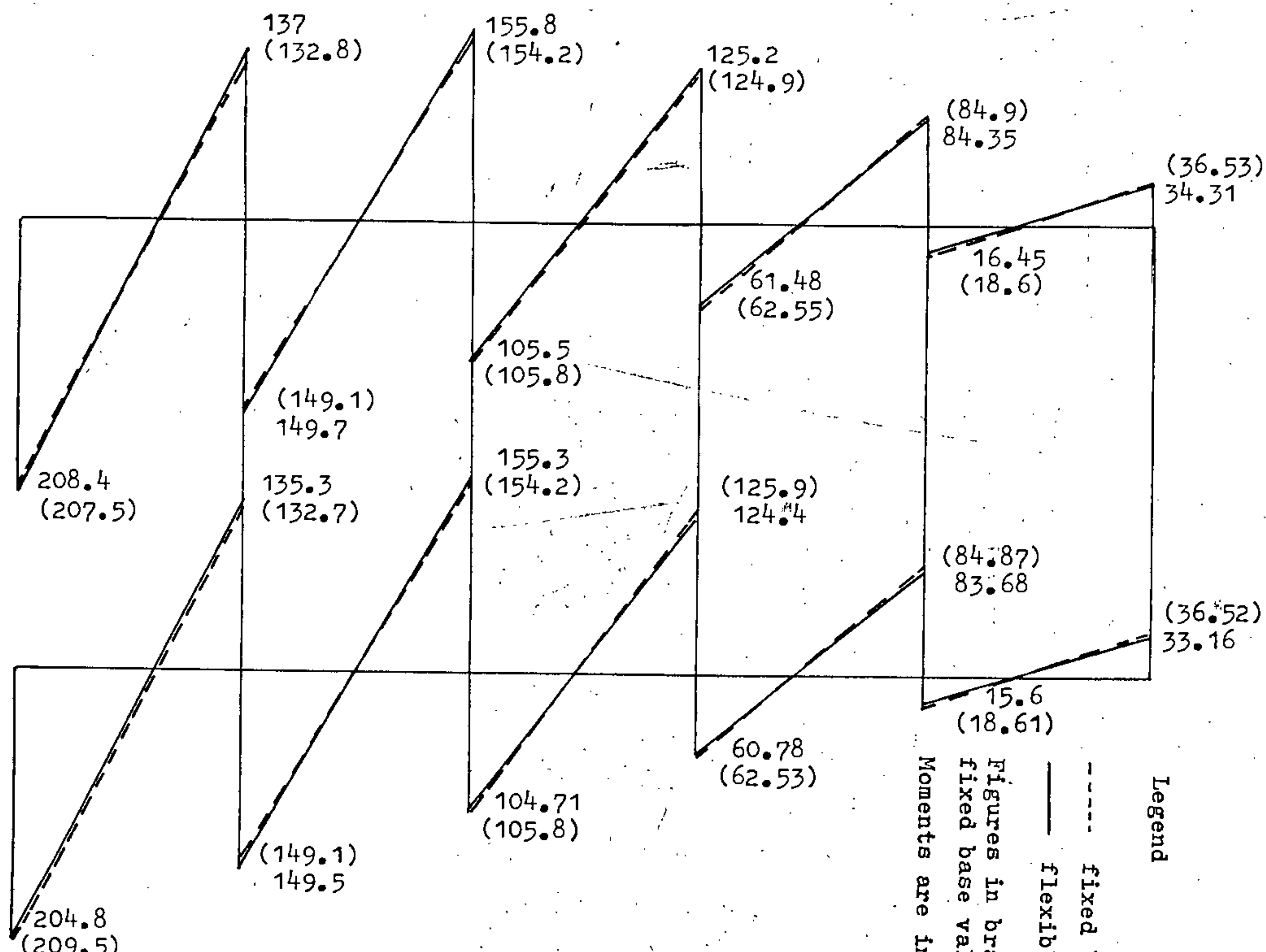

Legend

----- fixed base (1a)

—— flexible base (1c)

Figures in brackets are fixed base values

Moments are in KN-m

FIGURE 5.15 COLUMN BENDING MOMENTS OF THE INTERNAL FRAME OF STRUCTURE WITH SYMMETRIC PLAN: 1a AND 1c.

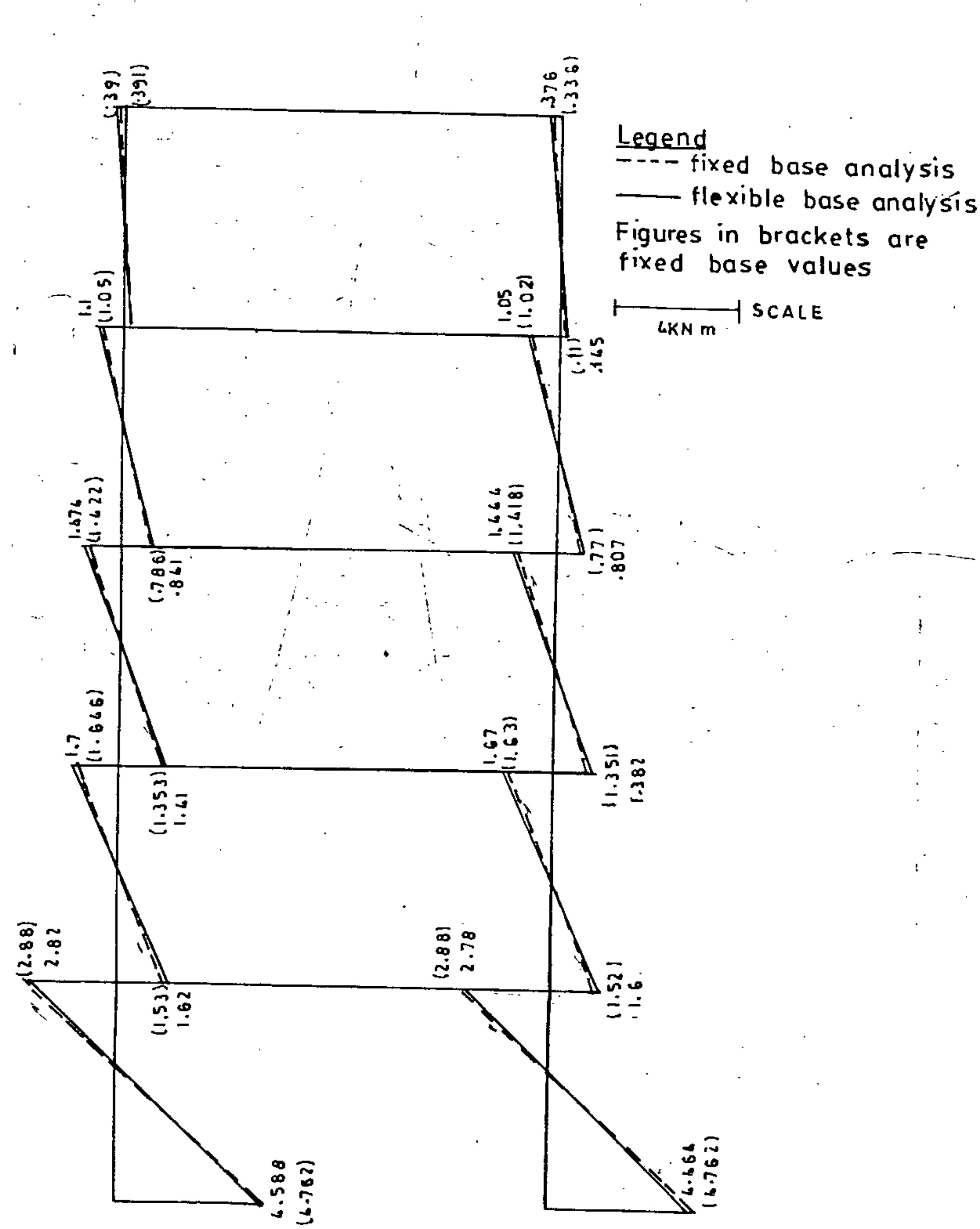

FIGURE 5.16 COLUMN BENDING MOMENTS OF THE INTERNAL FRAME OF STRUCTURE WITH SYMMETRIC PLAN: ANALYSIS CASES 1b AND 1d.

column moments may be due to the presence of a stiff continuous raft under the columns. Then bending moments are expected to be much different for the fixed base and interactive analyses if the columns were supported on isolated footings.

Variation of column bending moments with different floor levels for load case 1 is shown in Fig. 5.17a for bare frame analysis and in Fig. 5.17b for infilled frame. The influence of infill walls become evident when curves in Fig. 5.17b are compared with those in Fig. 5.17a. The infills not only reduce the column moments significantly, but also alter the nature of distribution of moments over the height of the structure.

The variation of bending moment in column EG of the internal frame with λ for bare and infilled frame analyses are illustrated in Fig. 5.18a and Fig. 5.18b respectively. By comparing these two figures, it is observed that infill walls decrease the rate of increase of column bending moments with increasing load.

Column and beam bending moments for the external frame CMOF of T-plan structure are shown in Fig. 5.19a and Fig.5.19b respectively for infilled frame analysis. Magnitude of bending moments diminishes with height, the maximum value being obtained for the bottom storey beams and columns. Bending moments obtained from the fixed base analysis are observed

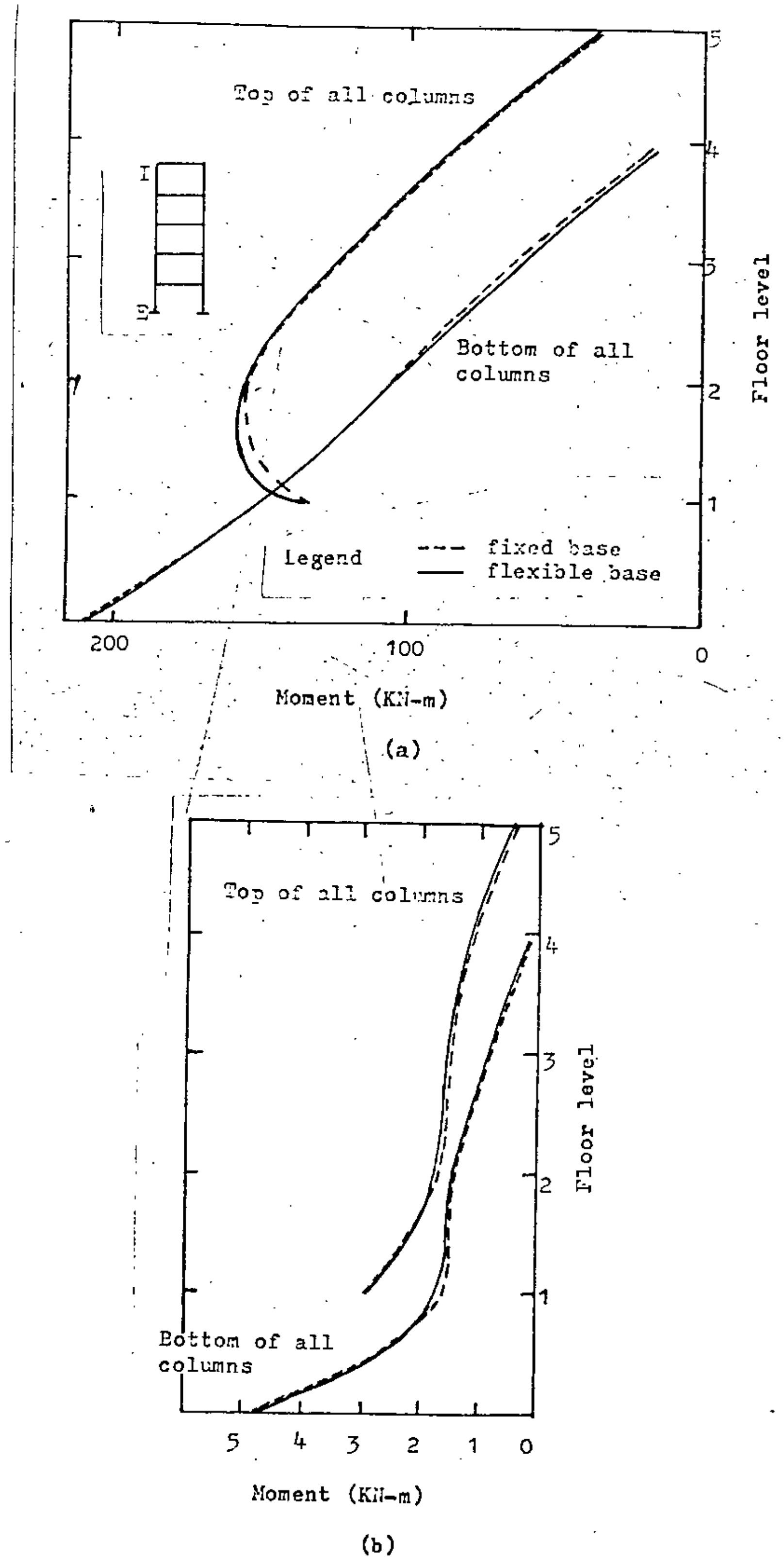

FIGURE 5.17 VARIATION OF BENDING MOMENTS OF COLUMNS FROM E TO I AT DIFFERENT FLOOR LEVEL OF THE STRUCTURE WITH SYMMETRIC PLAN (a) BARE FRAME ANALYSES (b) INFILLED FRAME ANALYSES.

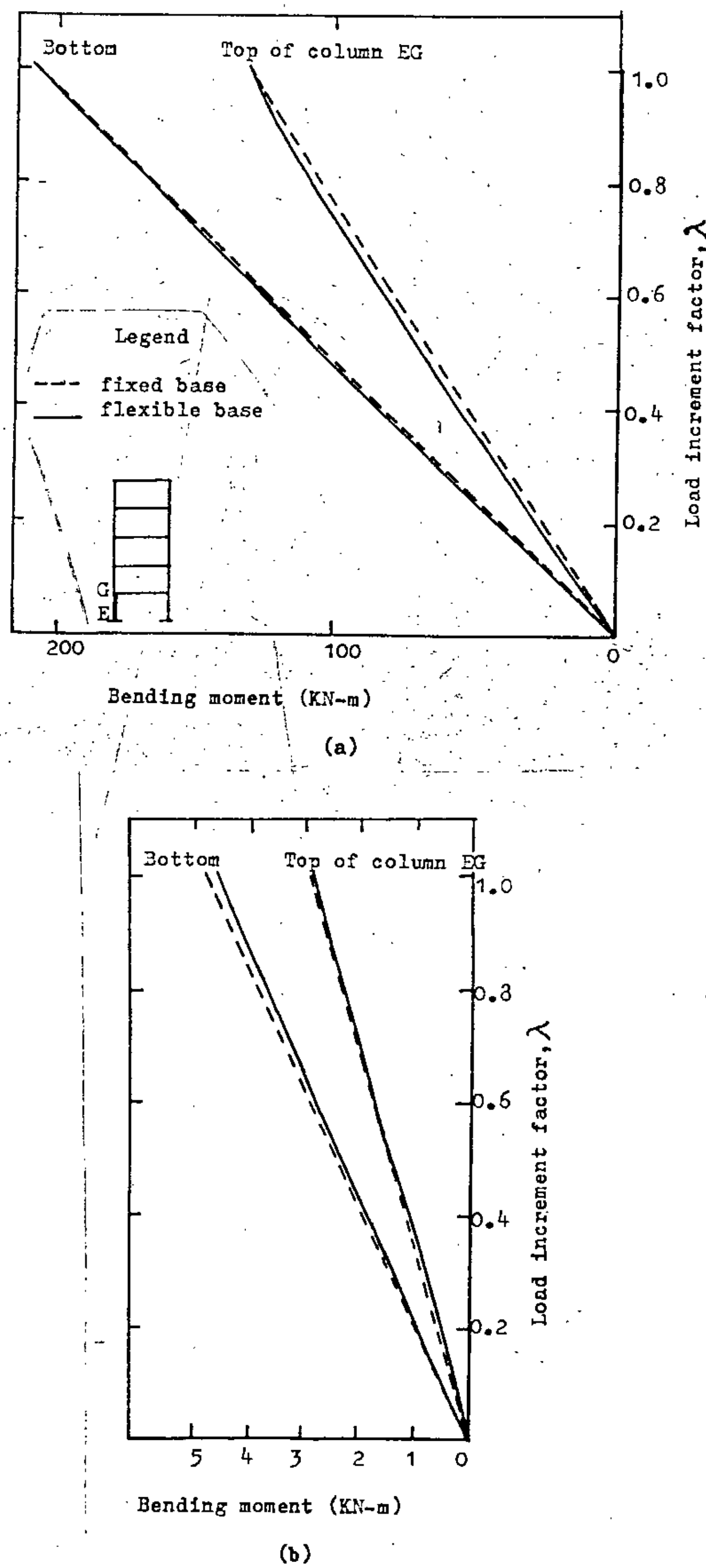

FIGURE 5.18 LOAD-BENDING MOMENT GRAPHS OF COLUMN EG OF THE STRUCTURE WITH SYMMETRIC PLAN (a) BARE FRAME ANALYSES (b) INFILLED FRAME ANALYSES.

to be higher than those from the interactive analysis. At the windward column base, the former exceeds the latter by 43.62%.

Fig. 5.20a and Fig. 5.20b show the column and beam bending moments respectively in the frame CMOF for bare frame analysis. In the absence of infills, bending moments from fixed base and flexible base analyses do not differ much; the windward column base moment from fixed base analysis exceeds that from interactive analysis by only 7.37%.

Comparing curves in Fig. 5.19 with corresponding curves in Fig. 5.20, the orthotropic infills are found to reduce the column and beam bending moments significantly for the T-plan structure as well. At windward column base this reduction is 97.88% for fixed base analysis and 98.41% for interactive analysis. At windward side of bottom storey beam the reduction is 98.34% for fixed base analysis and 98.7% for interactive analysis.

Column bending moments of the internal frame AKQI of T-plan structure for infilled frame analyses are shown in Fig. 5.21 and those for bare frame analyses are in Fig.5.22. The column moments in the internal frame are reduced highly due to presence of infills as in the external frame. Thus the leeward column base moment is reduced by 97.87% in the fixed base analysis and by 95.58% in the interactive analysis.

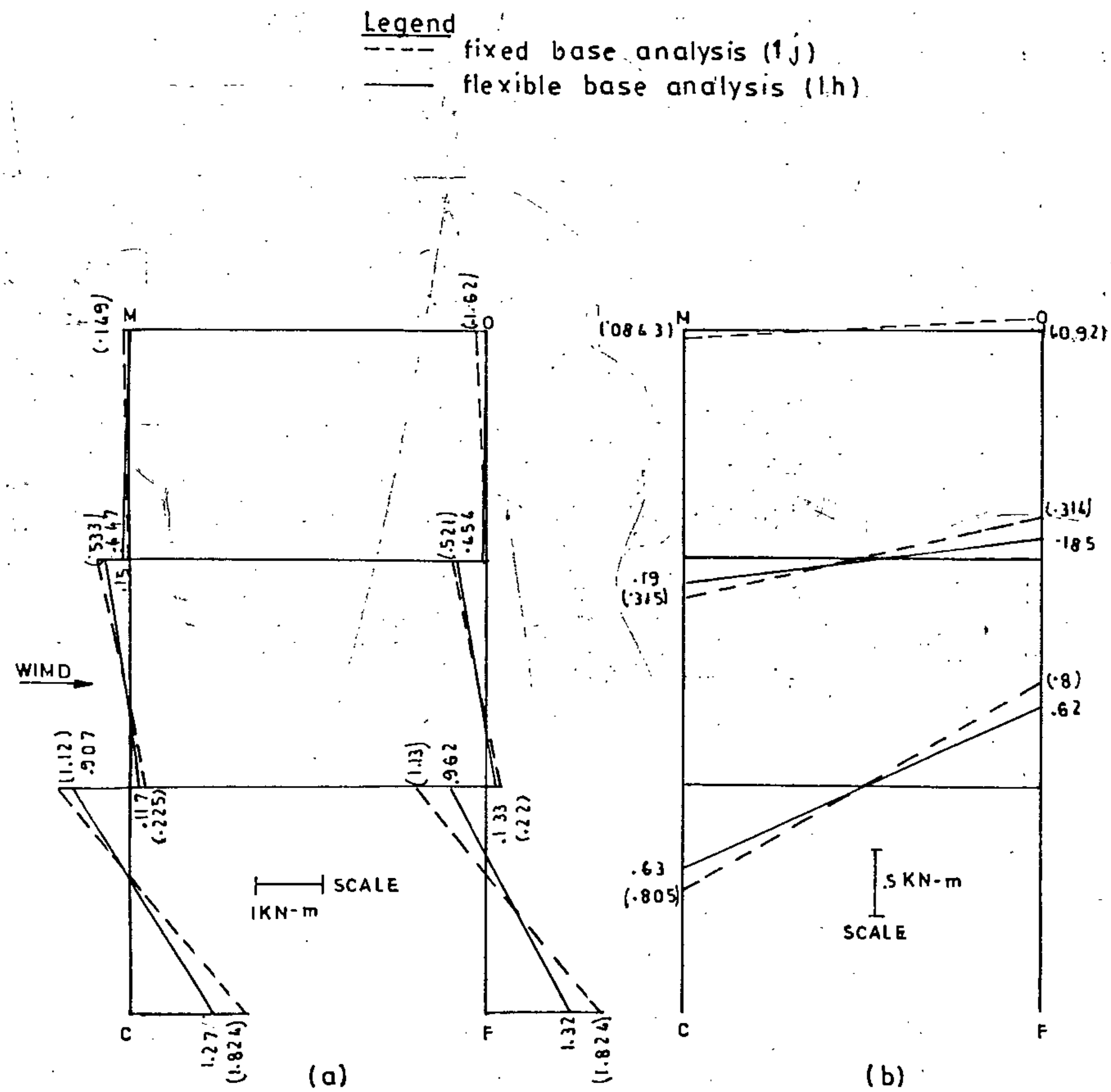

FIGURE 5.19 (a) COLUMN BENDING MOMENTS (b) BEAM BENDING MOMENTS OF EXTERNAL FRAME CMOF FOR ANALYSIS OF INFILLED T-PLAN STRUCTURE.

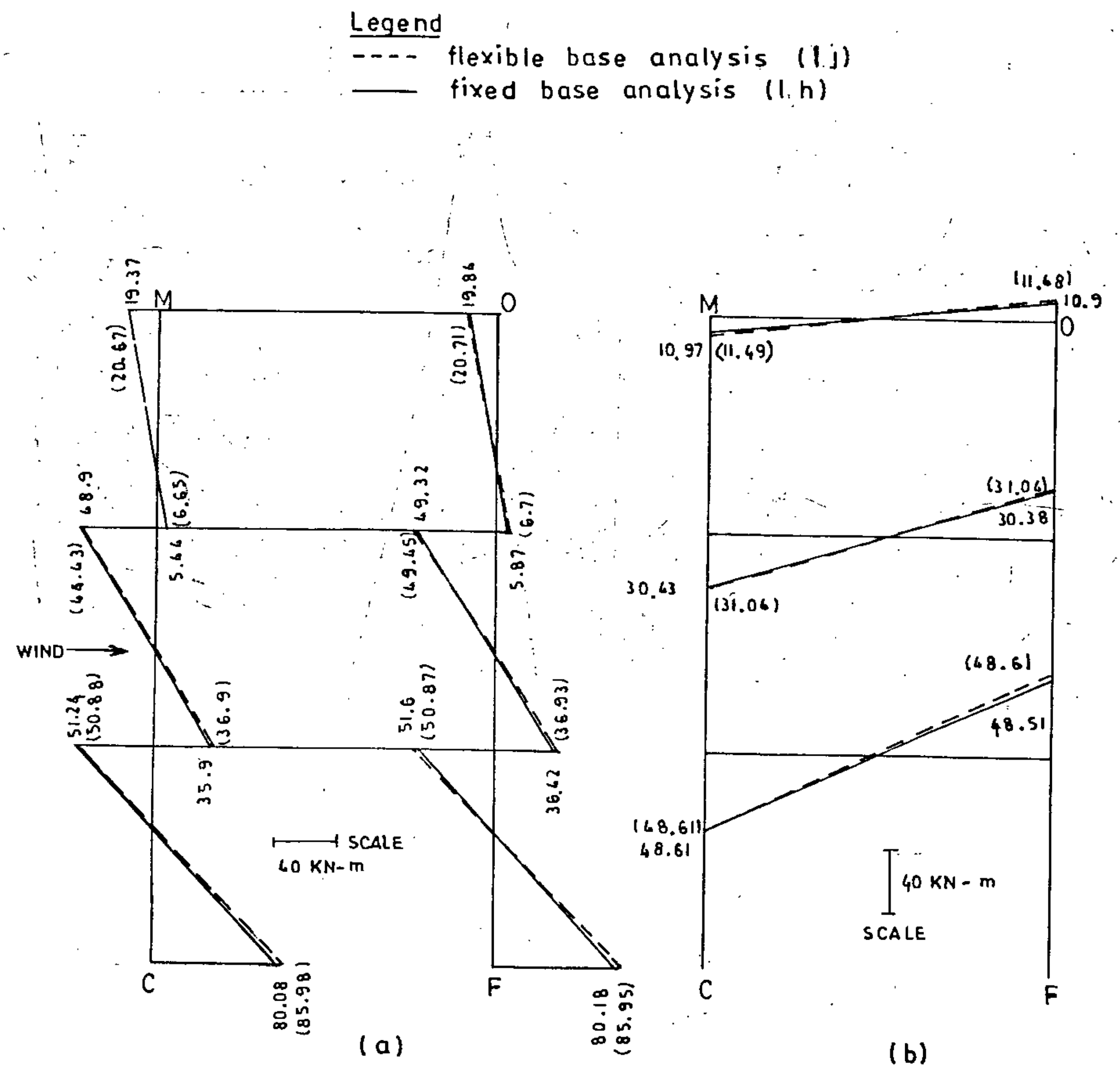

FIGURE 5.20 (a) COLUMN BENDING MOMENTS (b) BEAM BENDING MOMENTS OF EXTERNAL FRAME CMOF OF T-PLAN STRUCTURE FOR BARE FRAME ANALYSIS.

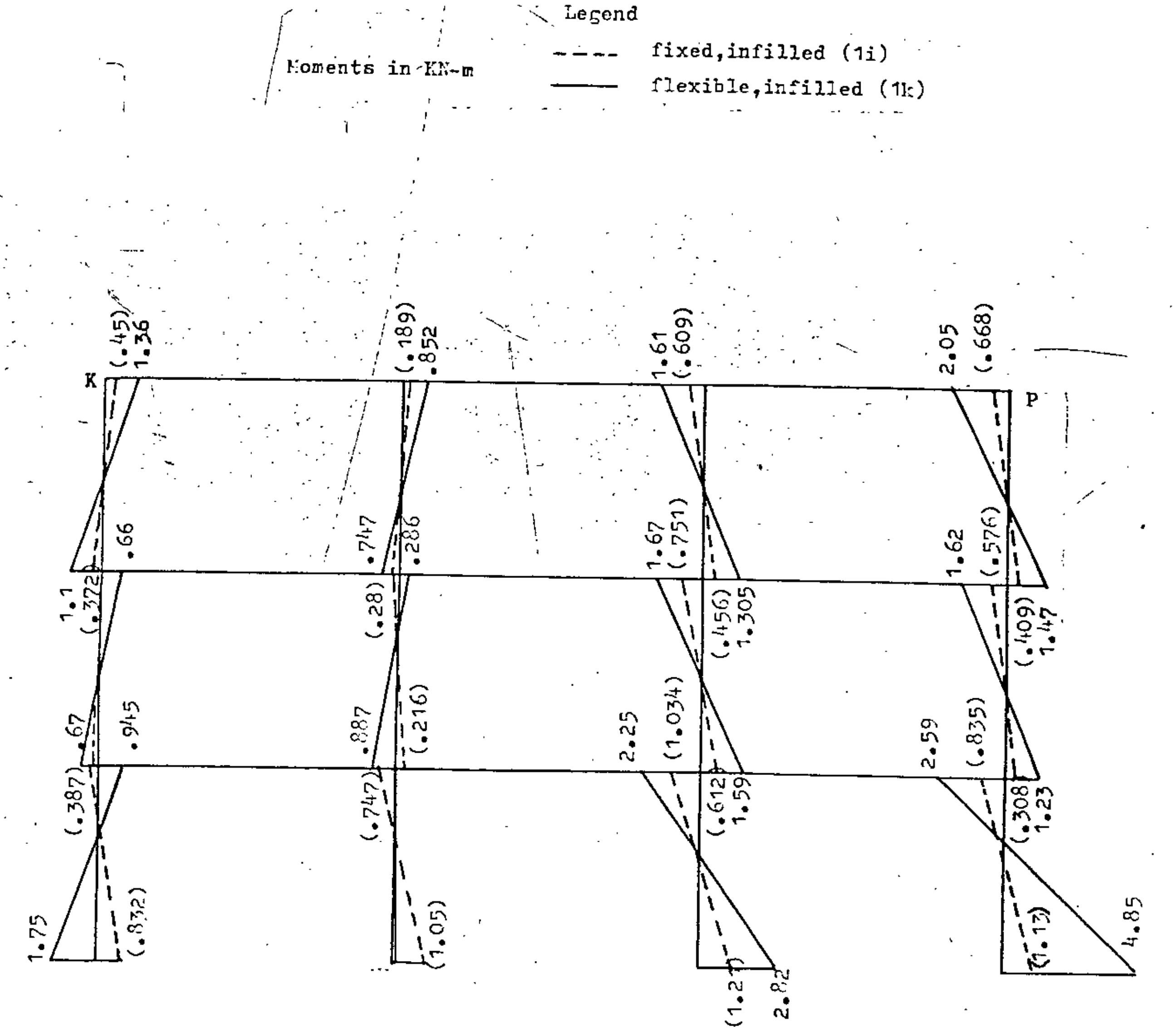

FIGURE 5.21 COLUMN BENDING MOMENTS OF INTERNAL FRAME AKQI OF T-PLAN STRUCTURE FOR INFILLED FRAME ANALYSES.

Legend

Moments in KN-m

Figures in brackets are fixed base values

---- fixed,bare (1h)

—— flexible,bare (1j)

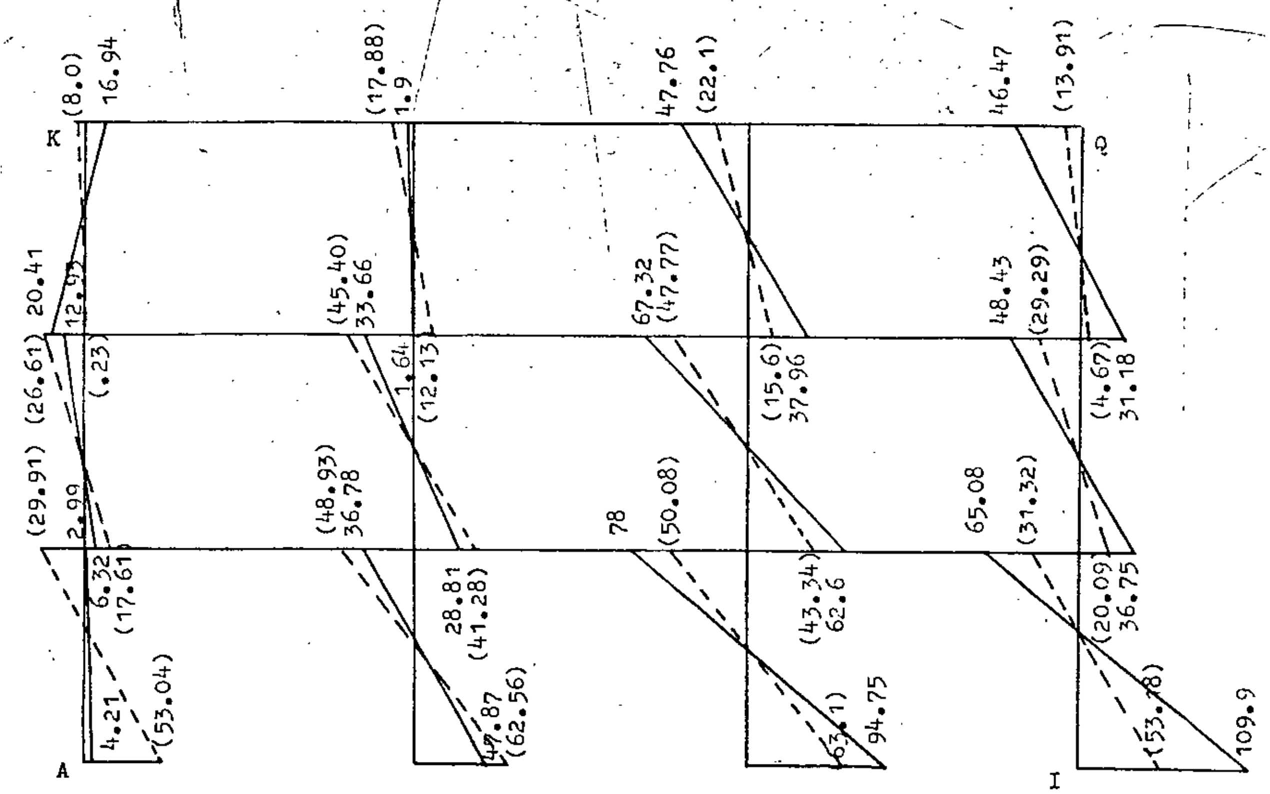

FIGURE 5.22 COLUMN BENDING MOMENTS OF INTERNAL FRAME AKQI OF T-PLAN STRUCTURE FOR ANALYSIS CASES 1h AND 1j.

Shifting of inflection points in certain columns due to interactive analysis is also interesting to note.

The redistribution of the bending moments is most significant at the base of the building in case of the infilled internal frame (Fig. 5.21). At point A the fixed base bending moment is 0.832 kNm and the flexible base moment is -1.78 kNm showing a reversal of the sign. In case of the bare frame, reversal of sign takes place at the top floor (Fig.5.22).

5.4 STRESSES IN SOIL

Distribution of vertical normal stress σ_y (nodal) along the transverse section F-F at soil depths 0,1,2,3, and 8 m under the rectangular structure is shown in Fig.5.23. The distributions are plotted for interactive analysis cases 1c and 1d. The stress variations for both the cases follow more or less the same nature at different depths. However, the presence of infills reduce σ_y slightly. The stress σ_y is also reduced with increasing depth and the maximum is attained under a node which is located at the extreme edge of the raft in the leeward side. The stress σ_y at the soil boundary are negligible but may be tensile, the intensity of which gradually reduces with depth.

vertical stress distribution along the longitudinal section E-E at various soil depths under the same structure is shown in Fig. 5.24 for interactive analyses. Considering the symmetry this has been plotted for the left half only. It is observed from the curves that presence of infill walls increases σ_y beyond the perimeter of the raft and decreases it directly below the raft. For both the cases of infilled or bare structure, the maximum σ_y in the longitudinal direction is recorded under the transverse axis of symmetry. The intensity of σ_y almost vanishes at the soil boundary in this direction also. The pressure distributions reveal that the greater stiffness of the infilled frames results in a more even distribution of soil pressure.

Fig. 5.25 illustrates the distribution of σ_y (nodal) along section F-F at different soil depths under the rectangular structure for interactive analysis with load case 2 (vertical load acting alone). The curves in Fig. 5.25 are symmetric, as expected. The distribution of σ_y in Fig. 5.25 and their general characteristics are identical to those of Fig. 5.23 for load case 1.

The variation of vertical pressure σ_y with depth under various points in plan are plotted in Fig. 5.26 for analysis case 1c. Maximum soil pressure occurs under the raft edge point D in the leeward side. This pressure remains approximately constant upto a depth of 1.5 m and then gradually decreases until it becomes again approximately steady below 3.5 m depth. The qualitative nature of σ_y distribution under other raft edge points J and I in leeward side are similar to that under point D but of reduced intensity. The σ_y

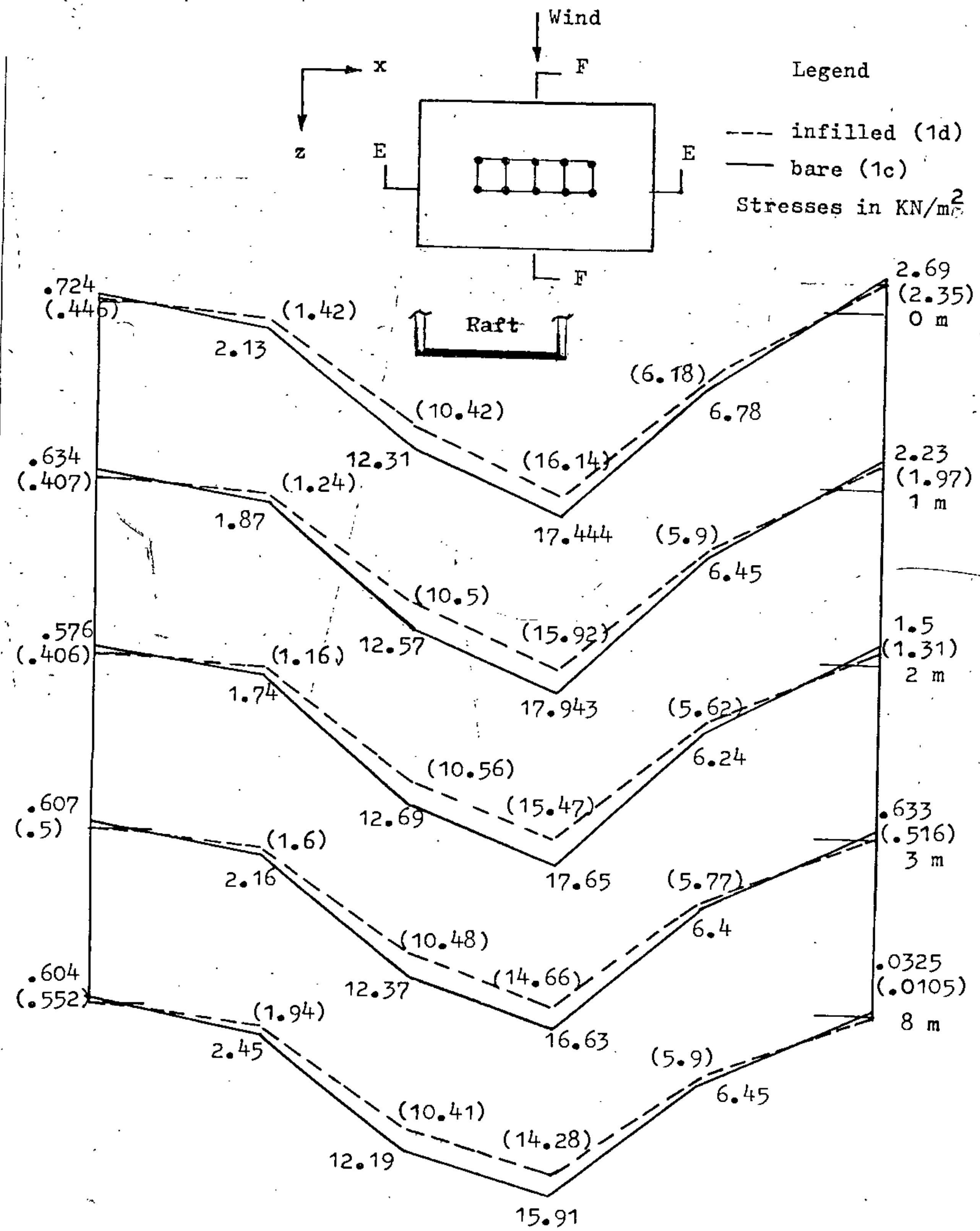

FIGURE 5.23 DISTRIBUTION OF σ_y (NODAL) ALONG SECTION F-F AT VARIOUS DEPTHS FOR ANALYSIS CASES 1c AND 1d.

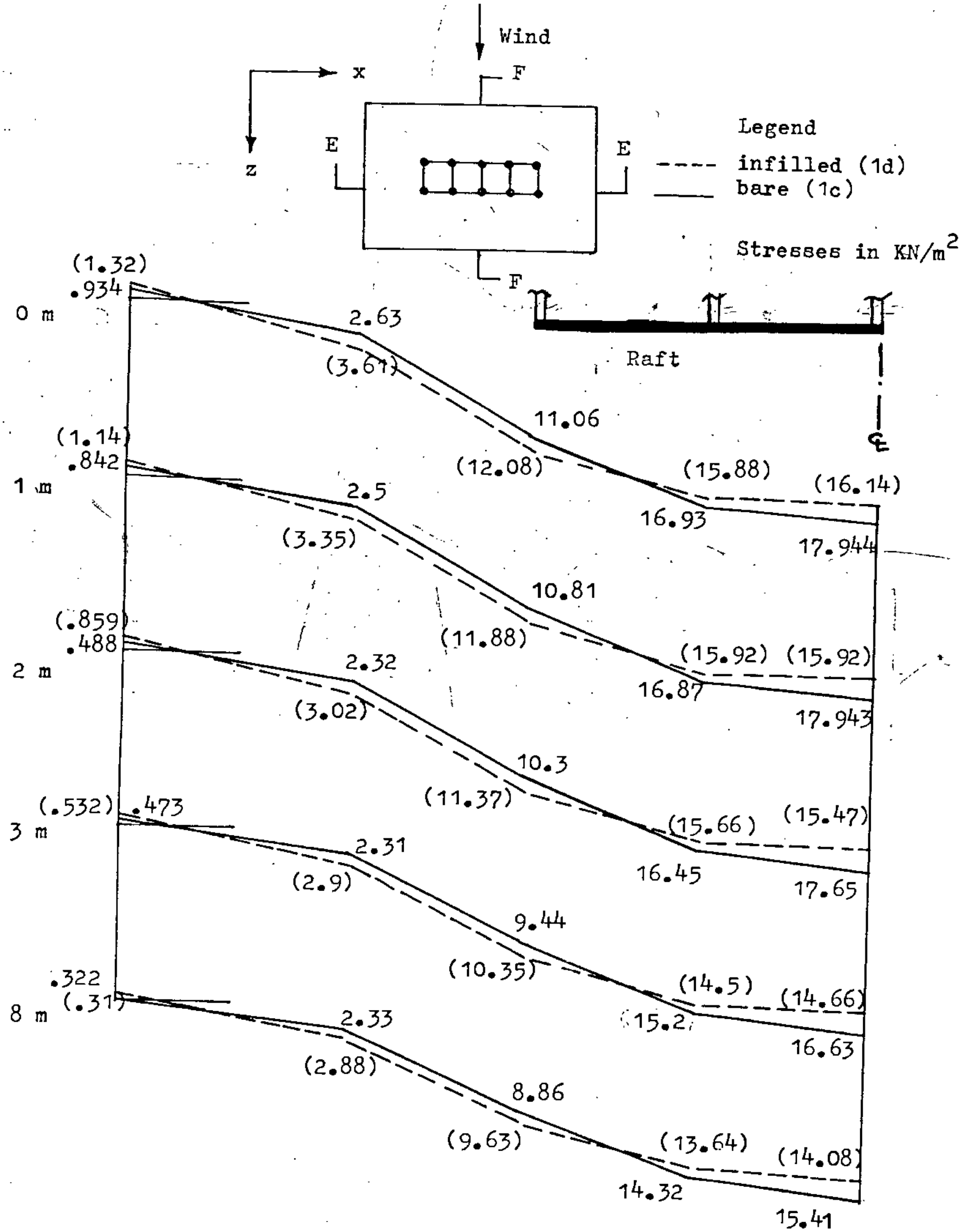

FIGURE 5.24 DISTRIBUTION OF σ_y (NODAL) ALONG SECTION E-E AT VARIOUS DEPTHS FOR ANALYSIS CASES 1c and 1d.

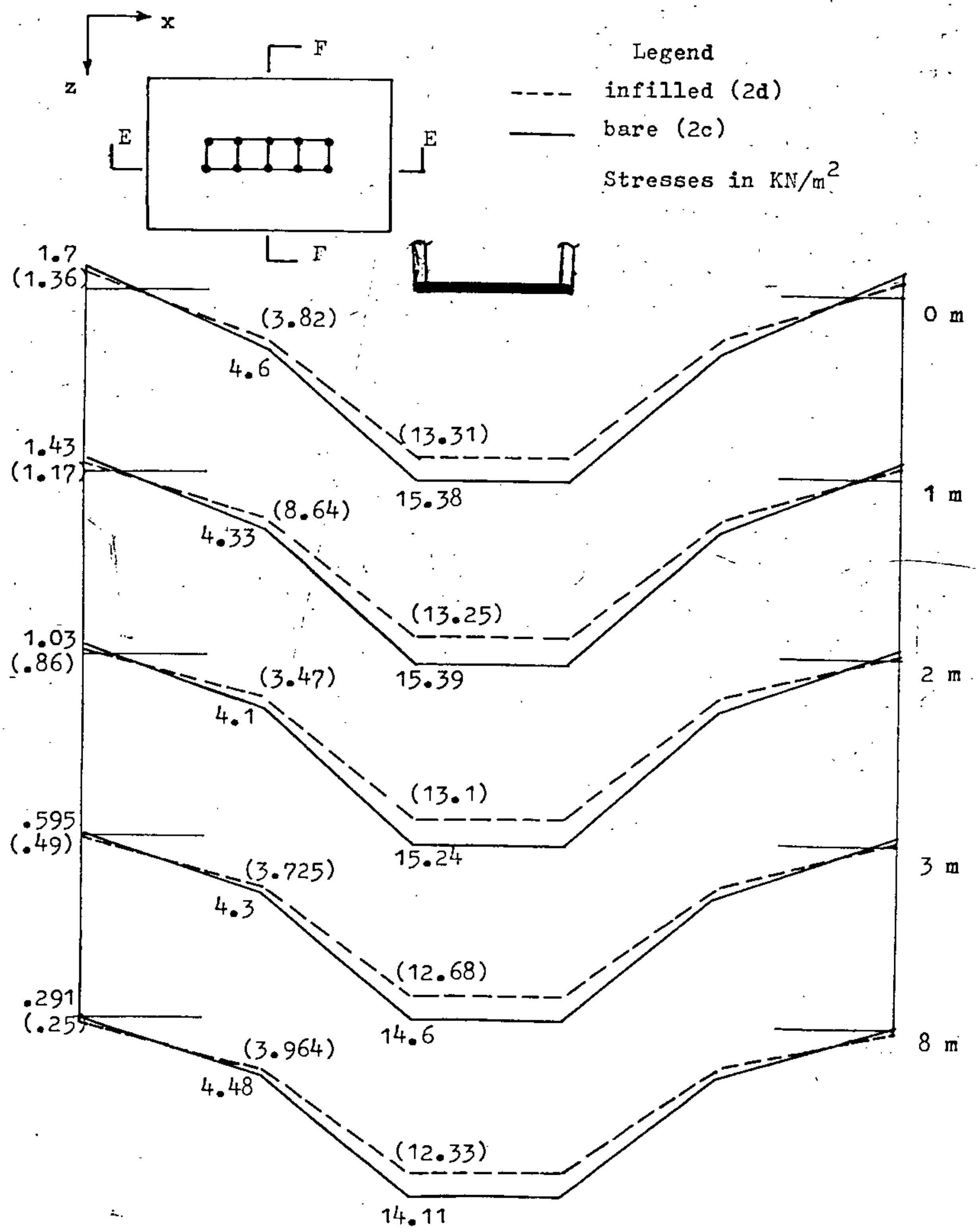

FIGURE 5.25 DISTRIBUTION OF σ_y (NODAL) IN Z-DIRECTION AT SECTION F-F AT VARIOUS DEPTHS FOR ANALYSIS CASES 2c AND 2d.

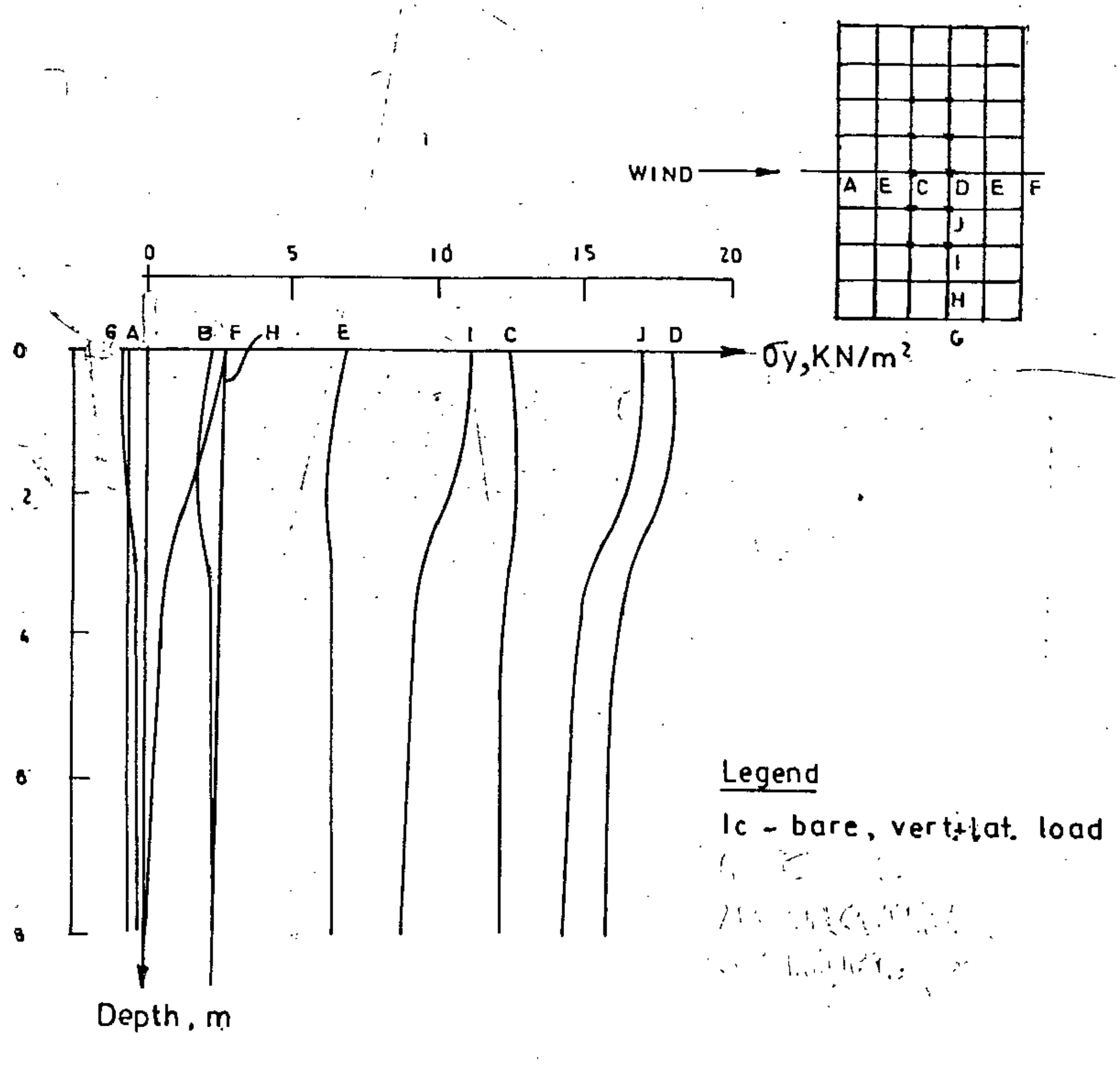

FIGURE 5.26 VARIATION OF VERTICAL PRESSURE WITH DEPTH AT VARIOUS POINTS SHOWN IN FIGURE FOR ANALYSIS CASE 1c.

distribution under leeward point H outside the raft is almost insensitive to depth. Under points G and A, both at soil boundary, soil pressure becomes tensile although of negligible magnitude. σ_y under points B and C and under other points as well, show variations only upto a depth of approximately 3.5 m and stabilizes at greater depths. It is worth mentioning that although soil pressure reduces with depth, the steep gradient of a Boussinesq type variation with a stress ordinate asymptotic to the upper soil boundary is not exhibited anywhere in the soil. The reason for this may be attributed to the stiffness of the raft and the superstructure not accounted for in the Boussinesq solution.

For the T-plan structure, the distribution of normal stress σ_y (nodal) along transverse section A-A at various soil depths are plotted in Fig. 5.27 for flexible base analysis with load case 2 (2j and 2k). The distribution is symmetric about the axis of symmetry because vertical load alone is acting. The presence of infills decreases σ_y directly below the raft but outside it σ_y for infilled structure slightly exceeds that for bare frame. Thus an important contribution of orthotropic infills present in a structure is that these help to distribute σ_y more uniformly in horizontal directions at various depths and reduce the maximum intensity of σ_y.

The distribution of σ_y (nodal) along longitudinal section B-B of the T-plan structure for the same analysis cases and soil depths are plotted in Fig. 5.28. The maximum σ_y is obtained under the junction of the web and the flange and occurs at a depth of 1 m. The asymmetry of the structure causes the distributions to be non-symmetric in the longitudinal direction even for vertical loads acting alone. The nature of σ_y distribution at various depths are identical to each other, although the intensity of σ_y gradually declines with depth after certain increase immediately below the raft.

For analyses with load case 1 (both vertical and lateral loads acting) of T-plan structure, the variation of σ_y (nodal) along transverse section A-A at specified depths are shown in Fig. 5.29. The influence on σ_y of wind load acting on T-plan structure seems to be less pronounced compared to that on rectangular plan structure (Fig. 5.23). This is considered to be due to the fact that the T-plan structure itself is stiffer than the rectangular one. However, the maximum σ_y occurs under the corner node at the junction of the flange and the web in the leeward side. Compared to stress under the other symmetrically located corner node of the windward side, the increase is not significant (3.78%) and much less compared to that for the rectangular plan structure (45.76%). Fig. 5.30 shows the distribution of σ_y in the soil along longitudinal section B-B of T-plan structures for cases 1j and 1k from which conclusions similar to those for the transverse

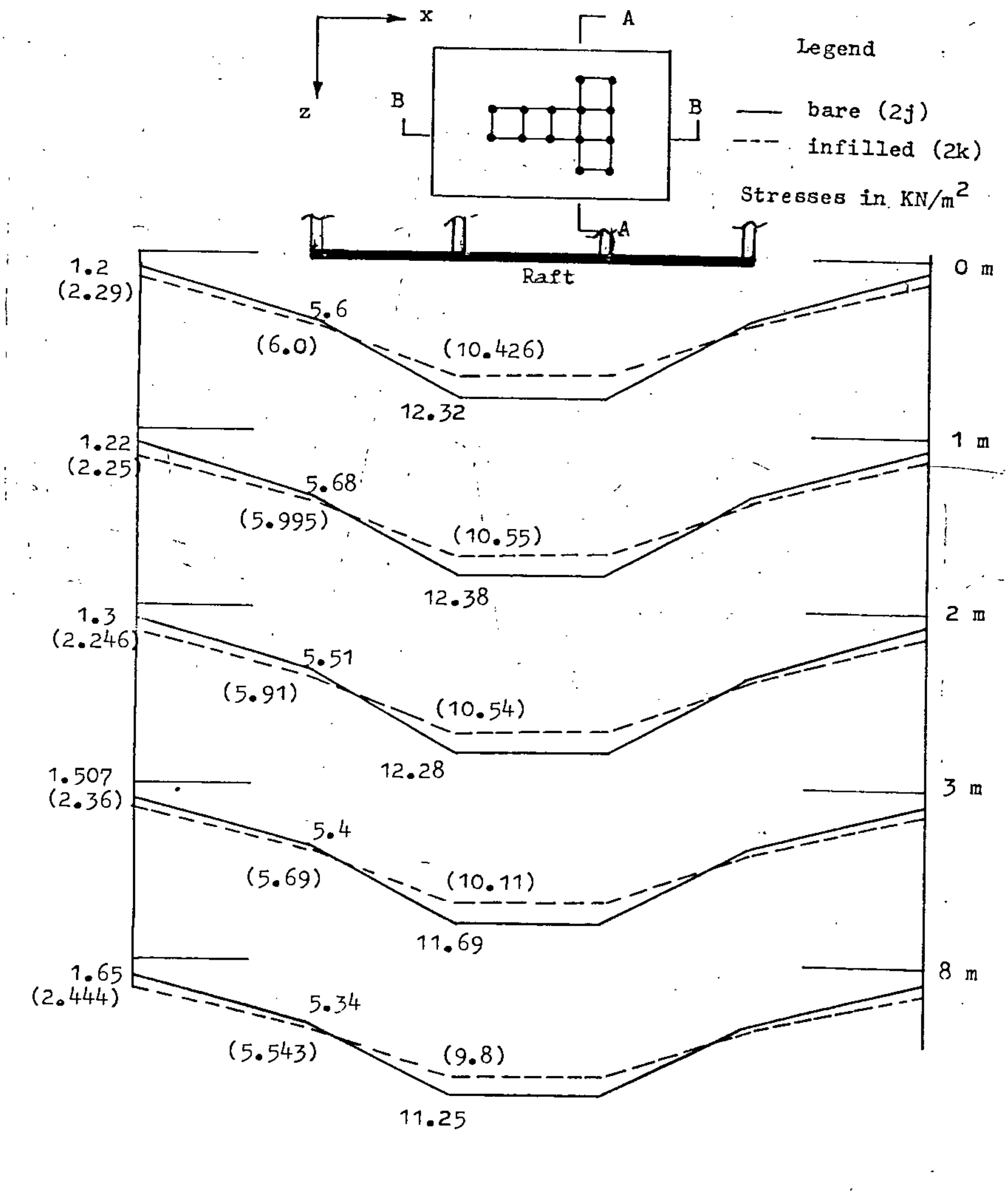

FIGURE 5.27 DISTRIBUTION OF σ_y (NODAL) ALONG SECTION A-A AT VARIOUS DEPTHS FOR ANALYSIS CASES 2j and 2k.

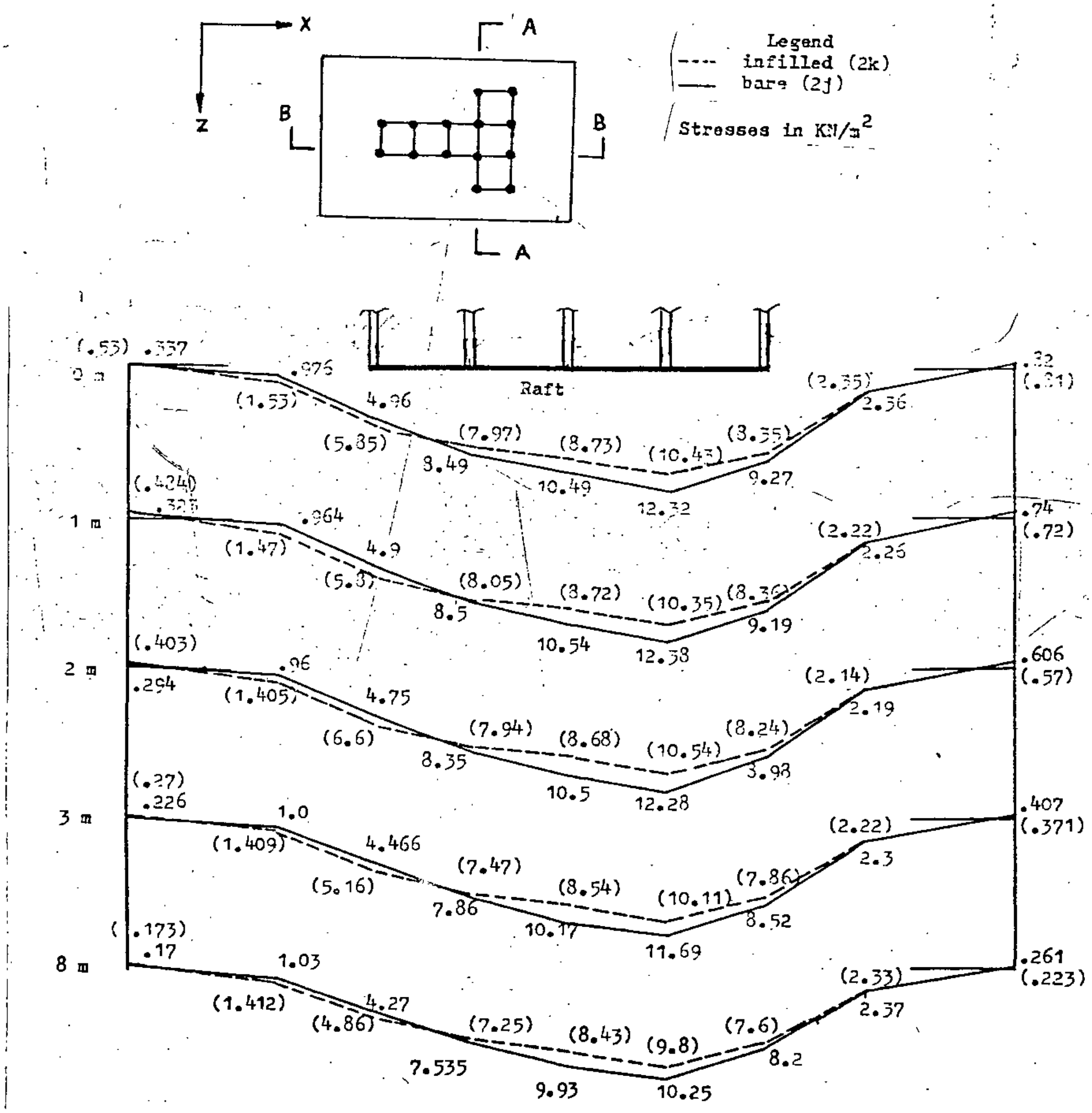

FIGURE 5.28 DISTRIBUTION OF σ_y (NODAL) ALONG SECTION B-B AT VARIOUS DEPTHS FOR ANALYSIS CASES 2J AND 2k.

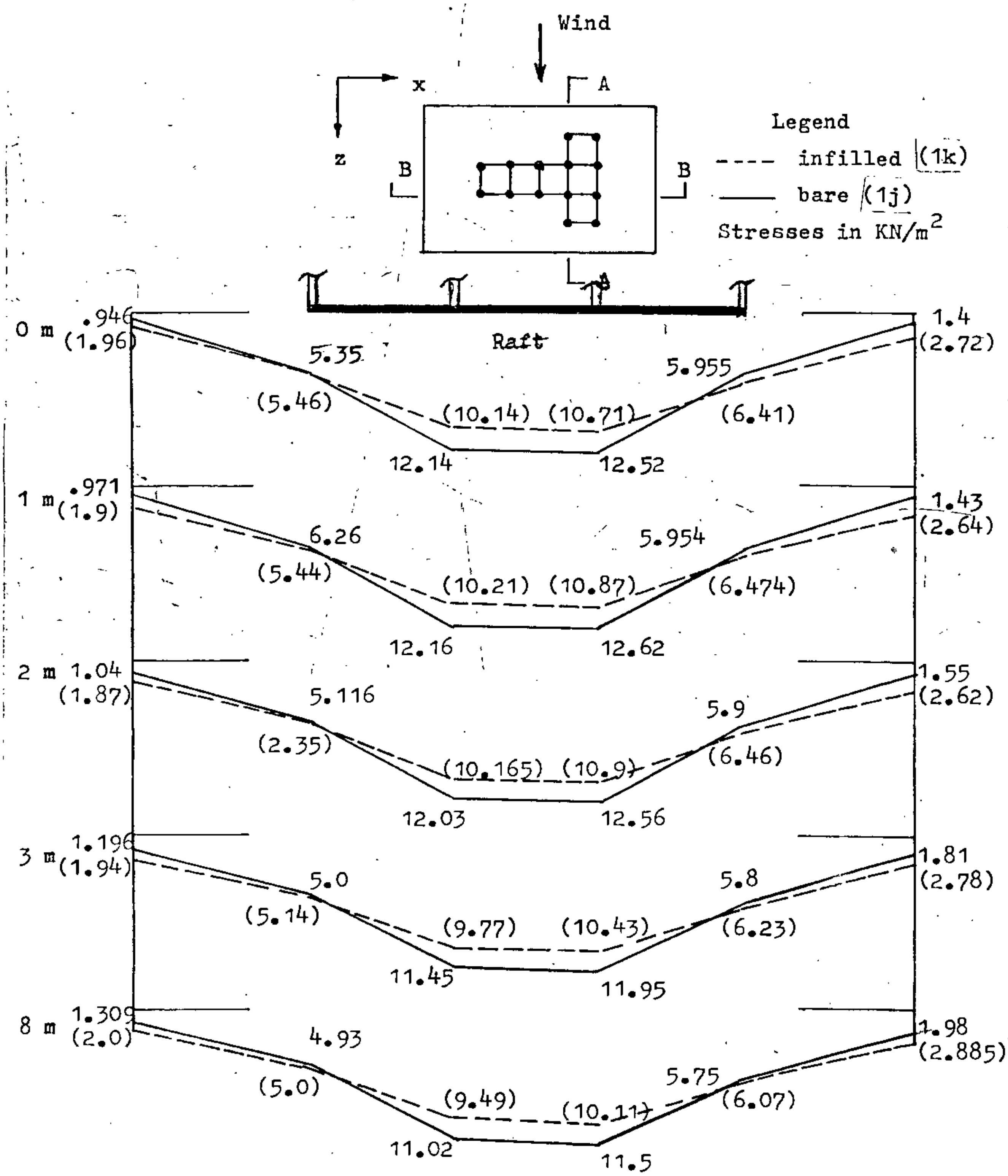

FIGURE 5.29 DISTRIBUTION OF σ_y (NODAL) ALONG SECTION A-A FOR ANALYSIS CASES 1j AND 1k.

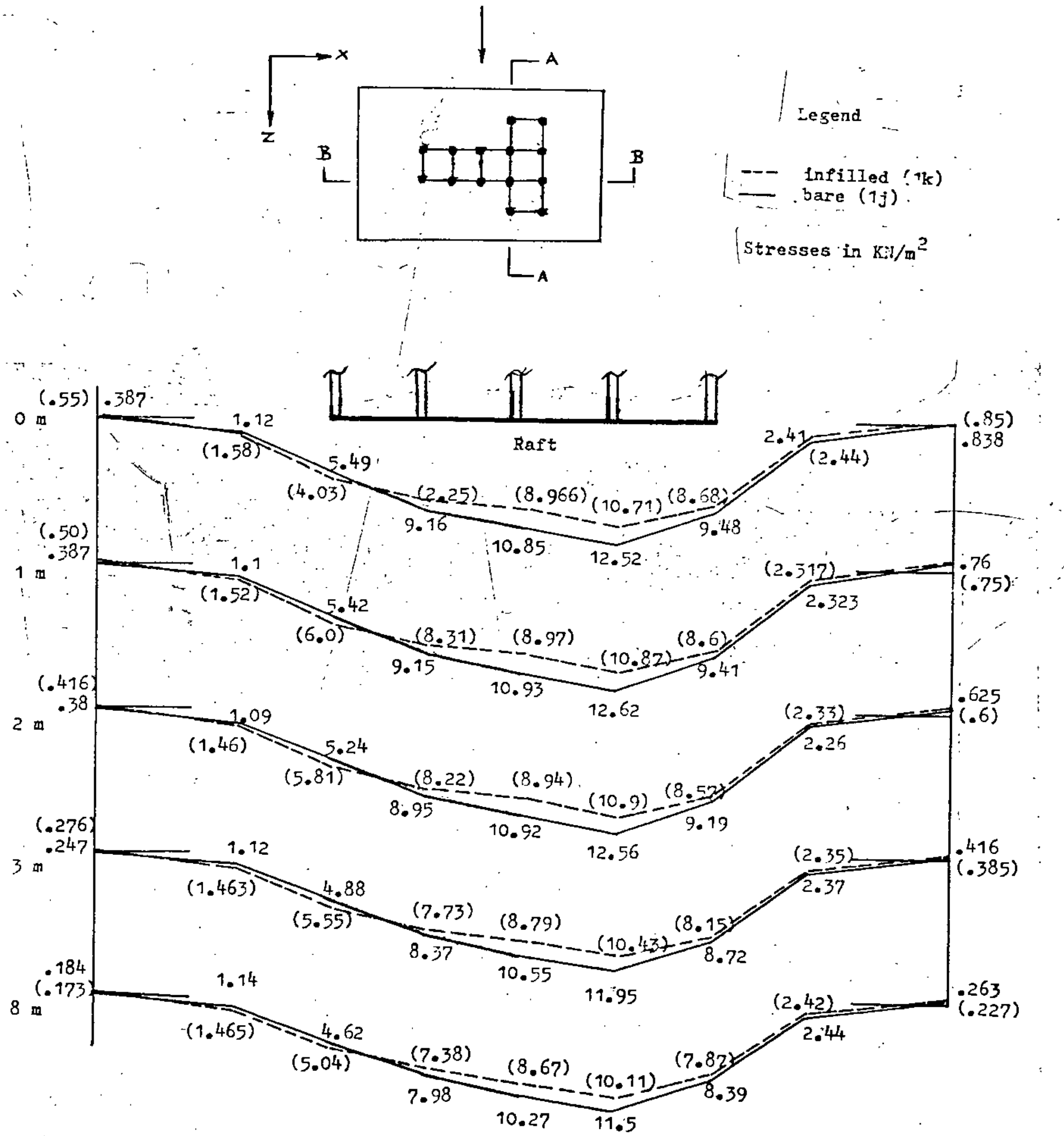

FIGURE 5.30 DISTRIBUTION OF σ_y (NODAL) IN kN/M^2 ALONG SECTION B-B AT VARIOUS SOIL DEPTHS OF T-PLAN STRUCTURE.

direction can be drawn. A general observation regarding soil stress distribution is that the maximum stress under any location occurs at a certain depth below the raft and not at the surface of contact of the raft and soil. Another observation is that the reduction in soil stresses with depth is not much dependent on the presence or absence of infill walls.

The stress-strain curves at the centroid of two solid elements in successive layers directly under the raft of the rectangular structure are shown in Fig. 5.31 for analysis case 1c. The soil immediately below the raft gets highly strained compared to soil at a deeper layer at the same stress level. This is because the soil elements at greater depths have a higher value of confining stress σ_{octi} and are therefore stiffer. This also demonstrates that contributions of soil at greater depths to the displacement of the structure are smaller even for the same level of stress in the elements. The argument is further substantiated by comparing the variations of stress and strain with depth under the same location in the raft, as shown in Fig. 5.32. The steep gradient of strain distribution along depth demonstrates that contributions of soil at greater depths in the deformation of structure diminish rapidly and the inclusion of a large extent of soil in the analysis is not necessary.

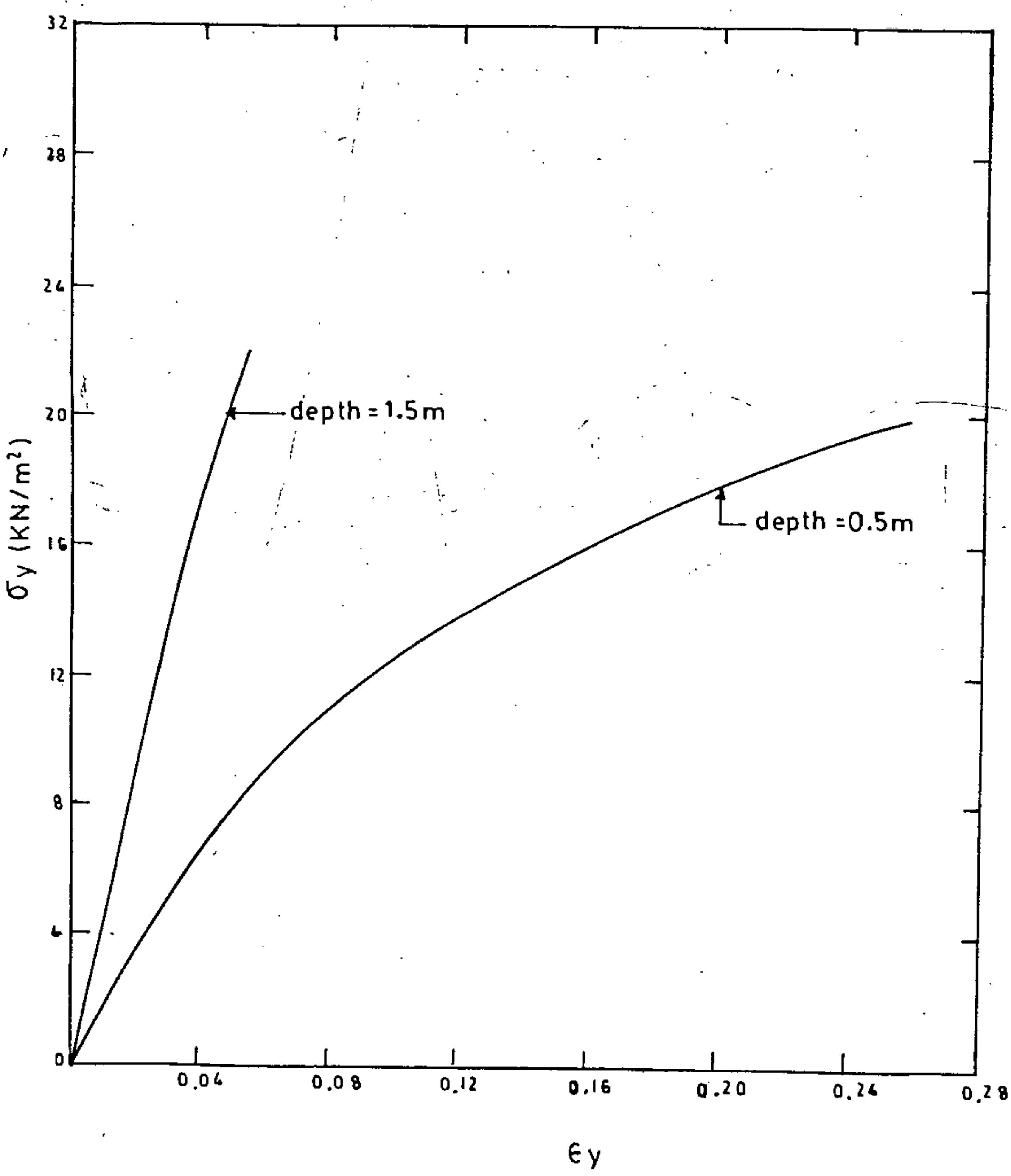

FIGURE 5.31 STRESS-STRAIN CURVES AT THE CENTROID OF TWO SOLID ELEMENTS DIRECTLY UNDER INTERNAL RAFT ELEMENT FOR ANALYSIS CASE 1c.

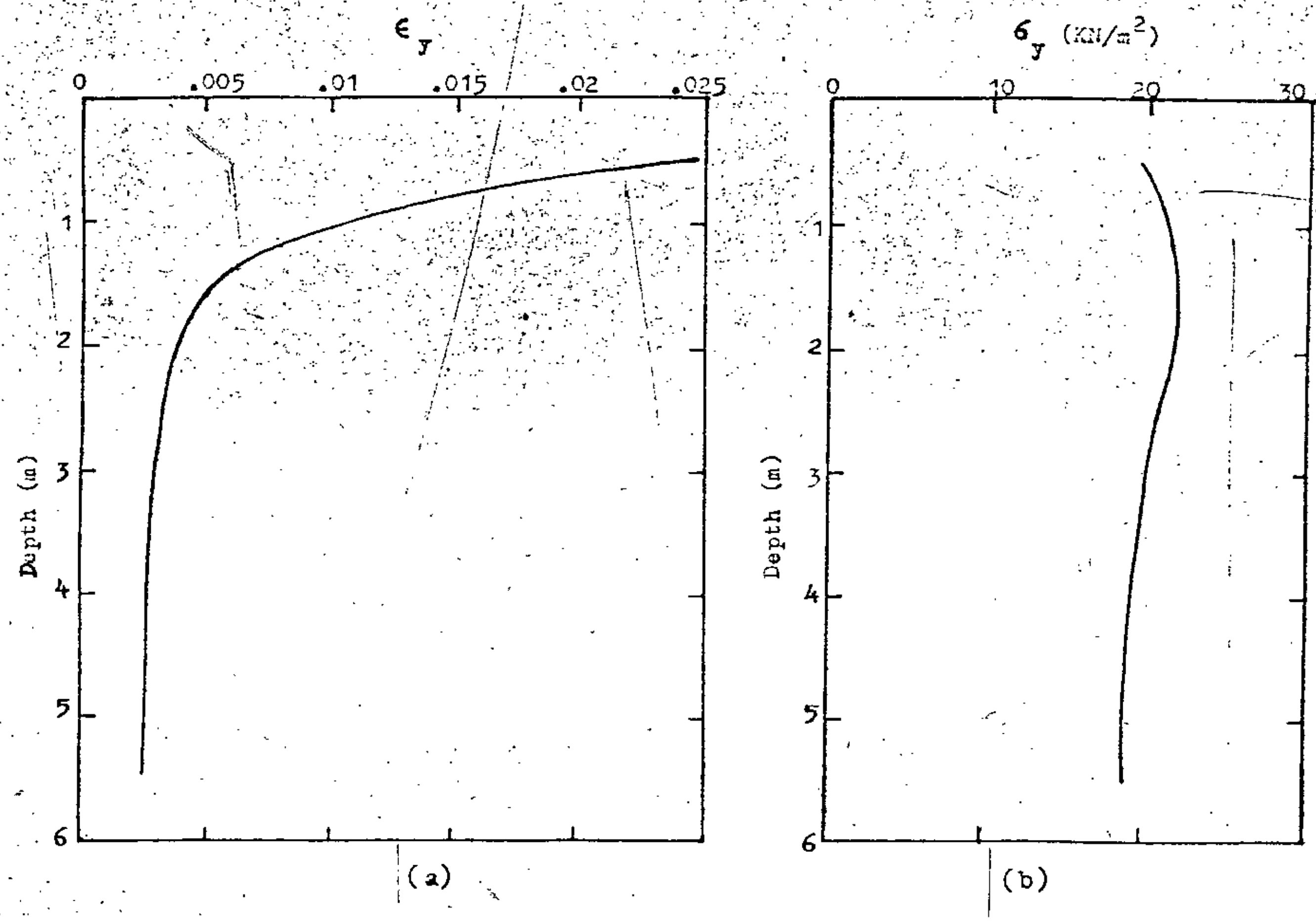

FIGURE 5.32 VARIATION OF (a) CENTROIDAL STRAIN AND (b) CENTROIDAL STRESS IN SOIL WITH DEPTH.

5.5 STRESSES IN INFILL WALLS

The variation in extreme fibre stresses perpendicular to bed joint at the centroid of bottom most infill wall of an external frame panel of rectangular plan structure with load increment factor λ is shown in Fig. 5.33a. Curves in Fig. 5.33b show the variation of column moment with λ. Curves in both of the two figures correspond to analysis cases 1d (wall with opening) and 1e (wall without opening). It may be observed from Fig. 5.33a that infill wall stresses increase with the load and at the same load these stresses in walls with opening are smaller than those in walls without openings. Curves in Fig. 5.33b show that openings in walls increase the column moment approximately two times. These facts indicate that the stiffer the wall becomes, the larger portion of the column moment it shares.

5.6 THE PROPAGATION OF CRACKS IN SOIL

The variation of the width of soil separation (crack) at the boundary joint under rectangular structure with increasing λ is shown in Fig. 5.34 for interactive analysis cases 1c and 1d. In the absence of infill walls (1c) the crack develops when load factor λ reaches 0.1. On the other hand, the presence of infill walls does not permit the crack to develop until the load factor reaches 0.9. The width of crack at the maximum load for infilled structure is only 13.4% of that for a bare structure. Thus the infill

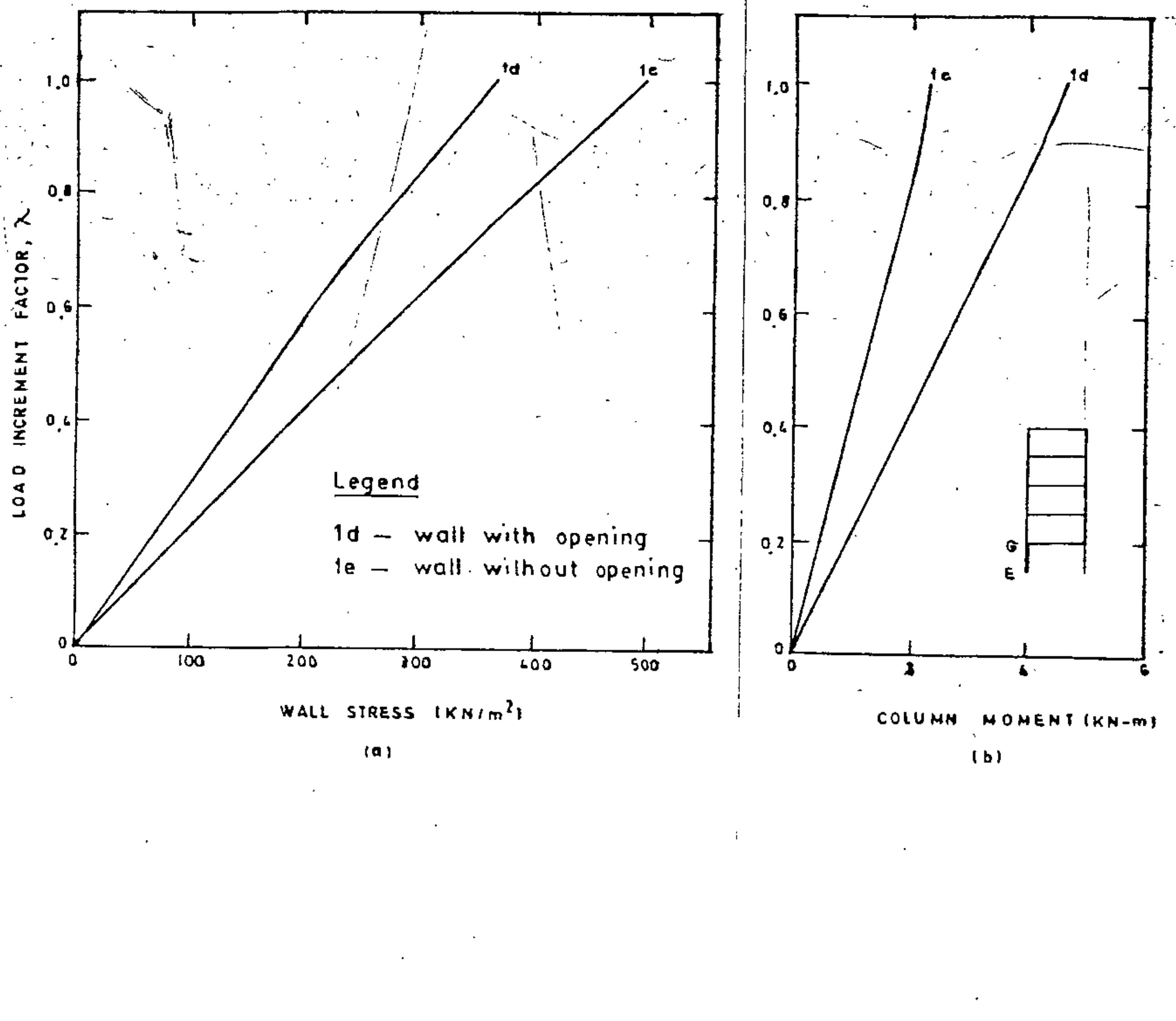

FIGURE 5.33 COMPARISON BETWEEN INFILL WITH OPENING AND WITHOUT OPENING (a) LOAD-STRESS CURVES (b) LOAD-MOMENT CURVES.

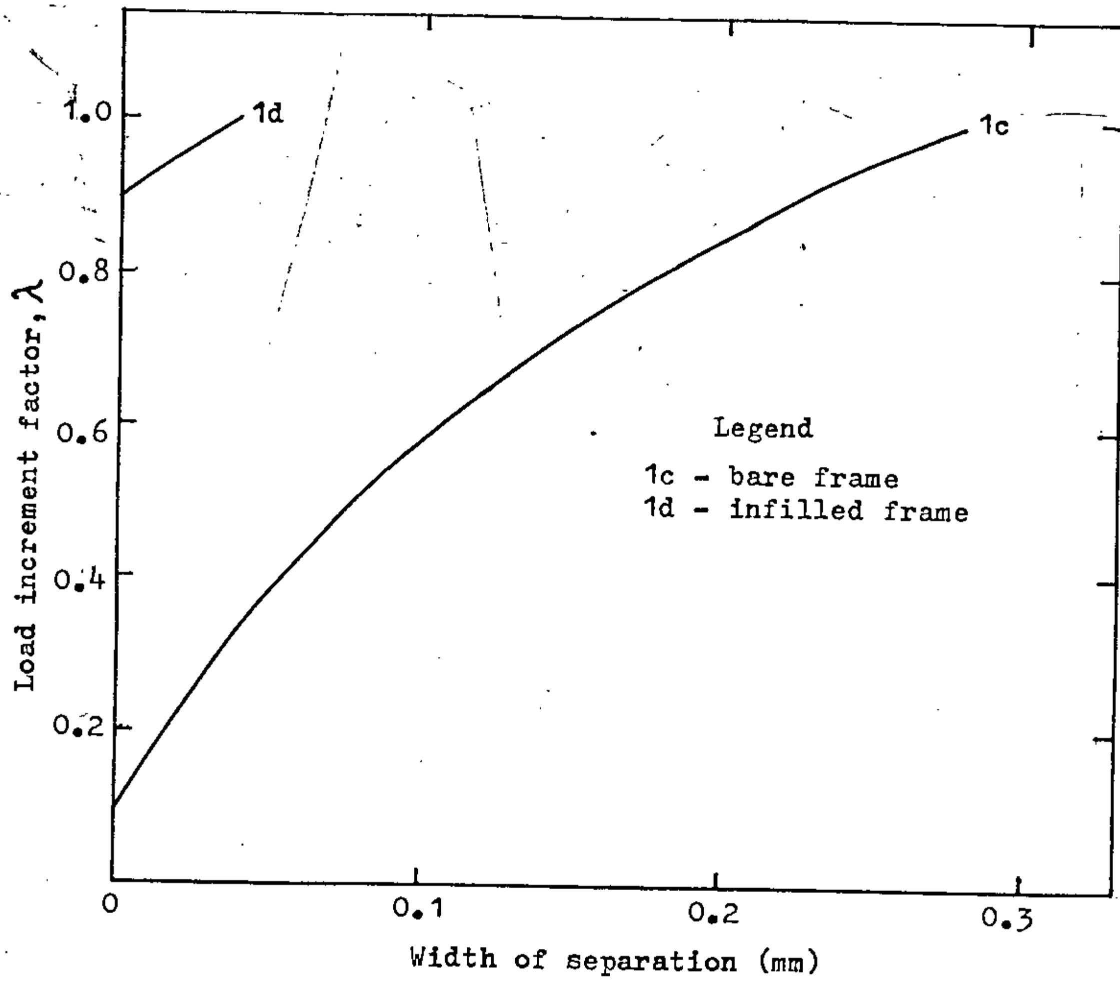

FIGURE 5.34 LOAD VS. WIDTH OF SEPARATION CURVE OF THE BOUNDARY JOINT FOR ANALYSIS CASES 1c AND 1d.

walls have a significant positive role in controlling the crack propagation and its width.

A summary of the deflections and stresses and bending moments obtained by the various analyses are given in Table 5.1 and Table 5.2 for better and clear understanding of the results.

Table 5.1 Deflections of the structures.

Analyses No.	Thickness of clay (m)	Sway at top (m)	Vertical deflection at top (cm)	Differential displacement (mm)	Maximum displacement (mm)
1a	8	.139	.524	0	0
1b	8	.00335	.215	0	0
1c	8	.262	7.6	40.78(e)* 46.4(i)**	7.09
1d	8	.116	6.02	42.0(e) 42.0(i)	5.83
1e	8	.111	5.8	40.5(e) 40.6(i)	5.67
1f	6	.257	7.04	38.24(e) 43.9(i)	6.53
1g	4	.256	6.62	35.6(e) 41.9(i)	6.11
2a	8	-	.435	0	0
2b	8	-	.176	0	0
2c	8	-	4.86	0	4.43
2d	8	-	3.63	0	3.47
1h	8	.0346	.0984	0	0
1i	8	.00062	.052	0	0
1j	8	.053	1.76	8.41(e) 1.2(i)	1.66(e) 2.93(i)
1k	8	.010	2.0	2.3(e) 1.6(i)	1.94(e) 2.12(i)
2i	8	-	.0859	0	0
2j	8	-	3.14	0	3.14
2k	8	-	2.10	0	2.1
2h	8	-	.215	0	0

*e = external frame

**i = internal frame

Table 5.2 Stresses and bending moments of the structures

Analyses No.	Column moment kN-m	Beam moment kN-m	Axial force (kN)	Infill wall stress (kN/m^2)	Soil (nodal) stress (kN/m^2)
1a	209.5(i)	123.9(e) 105.4(i)	654.0(e) 1160.0(i)	-	-
1b	4.764(i)	1.96(e) 1.92(i)	395.6(e) 481.9(i)	283.6(e) 391.7(i)	-
1c	208.4(i)	132.2(e) 106.4(i)	736.6(e) 1134(i)	-	11.06(e) 17.94(i)
1d	4.59(i)	1.96 (e) 1.92(i)	477.6(e) 440.8(i)	365.1(e) 343.6(i)	12.08(e) 16.14(i)
1e	2.273(i)	1.013(e) 1.007(i)	325.9(e) 281.1(i)	491.4(e) 435.5(i)	11.925(e) 16.18(i)
2a	.3147(i)	.966(i)	460.4(e) 912.0(i)	-	-
2b	.268(i)	.238 (i)	266.2(e) 367.6(i)	283.5(e) 391.6(i)	-
2c	48.04(e)	25.19(e)	514.8(e) 899.1(i)	-	8.53(e) 15.38(i)
2d	1.82(e)	1.006(e)	334.2(e) 324.5(i)	352.3(e) 345.6(i)	9.72(e) 13.31(i)
1h	85.98(e) 53.18(i)	48.61(e) 24.08(i)	318.3(e) 814.9(i)	-	-
1i	1.824(e) 1.13 (i)	.805 (e) .64 (i)	172.1(e) 270.7(i)	153.9(e) 287.3(i)	-
1j	80.08(e) 109.9(i)	48.61(e) 52.19(i)	331.9(e) 758.4(i)	-	5.49(e) 12.52(i)
1k	1.32(e) 4.85(i)	.63(e) 2.27(i)	195.7(e) 207.7(i)	199.8(e) 216.5(i)	6.03(e) 10.71(i)
2h	.376(i)	1.21(i)	274.2(e) 812.5(i)	-	-
2i	.198(i)	.28[illegible](i)	144.1(e) 269.6(i)	153.7(e) 287.1(i)	-
2j	50.35(i)	18.79(i)	290.4(e) 752.2(i)	-	4.98(e) 12.32(i)
2k	3.09(i)	1.65(i)	190.6(e) 203.2(i)	200.0(e) 216.9(i)	5.85(e) 10.426(i)

Chapter 6

CONCLUSIONS AND RECOMMENDATIONS FOR FUTURE RESEARCH

6.1 CONCLUSIONS

The following are the conclusions that can be drawn from the present investigation.

(1) The general finite element program for the non-linear three dimensional structure-soil interaction analysis with facilities for crack propagation has proven to be a varsatile and effective tool for investigating the phenomenon of interaction. The necessary computer storage and time are not prohibitively extensive.

(2) Orthotropic infill walls are found to reduce the structure sway significantly both in fixed base and interaction analyses. However, the reduction in sway due to infill walls is less when the contribution of the underlying soil is accounted for by an interaction analysis. The actual contribution of infill walls in increasing the lateral stiffness of framed structures may therefore be less than what is apparent from conventional fixed base analyses.

(3) Openings in infill walls increase the structure sway. However, the increase was not found to be significant when the openings were accounted for by the conventional approach of reducing the wall stiffness.

(4) Orthotropic wall infills reduce the absolute vertical displacements as well as relative vertical displacements of points on the structure, but the reduction in these displacements is less pronounced than the reduction in sway.

(5) Orthotropic infills increase the lateral stiffness of the structure with T-plan configuration in a more effective way than they increase the stiffness of rectangular plan structure.

(6) Orthotropic infills reduce the displacement of the raft to a lesser degree than the sway. Influence of wall infills on the displacement itself is more significant than that on the differential displacement.

(7) Structure sway, displacement and differential displacement all are influenced by the underlying soil strata included in an interaction analysis. However, increasing soil depths do not proportionately increase these deformations due to the diminishing values of strains at greater soil depths. Thus for a reasonable interaction analysis the extent of soil to be included in the mesh need not be very large.

(8) Orthotropic wall infills, due to their contribution to the structural stiffness, help to distribute the raft deformation more uniformly.

(9) In the T-plan structure, the wall infills reduce displacement but increase differential displacement under internal columns of an internal frame constituting the flange. While under an external web frame, the displacement is increased and the differential displacement is reduced by the presence of wall infills. However, the former conclusion may change completely if the displacements under the exterior columns of the internal frame are considered. This differential behaviour under the exterior and interior frames was unique for the T-plan structure.

(10) Orthotropic infill walls are found to reduce the column and beam bending moments in a very significant manner, while interactive analyses change these moments only negligibly. The lack of influence of the underlying soil on the bending moments is considered to be due to the stiffness of a continuous raft foundation as opposed to isolated column footings.

(11) Maximum vertical soil pressure occurred under the edges of the raft in the leeward side. The variation of this pressure with depth was less pronounced than a Boussinesq type distribution and the pressure became almost uniform at depths below 3.5 m for the rectangular plan structure.

(12) The presence of wall infills in the superstructure in general helps to distribute the vertical soil pressure more uniformly in the horizontal direction. Immediately below the raft the stress σ_y for bare structure exceeds that for infilled structure. On the other hand σ_y for infilled structure is more than for bare structure outside the extent of the raft. Thus maximum intensity of σ_y is reduced due to wall infills.

(13) The influence on soil pressure σ_y of the wind load acting on T-plan structure is less pronounced compared to that on rectangular structure. This is considered to be due to the increased lateral stiffness of the former.

(14) Strains in the soil at shallow depths are much larger than those at greater depths. This is because of the higher degree of confining pressure acting on the deeper soil elements. Thus the strain gradient with depth is steeper than the stress gradient. This goes to explain why it is not necessary to include a great depth of soil in an interaction analysis.

(15) Orthotropic wall infills due to their contribution to the structure stiffness help reduce the formation and propagation of cracks in the soil.

6.2 RECOMMENDATIONS FOR FUTURE RESEARCH

Following recommendations can be made to further develop the present research work:

(1) The generality of the finite element program developed here will permit to analyse various other structure-soil interaction problems besides those considered in this work. These may include buried structures, culverts, tunnels etc.

(2) The analyses performed in this work were based on the assumption that the orthotropic wall infills were in perfect fit with the frame panels. Lack of fit of the infill is a practical problem which may be tackled with some modification in the present work.

(3) The possible development of cracks within infill walls at wall frame boundary was not accounted for in this work. This aspect of infilled frame behaviour can be taken into consideration in future research.

REFERENCES

BENJAMIN J R and WILLIAMS H A (1958)
Behaviour of one-storey walls containing opening
Jnl. ACI, 30 (See HENDRY A W, 1981).

BENJAMIN J R and WILLIAMS H A (1960)
A Reinforced concrete shear wall assemblies
Jnl. Struct. Div., ASCE, August.

BRAY K H M (1973)
Computer analysis of large civil engineering structures
Ph.D Thesis, University of Aston in Birmingham.

BRYAN E R and DAVIES J M (1976)
Diaphragm action in multi-storey buildings
University of Salford, Dept. of Civil Engg., Report
No. 75-70, January (See THORBURN S, 1972).

CHAMECKI S (1956)
Structural rigidity in calculating settlements
Jnl. Soil Mech. Found. Div., Proc. A.S.C.E, 82, SM1.

CHAMECKI S (1969)
Calculation of progressive settlement of foundations in
interaction with structure and soil
Annales de L' Institute Technique du Batiment et des
Travaux Publics, Paris, No. 261 (See RAHMAN M A, 1978).

CHEUNG Y K and NAG D K (1968)
Plates and beams on elastic foundations-linear and non-
linear behaviour. Geotechnique, 18, pp 250-260.

CHEUNG Y K and ZIENKIEWICZ O C (1965)
Plates and tanks on elastic foundations-on application of
finite element method. Journ. Solids Struct., 1, pp. 451-461.

CHOUDHURY J R (1975)
Low-rise low cost housing and extreme wind related
problems in Bangladesh. Progress report on design criteria
and methodology for construction of low rise buildings to
better resist typhoons and hurricans. National Bureau of
Standards, Washington, D.C. 20234.

COATES R C, COUTIE M G and KONG F K (1972)
Structural analysis. Thomas Nelson and Sons Ltd., London.

CUNNEL M D (1974)
The application of finite elements to problems of soil.
Ph D thesis, University of Aston in Birmingham.

DEMENEGHI A (1981)
Analysis of soil-structure interaction
Proc. of tenth international conf. on Soil Mech. and Found. Engg. Vol. 2.

DESAI C S (1971)
Non-linear analysis using spline functions
Jnl. Soil. Mech. Found. Div., Proc. A.S.C.E, 97, SM10.

DESAI C S (1972)
Closure of discussion of the above paper
Jnl. Soil mech. Found. Div., Proc. A.S.C.E., 98, SM9.

DESAI C S, PHAN H V and PERUMPRAL J V (1982)
Mechanics of three-dimensional soil-structure interaction
Jnl. Eng. Mech. Div. ASCE, Vol. 108, no. EMS, October.

DESAI C S and SARGARO S (1984)
Hybrid F.E procedure for soil-structure interaction
Jnl. Struct. Div., ASCE, Vol. 110 no. 4, April.

EL-DAKHAKHNI W and DANIELS J H (1973)
Frame-floor wall system interaction in buildings.
Fritz. Engineri lab., Report no. 376-2 Lehigh Univ., April. (See THORBURN S, 1978).

FIORATO A E, SOZENOM A and GAMBLE W L (1970)
An investigation of the interaction of reinforced concrete frames with masonry filler walls.
Civ. Eng. Studies Structural Research Series no. 370.
Univ. of Illinois (See THORBURN S, 1978).

FLETCHER D Q and HERMANN L R (1971)
Elastic foundation representation of continuum.
Jnl. Eng. Mech. Div., ASCE., 97, EM1, pp 95-107.

GIRIJA VALLABHAN C V and JAIN R K (1972)
Octahedral stress approach to analysis of water resources structures. Proc. Symp. Application of finite element method to Geotechnical Eng., C S Desai (Ed.), U S Army Engr. Waterways Expt. Station, Soil Mech. information analysis centre, Vickburg, Mississippi, III, pp 1185-1213.

GIRIJA VALLABHAN C V and REESE Le (1968)
Finite element method for problems in soil mechanics.
Jnl. Soil Mech. Div., Proc. ASCE, 94, SM2.

HENDRY A W (1981)
Structural Brickwork
MacMillan Press Ltd.

HOLMES M (1961)
Steel frames with brickwork and concrete infilling
Proc. Inst. Civ. Engrs., 19.

JENNINGS A (1966)
A compact storage scheme for the solution of symmetric linear simultaneous equations
Computer Jnl., 9.

JENNINGS A (1979)
Matrix computation for engineers and scientists
John Wiley & Sons.

KADIR M R A (1974)
The structural behaviour of masonry infill panels in framed structure.
Ph D Thesis, University of Edinburgh (See HENDRY A W, 1981).

KADIR M R and HENDRY A W (1975)
The behaviour of brickwork infilled frames under racking load. Proc. 5th International Symposium on Load Bearing Brickwork, BCRA, London (See LIAUW T C and KWAN K H, 1985).

KARAMANSKI T (1967)
Calculating infilled frames by the method of finite element Symp. on Tall Buildings, ed. A Coull and B Stafford Smith (Pergamon, Oxford) (See HENDRY A W, 1981).

KING G J W and CHANDRASEKARAN V S (1974)
Interactive analysis of a rafted multi-storey space frame on an inhomogeneous clay stratum.
Proc. Conf. Finite Element Methods in Eng., Univ. N SW, pp 493-509.

KOMORNIK A and MAZURIK A (1974)
Interaction of superstructure-soil under restrained setting.
Canadian Geotechnical Journ., 11, No.4, pp. 470-479.

LARNACH W J (1970)
Calculation of settlements of building frames taking account of structural stiffness.
Civ. Engg. Public Works Review, September, pp 1040-1043.

LARNACH W J and WOOD L A (1972)
The effect of soil-structure interaction on settlement.
Proc. Int. Symp. Computer aided structural design, Univ. Warnick, Pergrinus Ltd., 2 pp G1. 1-G1.13.

LEE I K and HARRISON H B (1970)
Structure-foundation interaction theory
Jnl. Struct. Div., ASCE., 96, ST2, pp 177-198.

LIAUW T C (1970)
Elastic behaviour of infilled frames
Proc. ICE, Vol. 46, July.

LIAUW T C (1972)
An approximate method of analysis for infilled frames with or without openings
Bldg. Science, 7. (See HENDRY A W, 1981).

LIAUW T C (1973)
The composite characteristics of infilled frames
Int. Jnl. of Mech. Science, Vol. 15, No.7
(See LIAUW TC AND KAWAN K H, 1985).

LIAUW T C and KWAN K H (1982)
Non-linear analysis of multistory infilled frames
Proc. ICE, 73, Part 2, June.

LIAUW T C AND KWAN K H (1985)
Unified plastic analysis for infilled frames
Jnl. Struct. Div. ASCE, Vol. 111. No. 7 July.

LIAUW T C and LEE S W (1977)
On the behaviour and the analysis of multistorey infilled frames subjected to lateral loading.
Proc. ICE, 63 .

LITTLEJOHN G S and MACLEOD I A (1974)
(Editors) Structure-soil interaction in relation to buildings. Report by a special study group, Institution Struct. Engrs, London.

MAINSTONE R J (1971)
On the stiffness of infilled frames
Proc. ICE, Supplement (iv)

MAINSTONE R J (1974)
Supplementary note on the stiffness and strengths of infilled frames.
CP 13/74, Bldg. Research Establishment, Garston.
(See THORBURN S, 1978).

MAINSTONE R J and WEEKS G A (1970)
The influence of a bounding frame on the racking stiffness and strengths of brick walls
Proc. 2nd Int. Brick Conf. (See THORBURN S, 1978).

MAJID K I (1972)
The effect of irregularities on the finite element analysis of civil engineering structures.
Proc. Speciality Conf. Finite Element Methods in Civ.Eng., J O McCuleheo, M Saeed Mirza and A A Mufti (Editors), McGill University, Montreal, Quebec, Canada.

MAJID K I and AL-HASHIMI K (1976)
Failure of brittle materials due to crack propagation.
The Structural Engineer, 54, No.5, pp. 175-182.

MAJID K I and CRAIG J S (1972)
An incremental finite element analysis of structural interaction with soil of non-linear properties.
Proc. Conf. Soil-structure Interaction, Univ. Birmingham.

MAJID K.I and CUNNELL M D (1976)
A theoretical and experimental investigation into soil-structure interaction. Geotechnique, 26, No.2, pp 331-350.

MALLICK D V and GARG R P (1971)
Effect of openings on the lateral stiffness of infilled frames. Proc. of ICE, Vol. 49, June.

MALLICK D V and SEVERN R T (1967)
The behaviour of Infilled frames under static loading
Proc. ICE, 38.

MEYERHOF G G (1947)
The settlement analysis of building frames.
The Structural Engineer, London, 25, pp 369-409.

MILOVIC D M and TOURNIER J P (1974)
Stress and deformations in an elastic layer as a result of pressure across a rigid rectangular plate, (in German).
Der Baningeniever, 49, pp 63-66. (See RAHMAN M A, 1978).

NYBERG G (1976)
Diaphragm action of assembled C-shaped panels
Swedish Council for Building Research, Document D9.
(See THURBURN, 1978).

POLYAKOV S V (1960)
On the interaction between masonry filler walls and enclosing frame when loaded in the plane of the wall
Translations in earthquake engineering, Earthquake Eng. Research Institute, San Francisco (See THORBURN S, 1978).

RAHMAN M A (1978)
Interaction between foundations and structures
Ph D Thesis, Univ. of Aston, Birmingham.

RAHMAN M A and SAWKO F (1980)
Shear lag effect in brick diaphragm wall subjected to wind pressure
International Jnl. of Masonry Construction, Vol.1, No.1, March.

SACHANSKI S (1960)
Analysis of the earthquake resistance of frame building taking into consideration the carrying capacity of the filling masonry. Proc. 2nd World Conf. on Earthquake Engineering, Tokyo (See HENDRY A W, 1981).

SEDDON A E (1956)
The strength of concrete wall under axial and eccentric load. Symp. on strength of concrete structure (cement and concrete association, London) (See HENDRY A W, 1981).

SEETHARAMULU K and KUMAR A (1973)
Interaction of foundation beam and soil with frames. Proc. 8th Int. Conf. Soil Mech. Found. Eng., Moscow, Session 2. (See RAHMAN M A, 1978).

SIMMS L G (1967)
The behaviour of no-fine concrete panels as the infill in reinforced concrete frames.
Civ. Engg. and Pub.Wks. Rev., November.(See THORBURN S,1978).

STAFFORD SMITH B (1962)
Lateral stiffness of infilled frames
Jnl. Struct. Div. ASCE, 88, ST6.

STAFFORD SMITH B (1966)
Behaviour of square infilled frames
Jnl. Struct. Div., ASCE, January.

STAFFORD SMITH B and CARTER C (1969)
A method of analysis for infilled frames
Proc. ICE, 44, September.

SMITH I M (1970)
A finite element approach to elastic soil-structure interaction. Canadian Geotechnical jnl., 7, No.2, pp.95-105.

THORBURN S (1978)
(Editor) Structure-soil Interaction. State of the art report by an ad hoc committee, Inst. of Struct. Engrs., London.

WOOD R H (1958)
The stability of tall buildings
Proc. ICE, 11, September (LIAUW T C and KWAN KH , 1985).

WOOD R H (1978)
Plasticity, Composite action and collapse design of unreinforced shear wall pannels in frames.
Proc. ICE, Part 2, Vol. 65, June.

ZIENKIEWICZ O C (1977)
The Finite Element Method, 3rd ed. McGraw-Hill Book Co. Limited.

Appendix

THE FINITE ELEMENTS

A1.1 SPACE FRAME MEMBER ELEMENT

The element is shown in Fig. (A1.1) in which the direction of the p-axis is always from end 1 to end 2. Each end of the member can have all three translations and three rotations as shown in Fig. (A1.1b). The eight possible member forces and moments are shown in Fig. (A1.1c). These are the axial force P_a, two shear forces S_R and S_Q, torque T and the moments at the two ends about q and r axes M_{Q1}, M_{Q2}, M_{R1} and M_{R2}.

The irregularities due to the non-coincidence of the ends of the member with the specified joints and that of the centroid of the section with the shear centre are taken care of. In Fig. (A1.2a) i and j are the joints specified at the ends of the member while A and B are the actual centroids of the end sections. PCA and PCB are the distances in p direction of the ends A and B from the joints i and j respectively. QC and RC are the offsets in the q and the r directions of the member axis AB from the line ij. QS and RS in the figure are the distances in q and r directions between the centroid G and the shear centre C of the member cross section, as shown for the angle section in Fig. (A1.2b).

A1.2 RECTANGULAR PLATE ELEMENT

The node numbering and the local axes of the element are shown in Fig. (A1.3a). Each node can have a maximum of

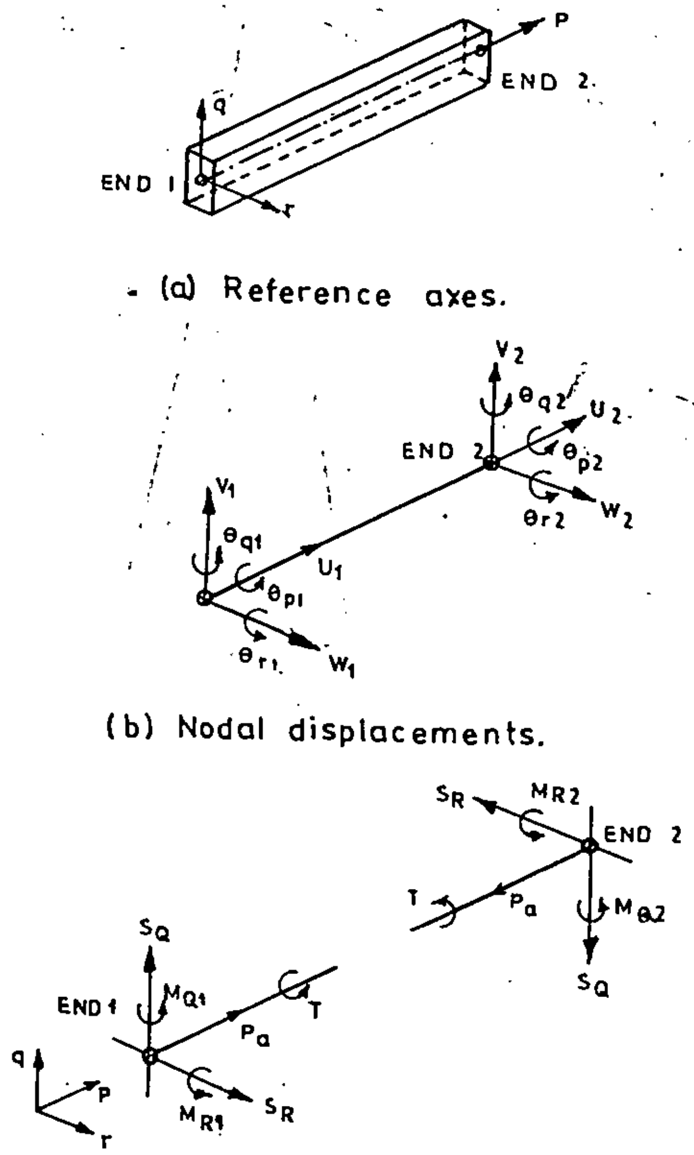

(a) Reference axes.

(b) Nodal displacements.

(c) Forces and moments.

FIGURE A1.1 SPACE FRAME MEMBER ELEMENT.

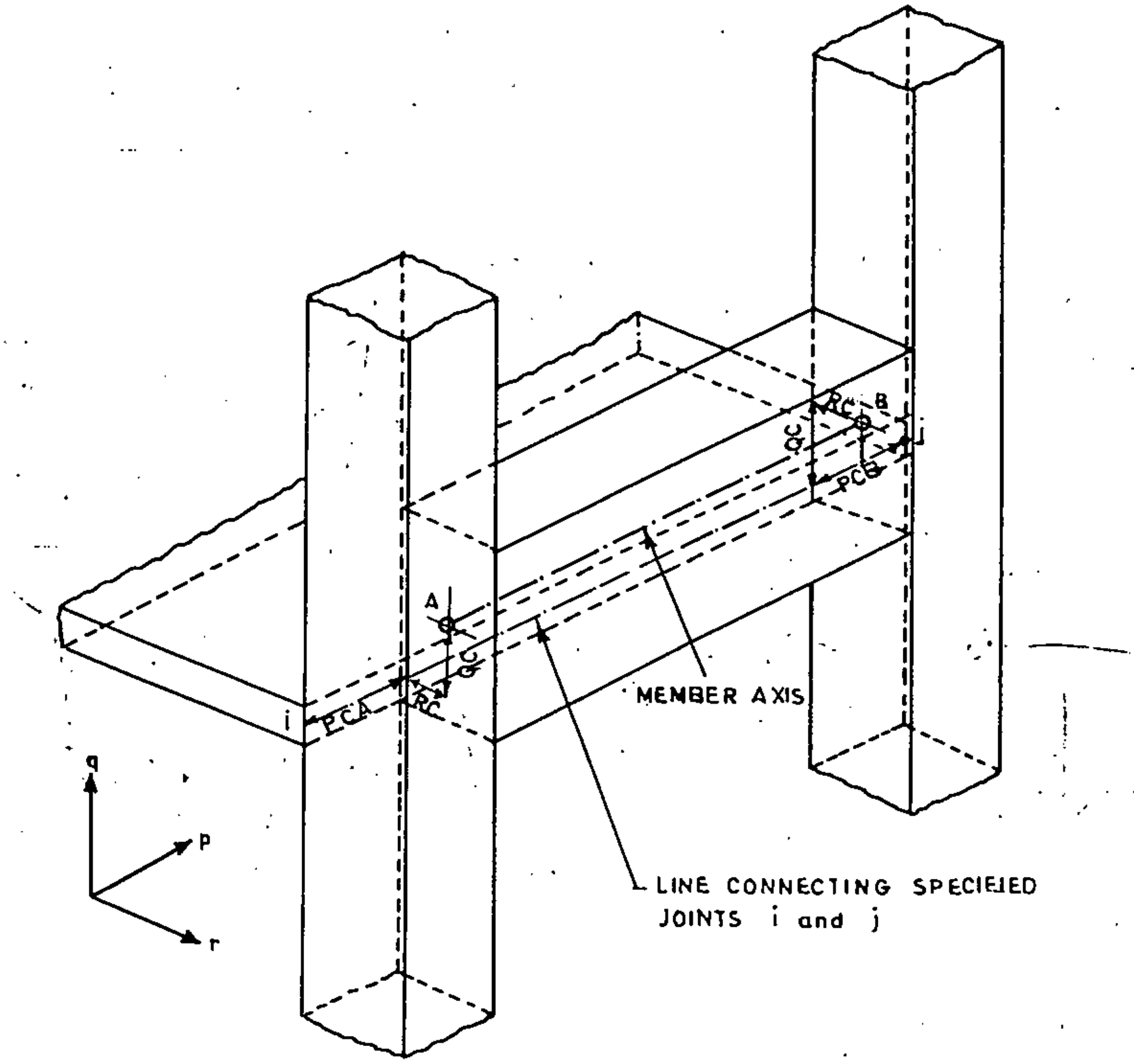

(a) Definition of end irregularities

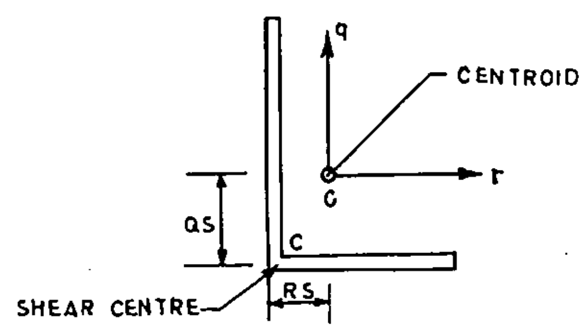

(b) Definition of QS and RS

FIGURE A1.2 END IRREGULARITIES OF THE SPACE MEMBER ELEMENT.

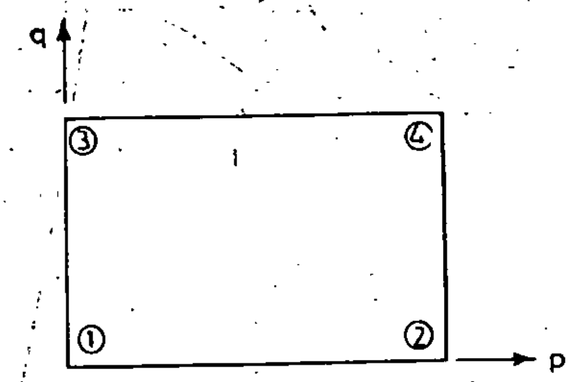

(a) Reference axes and node numbering.

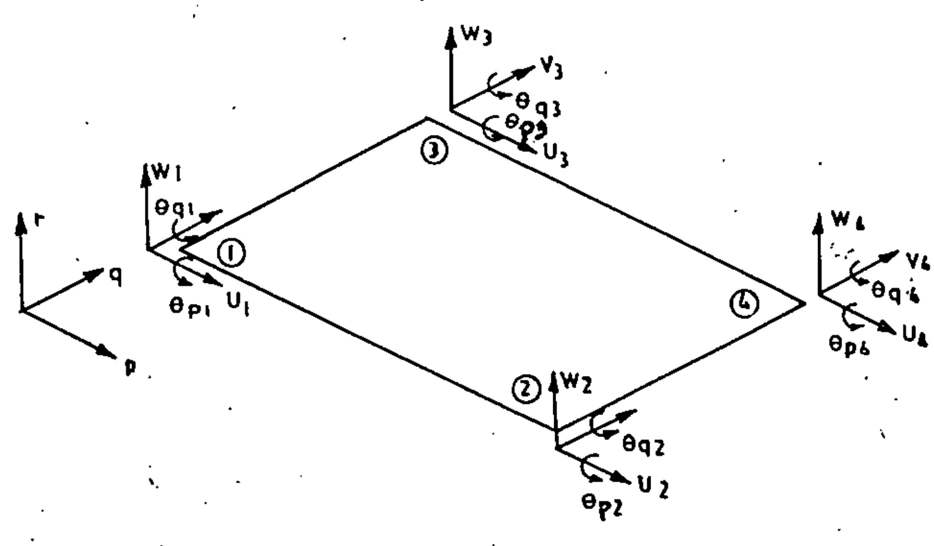

(b) Nodal displacements.

FIGURE A1.3 RECTANGULAR PLATE ELEMENT.

three translations and two rotations as shown in Fig.(A1.3b). The in-plane rotation of the nodes about the r axis is suppressed. The in-plane displacements u and v and the out of plane freedoms w, θ_p and θ_q are formulated separately. The element can be used either as a plane element by suppressing the out of plane displacements or as a bending element by allowing these.